# RADON-HAZARD-POTENTIAL AREAS IN SANDY, SALT LAKE COUNTY, AND PROVO, UTAH COUNTY, UTAH

*by*
*Barry J. Solomon, Bill D. Black*
*Dennis L. Nielson*
*Dane L. Finerfrock, John D. Hultquist*
*Cui Linpei*

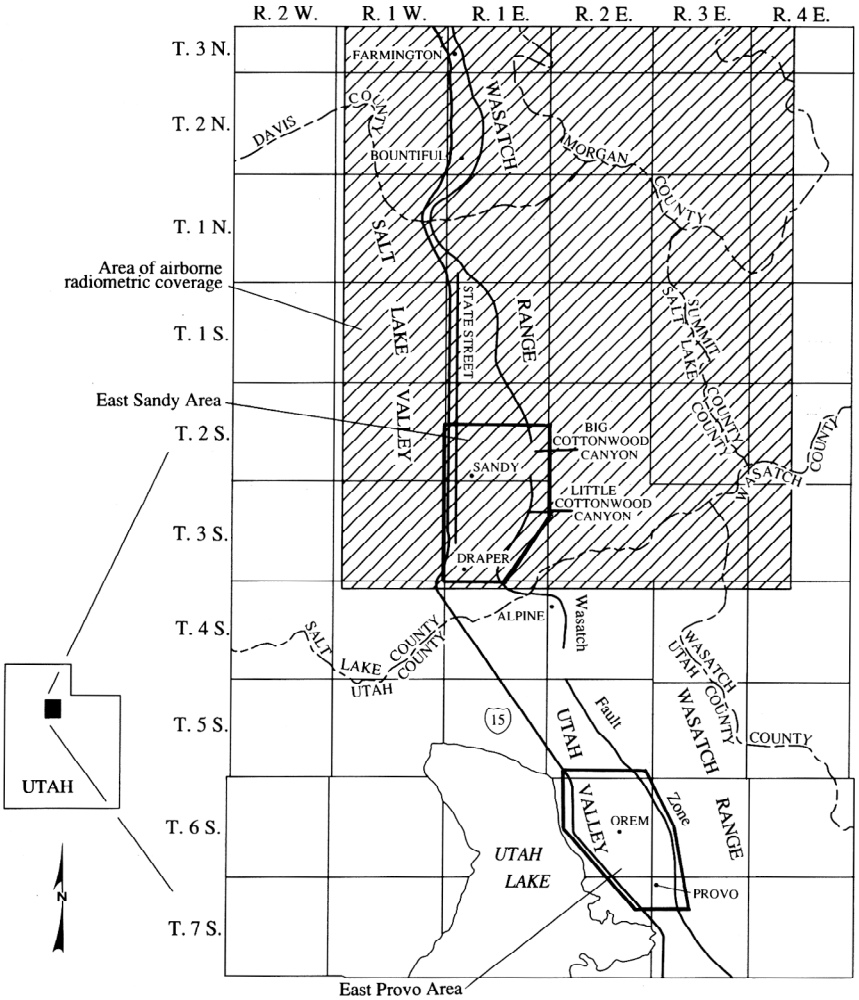


**Special Study 85** **1994**
**UTAH GEOLOGICAL SURVEY**
*a division of*
UTAH DEPARTMENT OF NATURAL RESOURCES
*in cooperation with*
U.S. ENVIRONMENTAL PROTECTION AGENCY

Solomon, Black, Nielson, Finerfrock, Hultquist, Cui RADON-HAZARD-POTENTIAL AREAS IN SANDY, SALT LAKE COUNTY, AND PROVO, UTAH COUNTY, UTAH UGS Special Study 85

**STATE OF UTAH**
*Michael O. Leavitt, Governor*

**DEPARTMENT OF NATURAL RESOURCES**
*Ted Stewart, Executive Director*

**UTAH GEOLOGICAL SURVEY**
*M. Lee Allison, Director*

**UGS Board**

| Member | Representing |
|---|---|
| Russell C. Babcock, Jr. (chairman) | Mineral Industry |
| D. Cary Smith | Mineral Industry |
| Richard R. Kennedy | Civil Engineering |
| Jo Brandt | Public-at-Large |
| C. William Berge | Mineral Industry |
| Jerry Golden | Mineral Industry |
| Milton E. Wadsworth | Economics-Business/Scientific |
| Scott Hirschi, Director, Division of State Lands and Forestry | *Ex officio member* |

**UGS Editorial Staff**

| | |
|---|---|
| J. Stringfellow | Editor |
| Vicky Clarke, Sharon Hamre | Editorial Staff |
| Patricia H. Speranza, James W. Parker, Lori Douglas | Cartographers |

**UTAH GEOLOGICAL SURVEY**
2363 South Foothill Drive
Salt Lake City, Utah 84109-1491
Phone: (801) 467-7970 Fax: (801) 467-4070

THE UTAH GEOLOGICAL SURVEY is organized into three geologic programs with Administration, Editorial, and Computer Resources providing necessary support to the programs. THE ECONOMIC GEOLOGY PROGRAM undertakes studies to identify coal, geothermal, uranium, hydrocarbon, and industrial and metallic mineral resources; to initiate detailed studies of the above resources including mining district and field studies; to develop computerized resource data bases, to answer state, federal, and industry requests for information; and to encourage the prudent development of Utah's geologic resources. THE APPLIED GEOLOGY PROGRAM responds to requests from local and state governmental entities for engineering geologic investigations; and identifies, documents, and interprets Utah's geologic hazards. THE GEOLOGIC MAPPING PROGRAM maps the bedrock and surficial geology of the state at a regional scale by county and at a more detailed scale by quadrangle. The Geologic Extension Service answers inquiries from the public and provides information about Utah's geology in a non-technical format.

The UGS manages a library which is open to the public and contains many reference works on Utah geology and many unpublished documents on aspects of Utah geology by UGS staff and others. The UGS has begun several computer data bases with information on mineral and energy resources, geologic hazards, stratigraphic sections, and bibliographic references. Most files may be viewed by using the UGS Library. The UGS also manages a sample library which contains core, cuttings, and soil samples from mineral and petroleum drill holes and engineering geology investigations. Samples may be viewed at the Sample Library or requested as a loan for outside study.

The UGS publishes the results of its investigations in the form of maps, reports, and compilations of data that are accessible to the public. For information on UGS publications, contact the Sales Office, 2363 South Foothill Drive, Salt Lake City, Utah 84109-1491, (801) 467-0401.

*The Utah Department of Natural Resources receives federal aid and prohibits discrimination on the basis of race, color, sex, age, national origin, or handicap. For information or complaints regarding discrimination, contact Executive Director, Utah Department of Natural Resources, 1636 West North Temple #316, Salt Lake City, UT 84116-3193 or Office of Equal Opportunity, U.S. Department of the Interior, Washington, DC 20240.*

Printed on recycled paper

# RADON-HAZARD-POTENTIAL AREAS IN SANDY, SALT LAKE COUNTY, AND PROVO, UTAH COUNTY, UTAH

*by*

*Barry J. Solomon and Bill D. Black*
*Utah Geological Survey*
*2363 South Foothill Drive, Salt Lake City, Utah 84109-1491*

*Dennis L. Nielson*
*University of Utah Research Institute*
*391-C Chipeta Way, Salt Lake City, Utah 84108*

*Dane L. Finerfrock and John D. Hultquist*
*Utah Department of Environmental Quality*
*Division of Radiation Control*
*168 North 1950 West, Salt Lake City, Utah 84114-4850*

*Cui Linpei*
*Institute of Geological Information*
*Beijing, People's Republic of China*

FIRST-YEAR GEOLOGIC STUDIES FOR THE
U.S. ENVIRONMENTAL PROTECTION AGENCY
STATE INDOOR RADON GRANT PROGRAM

Reference herein to any specific commercial product, process, or service by trade name, trademark, manufacturer, or otherwise, does not necessarily constitute or imply its endorsement, recommendation, or favoring by the Utah Geological Survey or the U.S. Environmental Protection Agency. The views and opinions of authors expressed herein do not necessarily state or reflect those of the U.S. Environmental Protection Agency.

# CONTENTS

**ABSTRACT** . . . . . 1
**INTRODUCTION** . . . . . 2
**LOCATION AND GEOLOGY OF STUDY AREAS** . . . . . 2
**DATA COLLECTION AND INTERPRETATION** . . . . . 12
Airborne-Radiometric Measurements . . . . . 12
Sampling and Analytical Techniques . . . . . 12
Data and Discussion . . . . . 12
Ground Measurements . . . . . 14
Sampling and Analytical Techniques . . . . . 14
Data and Discussion . . . . . 16
Potential Radon Hazard of Quaternary Geologic Units . . . . . 27
Cautions When Using This Report . . . . . 32
**A GEOLOGIC MODEL FOR PREDICTING INDOOR-RADON HAZARD ALONG THE WASATCH FRONT** . . . . . 32
**CONCLUSIONS** . . . . . 34
**ACKNOWLEDGMENTS** . . . . . 34
**REFERENCES CITED** . . . . . 35
**APPENDIX** - Ground-Survey Data (Except Soil-ATD Measurements) . . . . . 37

# FIGURES

**Figure 1.** Index map of study areas . . . . . 3
**Figure 2.** Surficial geologic map, east Sandy study area . . . . . 6
**Figure 3.** Surficial geologic map, east Provo study area . . . . . 10
**Figure 4.** eU concentrations from the airborne-radiometric survey . . . . . 12
**Figure 5.** eTh concentrations from the airborne-radiometric survey . . . . . 13
**Figure 6.** K concentrations from the airborne-radiometric survey . . . . . 13
**Figure 7.** Total gamma count from the airborne-radiometric survey . . . . . 14
**Figure 8.** eU/eTh ratios from the airborne-radiometric survey . . . . . 14
**Figure 9.** eU/K ratios from the airborne-radiometric survey . . . . . 15
**Figure 10.** eTh/K ratios from the airborne-radiometric survey . . . . . 15
**Figure 11.** Histogram of soil-gas-radon concentrations from ground-scintillometer surveys . . . . . 16
**Figure 12.** Scatter plot and linear regression of U and soil-gas radon . . . . . 19
**Figure 13.** Contour map of anomalous concentrations of radon in soil gas, east Sandy, from the ground-scintillometer survey . . 19
**Figure 14.** Contour map of indoor-radon concentrations, east Sandy "hot spot" . . . . . 21
**Figure 15.** Linear regression of radon in soil gas from the ATD survey . . . . . 21
**Figure 16.** Relationship between field and laboratory measurements of radon in soil gas . . . . . 22
**Figure 17.** Contour map of soil-gas radon measured in the field with ATDs, December, 1990 . . . . . 22
**Figure 18.** Contour map of soil-gas radon measured in the field with ATDs, March and April, 1991 . . . . . 24
**Figure 19.** Contour map of soil-gas radon measured in the field with ATDs, May, 1991 . . . . . 24
**Figure 20.** Contour map of depth-corrected soil-gas radon measured in the field with ATDs, March and April, 1991 . . . . . 25
**Figure 21.** Average levels of hazard-rating factors, east Sandy . . . . . 25
**Figure 22.** Average levels of hazard-rating factors, east Provo . . . . . 27
**Figure 23.** Normal probability diagram of eU concentrations . . . . . 28
**Figure 24.** Normal probability diagram of soil-gas radon concentrations from the ground-scintillometer survey . . . . . 28
**Figure 25.** Radon-hazard-potential map, east Sandy . . . . . 29
**Figure 26.** Radon-hazard-potential map, east Provo . . . . . 29
**Figure 27.** Indoor-radon concentrations and hazard ratings, east Sandy . . . . . 31
**Figure 28.** Indoor-radon concentrations and hazard ratings, east Provo . . . . . 31
**Figrue 29.** Regional geology, east Sandy . . . . . 33
**Figure 30.** Regional geology, east Provo . . . . . 33

# TABLES

**Table 1.** Statistical summary of east Sandy field data used as hazard factors for geologic units . . . . . 4
**Table 2.** Statistical summary of east Provo field data used as hazard factors for geologic units . . . . . 8

**Table 3.** Statistical summary of additional east Sandy ground-radiometric data for geologic units . . . . . 17
**Table 4.** Statistical summary of additional east Provo ground-radiometric data for geologic units . . . . . 18
**Table 5.** Soil-gas radon measurements from ATDs . . . . . 23
**Table 6.** Summary of indoor-radon measurements in selected schools . . . . . 26
**Table 7.** Radon-hazard-potential matrix . . . . . 26
**Table 8.** Radon-hazard-potential categories . . . . . 30
**Table 9.** Statistical summary of field data used as hazard factors for hazard-potential categories . . . . . 30
**Table 10.** Statistical summary of additional ground-radiometric data for hazard-potential categories . . . . . 30
**Table A-1.** Indoor-radon measurements, east Sandy . . . . . 38
**Table A-2.** Indoor-radon measurements, east Provo . . . . . 41
**Table A-3.** Ground-survey data, east Sandy, exclusive of indoor and soil-ATD measurements . . . . . 43
**Table A-4.** Ground-survey data, east Provo, exclusive of indoor and soil-ATD measurements . . . . . 47

# RADON-HAZARD-POTENTIAL AREAS IN SANDY, SALT LAKE COUNTY, AND PROVO, UTAH COUNTY, UTAH

*Barry J. Solomon and Bill D. Black*
*Utah Geological Survey*
*2363 South Foothill Drive, Salt Lake City, Utah 84109-1491*

*Dennis L. Nielson*
*University of Utah Research Institute*
*391-C Chipeta Way, Salt Lake City, Utah 84108*

*Dane L. Finerfrock and John D. Hultquist*
*Utah Department of Environmental Quality*
*Division of Radiation Control*
*168 North 1950 West, Salt Lake City, Utah 84114-4850*

*Cui Linpei*
*Institute of Geological Information*
*Beijing, People's Republic of China*

## ABSTRACT

Average indoor-radon levels in two areas of the Wasatch Front region of north-central Utah are considerably higher than the national average of 1.7 picocuries per liter (pCi/L) (63 Becquerels per cubic meter [Bq/m$^3$]). The average indoor-radon level on the east bench of Sandy near Little Cottonwood Canyon is 3.8 pCi/L (141 Bq/m$^3$) and on the east bench of Provo it is 2.9 pCi/L (107 Bq/m$^3$). However, indoor measurements are affected by construction type, building maintenance, occupant lifestyle, and weather and cannot be used to accurately estimate the radon-hazard potential in nearby, untested homes. Geologic characteristics of foundation materials which govern the potential for indoor radon are relatively uniform within geologic units that underlie the study areas, and were used to estimate the radon-hazard potential of Sandy and Provo.

The radon-hazard potential was estimated using three geologic factors: (1) uranium content of soils, (2) concentration of radon in soil gas, and (3) depth to ground water. Numerical scores were applied to each factor, and three radon-hazard-potential categories were established based on the cumulative totals of the three factors. The categories characterize the hazard potential of each major Quaternary geologic unit.

Geologic units with the highest potential for elevated indoor-radon concentrations are upper Pleistocene lacustrine deposits related to the transgressive phase of the Bonneville lake cycle, younger alluvial and colluvial deposits overlying the transgressive lacustrine units, and older, middle and upper Pleistocene glacial deposits. Well-drained, regressive-phase alluvium deposited on deltas on the margin of Lake Bonneville predominate. At the mouth of Little Cottonwood Canyon in east Sandy this alluvium contains abundant detritus from Tertiary granitic stocks and has high concentrations of both uranium (averaging 6.9 parts per million [ppm]) and radon (averaging 641 pCi/L [2.37 x 10$^4$ Bq/m$^3$]). The indoor-radon hazard potential is high where the alluvium occurs near Little Cottonwood Canyon. At the mouth of Provo Canyon in east Provo this alluvium contains detritus from uraniferous rocks of the Penn-

sylvanian to Mississipian Manning Canyon Shale and Precambrian Mineral Fork Formation, mixed with a significant fraction of material from less uraniferous rocks. Uranium (averaging 2.3 ppm) and radon (averaging 394 pCi/L [1.46 x $10^4$ Bq/$m^3$] levels in this alluvium are lower in east Provo than in east Sandy, but are sufficiently high to indicate a moderate potential indoor-radon hazard where the alluvium occurs in east Provo.

Characterization of the uranium concentration, soil-gas radon level, and ground-water depth in geologic units underlying large areas can be accomplished rapidly, and can serve as a predictive indicator of the potential for high indoor-radon levels. This relative radon-hazard potential can then be used to prioritize indoor testing in existing buildings and evaluate the need for radon-resistant new construction.

## INTRODUCTION

Concentrations of indoor radon (Rn) are a function of a number of non-geologic factors including weather, building construction, and ventilation. Ultimately, however, the source of the radon is uranium (U) in the geologic units surrounding a building's foundation. Identification of areas with high concentrations of uranium is the first step in determining the potential for high concentrations of indoor radon. One radon isotope, $^{222}$Rn, is the most significant contributor to the indoor-radon problem and forms as a product in the $^{238}$U decay series. Subsequent references to radon and uranium refer to these isotopes, unless otherwise noted.

The problem of radon in the domestic environment was first recognized in 1984 when a house in Boyertown, Pennsylvania was discovered to have indoor-radon concentrations of greater than 2,500 pCi/L (9.25 x $10^4$ Bq/$m^3$). This occurrence is associated with Precambrian gneiss containing high levels of uranium. The radon levels in homes overlying this gneiss increase when it is sheared (Gundersen and others, 1988).

Sprinkel (1987) used regional geologic data to map potential radon-hazard areas in Utah. These areas were identified by known uranium occurrences; uranium-enriched rocks at the surface or beneath well-drained, porous, and permeable soils; and anomalous surficial uranium concentrations. The vicinity of the surface trace of the Wasatch fault zone, a large, permeable conduit in which uraniferous fluids and radon may readily migrate, was also considered a potential radon-hazard area. Quaternary units were not included in the compilation unless already documented as a radon source.

In 1988, in response to growing national concern over the threat of radon gas, Congress enacted Title III, Indoor Radon Abatement Act (IRAA), as an amendment to the Toxic Substances Control Act. The IRAA has the overall goal of reducing public health risks from radon gas by rendering air within buildings in the United States free of radon. Section 306 of the IRAA, the State Indoor Radon Grant (SIRG) Program, authorizes the U.S. Environmental Protection Agency (EPA) to provide grants to states to support development and implementation of state radon assessment and mitigation programs. A principal SIRG activity of the Utah Geological Survey (UGS) is to identify areas throughout the state that have geologic factors conducive to elevated indoor-radon levels, and assess the radon-hazard potential of those areas.

Indoor-radon levels were measured statewide during a 1988 survey conducted by the Utah Division of Radiation Control (UDRC) (Sprinkel and Solomon, 1990). Volunteers were solicited from cities or towns in radon-hazard areas defined by Sprinkel (1987); homes selected for testing were owner-occupied, single-family dwellings. Alpha-track detectors (ATDs) were placed in 631 homes to measure indoor-radon levels. The statewide average indoor-radon level was 2.7 picocuries per liter (pCi/L) (100 Becquerels per cubic meter [Bq/$m^3$]), with 14 percent of measurements greater than 4 pCi/L (148 Bq/$m^3$), the level above which hazard-reduction procedures are suggested (U.S. Environmental Protection Agency and others, 1992). Comparable figures for the United States are an average of 1.7 pCi/L (63 Bq/$m^3$) with 6 percent of measurements greater than 4 pCi/L (148 Bq/$m^3$) (Sextro, 1988). Clusters of high indoor-radon values occur in several areas of the state. Two of these areas, east Sandy and east Provo, occur along the populous Wasatch Front (figure 1) and were selected for detailed investigation during the first year of the multi-year SIRG program. This study included collection and interpretation of ground radiometric and geologic data in both areas, collection of additional indoor-radon measurements in homes and schools by the UDRC, and interpretation of airborne radiometric data in east Sandy and adjacent portions of the Salt Lake Valley and Wasatch Range. Preliminary results of this study were reported in Solomon and others (1991).

The objective of this investigation was to use rapid and inexpensive field methods to identify radon-hazard-potential areas based on geologic factors which influence areal radon distribution. These methods can be used elsewhere to assess the radon hazard prior to expenditure of considerable time and expense testing existing construction and using radon-resistant techniques in new construction.

## LOCATION AND GEOLOGY OF STUDY AREAS

The east Sandy study area is in the Salt Lake Valley of eastern Salt Lake County. The study area extends from the mouth of Big Cottonwood Canyon on the north to the city of Draper on the south, and is approximately bounded by State Street on the west and the Wasatch Range on the east (figure 1). The average indoor-radon level in east Sandy is 3.0 pCi/L (111 Bq/$m^3$), with 18 percent of measurements greater than 4 pCi/L (148 Bq/$m^3$) (tables 1 and A-1).

The valley in Sandy is underlain by a complex sequence of Quaternary unconsolidated alluvial, colluvial, deltaic, lacustrine, eolian, and glacial deposits (figure 2) (Personius and Scott, 1992). The dominant influence on surficial geology and physiography was the last cycle of Pleistocene Lake Bonneville, which was present from about 28,000 to 13,000 years ago (Oviatt and others, 1992). The lake underwent several major periods of stability resulting in the creation of four basin-wide shorelines. Two of these, the transgressive Bonneville and regressive Provo shorelines, occur in the study area.

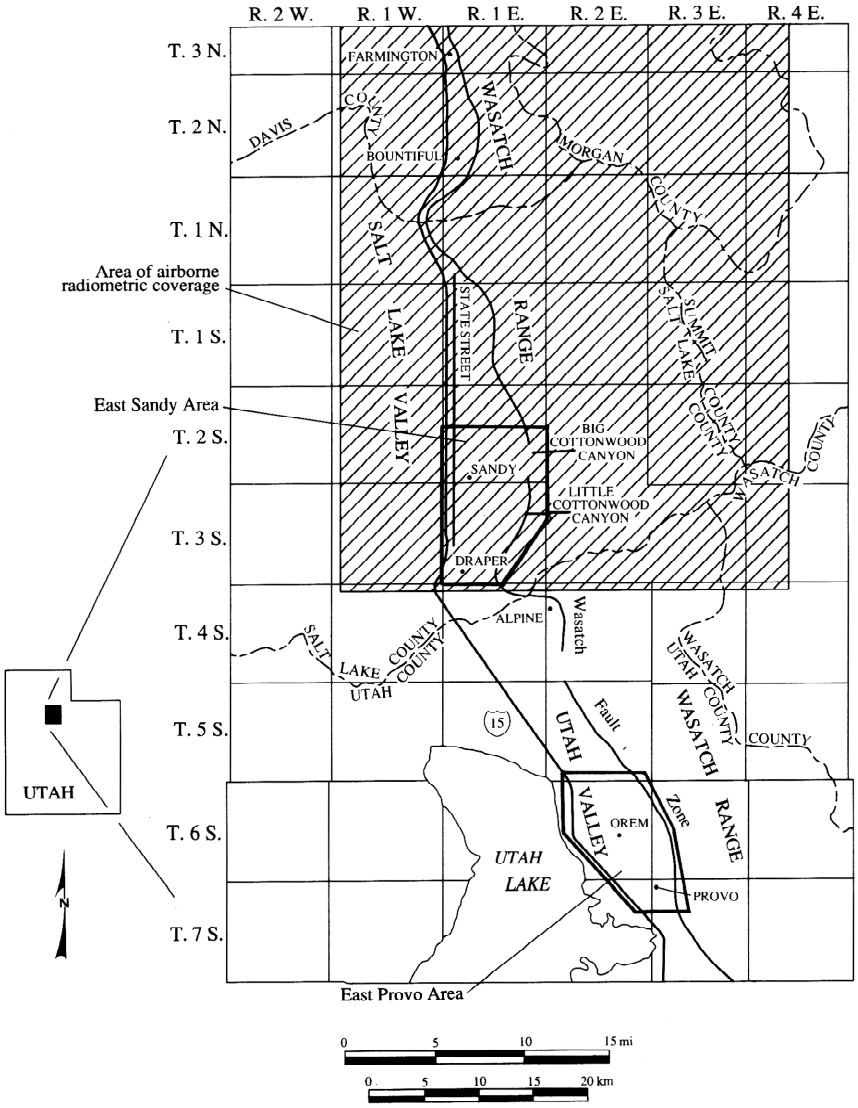


***Figure 1.*** *Index map of study areas.*

Compound deltas at both the Bonneville and Provo levels were formed at the mouths of Big and Little Cottonwood Canyons by rivers which incised middle and upper Pleistocene glacial material and drained into the lake from the Wasatch Range. Uppermost Pleistocene and Holocene fluvial, alluvial-fan, colluvial, and eolian deposits overlie older, upper Pleistocene lacustrine and deltaic material. Coarser deposits in the valley generally occur to the east beneath elevated shoreline benches along the range front. Ground water is deeper than 50 feet (15 m) beneath the benches, but is less than 10 feet (3 m) deep beneath the valley floor to the west and beneath alluvial channels which dissect the benches (Anderson and others, 1986b). In Sandy, the active Wasatch fault zone separates unconsolidated deposits of the Salt Lake Valley from bedrock in the Wasatch Range.

A variety of bedrock crops out in the Wasatch Range, but three lithologies are potential sources of uranium for valley deposits. Of primary importance are Oligocene granitic rocks of the Little Cottonwood, Alta, and Clayton Peak stocks, which underlie extensive parts of the Little Cottonwood Canyon drainage and smaller parts of the Big Cottonwood Canyon drainage (Crittenden, 1976). Of secondary importance are informally named Precambrian metamorphic rocks and the Precambrian Mineral Fork Formation, a diamictite derived from older granitic rocks (Condie, 1967). These units underlie small parts of both canyon drainages. Quartzite, shale, and slate are widespread in the Precambrian Big Cottonwood Formation in the Big Cottonwood Canyon drainage (James, 1979), and provide source material low in uranium for valley deposits.

The east Provo study area is in the Utah Valley of central

*Table 1.*

*Statistical summary of field data, factor ratings, hazard ratings, and hazard potential for Quaternary geologic units in the east Sandy area. Geologic units were mapped by Personius and Scott (1990, 1992) (figure 2), but units ca, alp, and lbg have been subdivided for this study where they occur on the Big Cottonwood and Little Cottonwood deltas. Soil textures are described using the classification of the U.S. Soil Conservation Service (1975) and reflect the predominant texture of the material at sample sites. Because of textural variability within geologic units, textures do not necessarily correspond to unit descriptions. N for eU and soil-gas Rn is the number of sample sites; N for ground-water depth is the number of sites with ground-water depth greater than 50 feet (15 m); N for indoor Rn is the number of sample sites for both this study and the statewide survey (Sprinkel and Solomon, 1990). Factor ratings for units with no samples collected were estimated from geologically similar units and indoor measurements. See tables 7 and 8 for a description of the factor ratings, hazard ratings, and hazard potential.*

| Geologic Unit | Soil Texture | eU | | | | | Rn in soil gas | | | | | Depth to ground water | | | Indoor Rn | | | | Hazard Rating and Potential |
|---|---|---|---|---|---|---|---|---|---|---|---|---|---|---|---|---|---|---|---|
| | | N | %>3 ppm | Avg. ppm | Max. ppm | Rating | N | %>500 pCi/L | Avg. pCi/L | Max. pCi/L | Rating | N | %>50 ft | Rating | N | %>4 pCi/L | Avg. pCi/L | Max. pCi/L | |
| Lacustrine Deposits | | | | | | | | | | | | | | | | | | | |
| Deposits postdating the Bonneville lake cycle | | | | | | | | | | | | | | | | | | | |
| Lacustrine, marsh, and alluvial deposits (laly) | CL | 2 | 50 | 3.2 | 3.3 | 2 | 2 | 50 | 522 | 905 | 3 | 0 | 0 | 1 | 0 | – | – | – | 6 - Mod |
| Regressive-phase deposits of Bonneville lake cycle | | | | | | | | | | | | | | | | | | | |
| Deltaic deposits (lpd) | Sg | 7 | 86 | 7.1 | 9.0 | 4 | 3 | 33 | 315 | 613 | 2 | 1 | 11 | 1 | 2 | 0 | 1.1 | 1.3 | 7 - Mod |
| Lacustrine gravel (lpg) | Sg | 33 | 76 | 4.8 | 10.6 | 3 | 19 | 47 | 539 | 1,434 | 3 | 44 | 59 | 3 | 42 | 7 | 2.2 | 8.8 | 9 - Mod |
| Transgressive-phase deposits of Bonneville lake cycle | | | | | | | | | | | | | | | | | | | |
| Lacustrine gravel (lbg) | Sg | 17 | 82 | 4.8 | 8.6 | – | 8 | 38 | 565 | 1,198 | – | 26 | 74 | – | 18 | 22 | 3.5 | 26.2 | – |
| Big Cottonwood | Sg | 2 | 100 | 7.1 | 8.6 | 4 | 2 | 0 | 296 | 327 | 2 | 0 | 0 | 1 | 2 | 0 | 0.8 | 1.1 | 7 - Mod |
| Little Cottonwood | Sg | 15 | 80 | 4.5 | 7.9 | 3 | 6 | 50 | 654 | 1,198 | 3 | 26 | 84 | 4 | 16 | 25 | 3.8 | 26.2 | 10 - Hi |
| Undivided deposits of Bonneville lake cycle | | | | | | | | | | | | | | | | | | | |
| Lacustrine clay and silt (lbpm) | CL | 2 | 50 | 3.8 | 5.1 | 2 | 2 | 50 | 445 | 580 | 2 | 0 | 0 | 1 | 1 | 0 | 0.8 | 0.8 | 5 - Low |
| Alluvial Deposits | | | | | | | | | | | | | | | | | | | |
| Stream alluvium | | | | | | | | | | | | | | | | | | | |
| Unit 1 (al1) | Sg | 6 | 83 | 6.8 | 9.0 | 3 | 3 | 0 | 270 | 482 | 2 | 0 | 0 | 1 | 1 | 0 | 1.1 | 1.1 | 6 - Mod |
| Unit 2 (al2) | Slg | 1 | 100 | 3.7 | 3.7 | 2 | 0 | – | – | – | 4 | 0 | 0 | 1 | 5 | 80 | 9.0 | 26.2 | 7 - Mod |
| Regressive-phase alluvium (alp) | LSg | 34 | 97 | 6.7 | 8.7 | – | 16 | 50 | 641 | 2,398 | – | 78 | 64 | – | 88 | 27 | 3.7 | 13.7 | – |
| Big Cottonwood | LSg | 2 | 50 | 4.1 | 5.5 | 2 | 0 | – | – | – | 3 | 0 | 0 | 1 | 4 | 0 | 2.5 | 3.8 | 6 - Mod |
| Little Cottonwood | LSg | 32 | 100 | 6.9 | 8.7 | 4 | 16 | 50 | 641 | 2,398 | 3 | 78 | 67 | 3 | 84 | 29 | 3.8 | 13.7 | 10 - Hi |

*Table 1 (continued)*

| | | | | | | | | | | | | | | | | | | | |
|---|---|---|---|---|---|---|---|---|---|---|---|---|---|---|---|---|---|---|---|
| Fan alluvium | | | | | | | | | | | | | | | | | | | |
| Unit 1 (af1) | Sg | 1 | 100 | 4.2 | 4.2 | 2 | 0 | – | – | – | 1 | 1 | 100 | 4 | 0 | – | – | – | 7 - Mod |
| Unit 2 (af2) | Sg | 6 | 67 | 4.0 | 6.0 | 2 | 1 | 0 | 120 | 120 | 1 | 6 | 55 | 3 | 5 | 0 | 2.5 | 3.2 | 6 - Mod |
| Glacial Deposits | | | | | | | | | | | | | | | | | | | |
| Outwash of Bells Canyon age (gbco) | Sg | 2 | 100 | 7.0 | 7.4 | 4 | 0 | – | – | – | 3 | 3 | 100 | 4 | 1 | 0 | 2.7 | 2.7 | 11 - Hi |
| Till of Bells Canyon age (gbct) | Sg | 2 | 100 | 5.7 | 6.3 | 3 | 0 | – | – | – | 3 | 3 | 100 | 4 | 1 | 100 | 6.1 | 6.1 | 10 - Hi |
| Eolian Deposits | | | | | | | | | | | | | | | | | | | |
| Sand (es) | S | 8 | 88 | 5.1 | 8.2 | 3 | 0 | – | – | – | 2 | 30 | 83 | 4 | 28 | 0 | 1.7 | 3.4 | 9 - Mod |
| Colluvial Deposits | | | | | | | | | | | | | | | | | | | |
| Debris-flow deposits 1 (cd1) | Sg | 0 | – | – | – | 3 | 0 | – | – | – | 2 | 2 | 100 | 4 | 2 | 0 | 1.6 | 1.9 | 9 - Mod |
| Hillslope colluvium (chs) | Sg | 2 | 100 | 5.7 | 5.7 | 3 | 0 | – | – | – | 3 | 3 | 100 | 4 | 1 | 0 | 2.4 | 2.4 | 10 - Hi |
| Colluvium and alluvium (ca) | Sg | 8 | 100 | 5.9 | 8.4 | – | 2 | 0 | 375 | 467 | – | 12 | 67 | – | 10 | 10 | 2.1 | 4.4 | – |
| Big Cottonwood | Sg | 4 | 100 | 5.5 | 8.4 | 3 | 2 | 0 | 375 | 467 | 2 | 1 | 20 | 1 | 1 | 0 | 2.2 | 2.2 | 6 - Mod |
| Little Cottonwood | Sg | 4 | 100 | 6.4 | 7.7 | 3 | 0 | – | – | – | 3 | 11 | 85 | 4 | 9 | 11 | 2.1 | 4.4 | 10 - Hi |
| Fill Deposits | | | | | | | | | | | | | | | | | | | |
| Man-made fill (f) | Sg | 0 | – | – | – | 4 | 0 | – | – | – | 3 | 1 | 100 | 4 | 1 | 0 | 2.2 | 2.2 | 11 - Hi |
| EAST SANDY TOTAL | – | 131 | 86 | 5.6 | 10.6 | – | 56 | 41 | 528 | 2,398 | – | 210 | 62 | – | 206 | 18 | 3.0 | 26.2 | – |

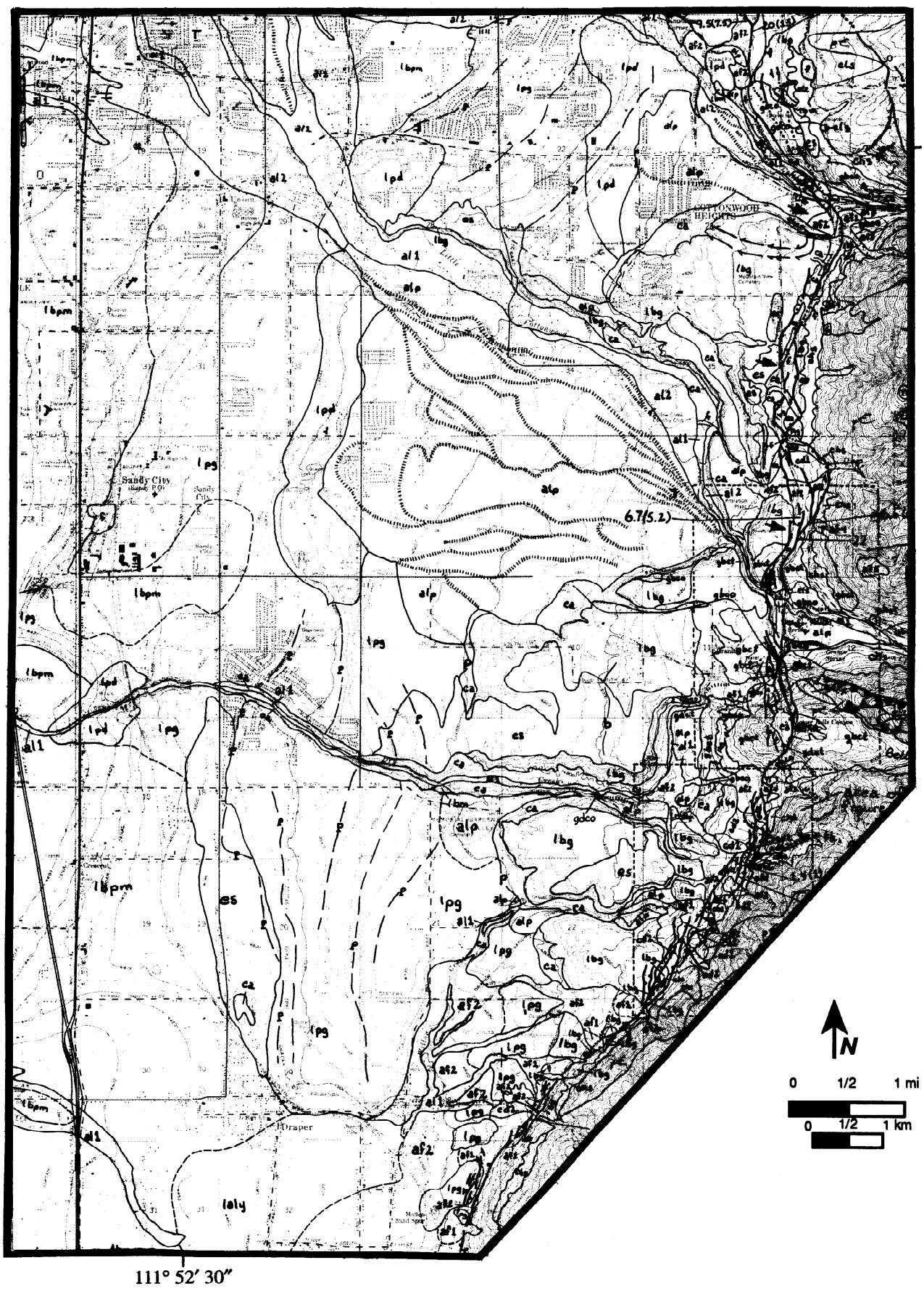


*Figure 2. Surficial geologic map of the east Sandy study area, modified from Personius and Scott (1990).*

***Figure 2** (continued)*

**CORRELATION OF MAP UNITS**

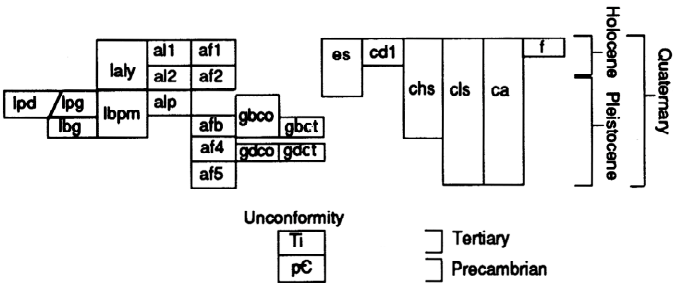


—- - **Contact** — Dashed where approximately located

12 (9) • • • **Normal fault** — Bar and ball on downdropped side. Dotted where concealed. Height of fault scarp and amount of geomorphic surface offset (in parentheses) shown in meters.

▲▲▲ **Thrust fault** — Sawteeth on overriding plate or block

**Major shorelines related to levels of the Bonneville lake cycle** — Coincide with geologic contacts in some places

- - B - - - Bonneville shoreline

- - b - - - Other shorelines of the transgressive phase

- - P - - - Provo shoreline

- - p - - - Other shorelines of the regressive phase

**Topographic escarpment** — Formed primarily by fluvial processes; coincide with geologic contacts in some places; tear drops point up slope

**Paleostream channels** — Preserved as abandoned channels

**Tilted geomorphic surface** — Arrow points in general direction of downward tilt

**DESCRIPTION OF MAP UNITS**

**LACUSTRINE DEPOSITS**

**Deposits Postdating the Bonneville Lake Cycle**

laly — Lacustrine, marsh and alluvial deposits

**Regressive-Phase Deposits of Bonneville Lake Cycle**

lpd — Deltaic deposits related to regressive phase

lpg — Lacustrine sand and gravel related to regressive phase

**Transgressive-Phase Deposits of Bonneville Lake Cycle**

lbg — Lacustrine sand and gravel related to transgressive phase

**Undivided Deposits of Bonneville Lake Cycle**

lbpm — Lacustrine clay and silt, undivided

**ALLUVIAL DEPOSITS**

**Stream Alluvium**

al1 — Stream alluvium 1

al2 — Stream alluvium 2

alp — Stream alluvium related to regressive phase

**Fan Alluvium**

af1 — Fan alluvium 1

af2 — Fan alluvium 2

afb — Fan alluvium related to transgressive phase

af4 — Fan alluvium 4

af5 — Fan alluvium 5

**GLACIAL DEPOSITS**

gbco — Outwash of Bells Canyon age

gbct — Till of Bells Canyon age

gdco — Outwash of Dry Creek age

gdct — Till of Dry Creek age

**EOLIAN DEPOSITS**

es — Eolian sand

**COLLUVIAL DEPOSITS**

cd1 — Debris-flow deposits 1

chs — Hillslope colluvium

cls — Landslide deposits

ca — Colluvium and alluvium, undivided

**FILL DEPOSITS**

f — Manmade fill

**BEDROCK**

Ti — Tertiary intrusive igneous rocks

p€ — Precambrian metamorphic rocks

Utah County. The study area extends from the city of Orem on the north to Provo on the south, and is approximately bounded by Interstate 15 on the west and the Wasatch Range on the east (figure 1). The average indoor-radon level in east Provo is 2.5 pCi/L (93 Bq/m$^3$), with 12 percent of measurements greater than 4 pCi/L (148 Bq/m$^3$) (tables 2 and A-2). Although the average indoor-radon level in the study area is lower than the statewide average, Sprinkel and Solomon (1990) demonstrated that part of east Provo has average indoor-radon concentrations in excess of the statewide average.

The valley in Provo is underlain by Quaternary sediments deposited in similar paleoenvironments to those of east Sandy (figure 3) (Machette, 1989). A compound delta at both the Bonneville and Provo levels was formed at the mouth of Provo Canyon by a river which drained into Lake Bonneville from the Wasatch Range. Ground water is deeper than 50 feet (15 m) in coarser deposits underlying elevated shoreline benches along the range front, but is less than 10 feet (3 m) deep beneath the valley floor to the west and beneath alluvial channels which dissect the benches (Anderson and others, 1986a). As in Sandy, the Wasatch fault zone separates unconsolidated deposits of the valley from bedrock in the mountains.

A variety of bedrock crops out in the Wasatch Range adjacent to the east Provo area. Two units are potential sources of uranium for valley deposits: (1) the Pennsylvanian to Mississippian Manning Canyon Shale, a dark, organic shale which underlies a large portion of the range front; and (2) diamictite of the Precambrian Mineral Fork Formation, similar to that near Sandy, which underlies the Rock and Slate Canyon drainages (Baker, 1964, 1972, 1973). Limestone and quartzite of the Pennsylvanian and Permian Oquirrh Formation provide source material low in uranium for valley deposits, and underlie much of the Provo Canyon drainage.

## *Table 2.*

*Statistical summary of field data, factor ratings, hazard ratings, and hazard potential for Quaternary geologic units in the east Provo area. Geologic units were mapped by Machette (1989) (figure 3). Soil textures are described using the classification of the U.S. Soil Conservation Service (1975) and reflect the predominant texture of the material at sample sites. Because of textural variability within geologic units, textures do not necessarily correspond to unit descriptions. N for eU and soil-gas Rn is the number of sample sites; N for ground-water depth is the number of sites with ground-water depth greater than 50 feet (15 m); N for indoor Rn is the number of sample sites for both this study and the statewide survey (Sprinkel and Solomon, 1990). Factor ratings for units with no samples collected were estimated from geologically similar units and indoor measurements. See tables 7 and 8 for a description of the rating factors and hazard ratings.*

| Geologic Unit | Soil Texture | eU | | | | | Rn in soil gas | | | | | Depth to ground water | | | Indoor Rn | | | | Hazard Rating and Potential |
|---|---|---|---|---|---|---|---|---|---|---|---|---|---|---|---|---|---|---|---|
| | | N | % > 3 ppm | Avg. ppm | Max. ppm | Rating | N | % > 500 pCi/L | Avg. pCi/L | Max. pCi/L | Rating | N | % > 50 ft | Rating | N | % > 4 pCi/L | Avg. pCi/L | Max. pCi/L | |
| Lacustrine Deposits | | | | | | | | | | | | | | | | | | | |
| Regressive-phase deposits of Bonneville lake cycle | | | | | | | | | | | | | | | | | | | |
| Deltaic deposits (lpd) | Lg | 2 | 0 | 2.1 | 2.2 | 2 | 2 | 0 | 190 | 205 | 1 | 0 | 0 | 1 | 5 | 0 | 1.7 | 2.3 | 4 - Low |
| Lacustrine gravel (lpg) | Lg | 3 | 0 | 1.9 | 2.4 | 1 | 2 | 0 | 384 | 419 | 2 | 0 | 0 | 1 | 8 | 0 | 1.9 | 2.5 | 4 - Low |
| Lacustrine sand (lps) | CLg | 4 | 0 | 2.3 | 2.9 | 2 | 4 | 50 | 421 | 619 | 2 | 0 | 0 | 1 | 3 | 0 | 1.4 | 1.7 | 5 - Low |
| Lacustrine silt and clay (lpm) | CL | 0 | – | – | – | 1 | 0 | – | – | – | 1 | 0 | 0 | 1 | 5 | 0 | 1.2 | 1.9 | 3 - Low |
| Transgressive-phase deposits of Bonneville lake cycle | | | | | | | | | | | | | | | | | | | |
| Lacustrine gravel (lbg) | Lg | 2 | 50 | 3.1 | 3.8 | 2 | 0 | – | – | – | 3 | 6 | 100 | 4 | 4 | 0 | 2.8 | 3.7 | 9 - Mod |
| Lacustrine sand (lbs) | Lg | 9 | 44 | 2.7 | 3.4 | 2 | 3 | 0 | 154 | 207 | 1 | 25 | 96 | 4 | 17 | 6 | 1.8 | 9.9 | 7 - Mod |
| Lacustrine silt and clay (lbm) | Lg | 10 | 50 | 2.9 | 3.6 | 2 | 7 | 57 | 602 | 1,463 | 3 | 18 | 51 | 3 | 24 | 25 | 3.7 | 13.6 | 8 - Mod |
| Alluvial Deposits | | | | | | | | | | | | | | | | | | | |
| Stream alluvium | | | | | | | | | | | | | | | | | | | |
| Unit 1 (al1) | SLg | 2 | 50 | 3.0 | 4.0 | 2 | 1 | 0 | 187 | 187 | 1 | 0 | 0 | 1 | 0 | – | – | – | 7 - Mod |
| Unit 2 (al2) | SLg | 8 | 13 | 2.4 | 3.9 | 2 | 3 | 67 | 604 | 887 | 3 | 0 | 0 | 1 | 2 | 50 | 3.8 | 6.5 | 6 - Mod |
| Regressive-phase alluvium (alp) | Lg | 24 | 17 | 2.3 | 3.3 | 2 | 11 | 27 | 394 | 734 | 2 | 21 | 38 | 2 | 31 | 6 | 2.5 | 6.3 | 6 - Mod |

*Table 2 (continued)*

| | | | | | | | | | | | | | | | | | | | |
|---|---|---|---|---|---|---|---|---|---|---|---|---|---|---|---|---|---|---|---|
| Fan alluvium | | | | | | | | | | | | | | | | | | | |
| Unit 2 (af2) | Lg | 8 | 25 | 2.5 | 3.4 | 2 | 6 | 33 | 679 | 1,455 | 3 | 0 | 0 | 1 | 1 | 100 | 8.2 | 8.2 | 6 - Mod |
| Younger fan alluvium (afy) | Lg | 19 | 32 | 2.9 | 4.6 | 2 | 11 | 45 | 517 | 1,405 | 3 | 26 | 49 | 2 | 34 | 18 | 2.7 | 10.2 | 7 - Mod |
| Regressive-phase fan alluvium (afp) | Lg | 6 | 33 | 2.8 | 3.6 | 2 | 5 | 0 | 234 | 468 | 1 | 1 | 6 | 1 | 10 | 10 | 1.9 | 8.1 | 4 - Low |
| Transgressive-phase fan alluvium (afb) | Lg | 0 | – | – | – | 1 | 0 | – | – | – | 3 | 1 | 100 | 4 | 1 | 0 | 1.4 | 1.4 | 8 - Mod |
| Unit 4 (af4) | Lg | 0 | – | – | – | 1 | 0 | – | – | – | 3 | 1 | 100 | 4 | 1 | 0 | 0.9 | 0.9 | 8 - Mod |
| Eolian Deposits | | | | | | | | | | | | | | | | | | | |
| Sand and silt (es) | SCL | 2 | 0 | 1.8 | 1.8 | 1 | 2 | 0 | 419 | 490 | 2 | 0 | 0 | 1 | 5 | 0 | 2.0 | 3.8 | 4 - Low |
| Colluvial Deposits | | | | | | | | | | | | | | | | | | | |
| Older landslide deposits (clso) | Lg | 0 | – | – | – | 2 | 0 | – | – | – | 3 | 1 | 100 | 4 | 1 | 0 | 3.4 | 3.4 | 9 - Mod |
| EAST PROVO TOTAL | – | 99 | 26 | 2.6 | 4.6 | – | 57 | 32 | 449 | 1,463 | – | 100 | 40 | – | 152 | 12 | 2.5 | 13.6 | – |

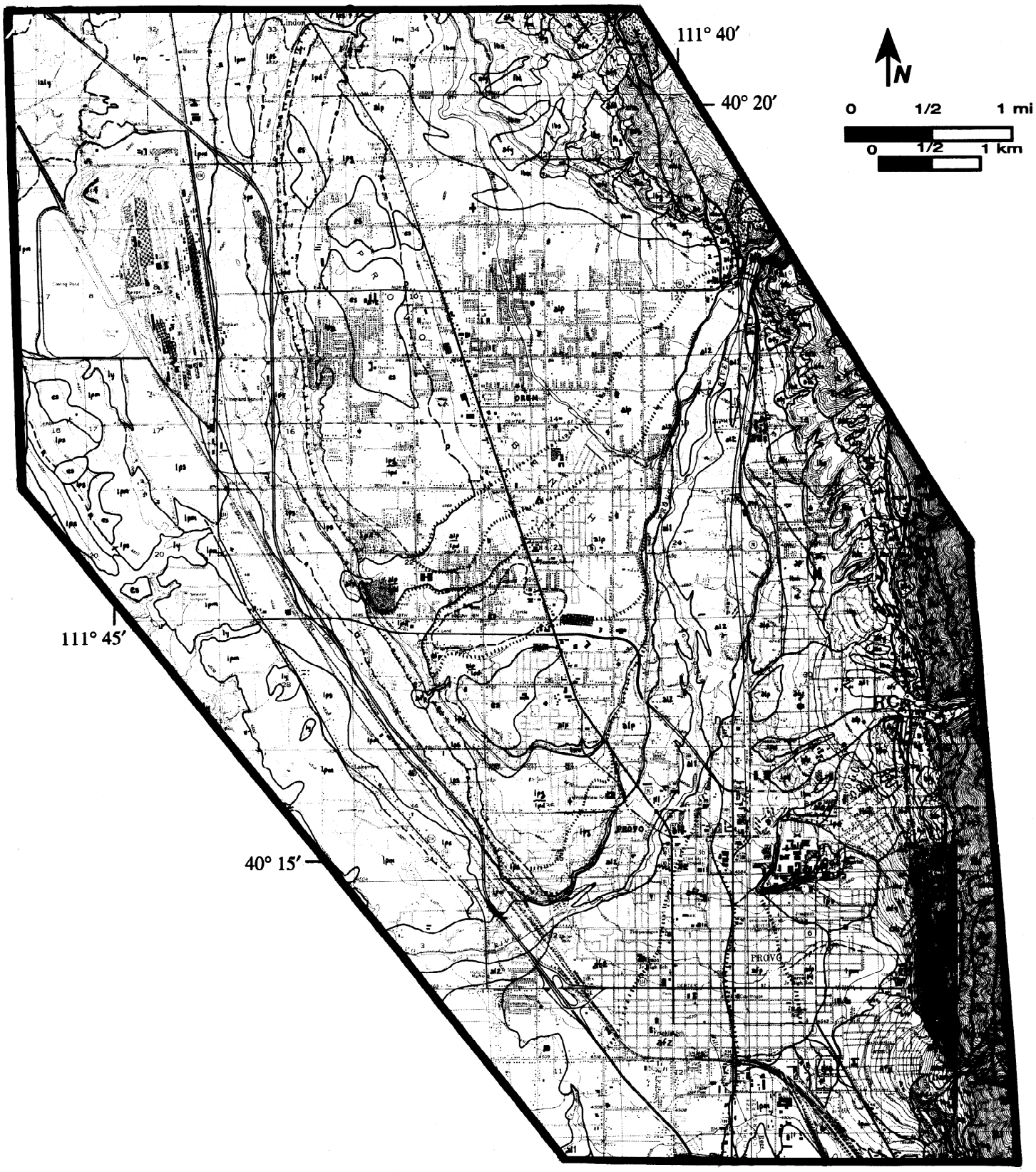


*Figure 3. Surficial geologic map of the east Provo study area, modified from Machette (1989).*

***Figure 3** (continued)*

## CORRELATION OF MAP UNITS

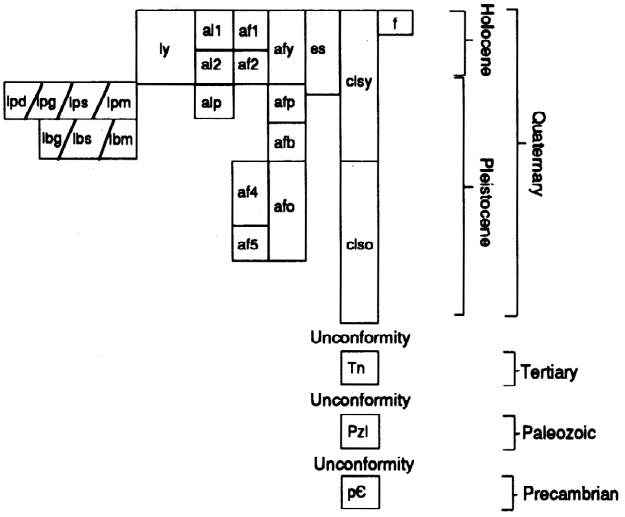


**Contact** — Dashed where approximately located

**Gradational contact** — Contact between differentiated units and undifferentiated counterparts.

12 (9) RC **Normal fault** — Bar and ball on downdropped side. Dotted where concealed. Height of fault scarp and amount of geomorphic surface offset (in parentheses) shown in meters. RC shows location of exploratory trench

**Major shorelines related to levels of the Bonneville lake cycle** — Coincide with geologic contacts in some places

- - B - - - Bonneville shoreline

- - P - - - Provo shoreline

- - p - - - Other shorelines of the regressive phase

**Topographic escarpment** — Formed primarily by fluvial processes; coincide with geologic contacts in some places; where escarpment coincides with the contact between map units, hachures face up slope

**Tilted geomorphic surface** — Arrow points in general direction of downward tilt

## DESCRIPTION OF MAP UNITS

### LACUSTRINE DEPOSITS

**Deposits Postdating the Bonneville Lake Cycle**

| | |
|---|---|
| ly | Younger lacustrine and marsh deposits |

**Regressive-Phase Deposits of Bonneville Lake Cycle**

| | |
|---|---|
| lpd | Deltaic deposits related to regressive phase |
| lpg | Lacustrine gravel related to regressive phase |
| lps | Lacustrine sand related to regressive phase |
| lpm | Lacustrine silt and clay related to regressive phase |

**Transgressive-Phase Deposits of Bonneville Lake Cycle**

| | |
|---|---|
| lbg | Lacustrine gravel related to transgressive phase |
| lbs | Lacustrine sand related to transgressive phase |
| lbm | Lacustrine silt and clay related to transgressive phase |

### ALLUVIAL DEPOSITS

**Stream Alluvium**

| | |
|---|---|
| al1 | Stream alluvium 1 |
| al2 | Stream alluvium 2 |
| alp | Stream alluvium related to regressive phase |

**Fan Alluvium**

| | |
|---|---|
| af1 | Fan alluvium 1 |
| af2 | Fan alluvium 2 |
| afy | Younger fan alluvium, undivided |
| afp | Fan alluvium related to regressive phase |
| afb | Fan alluvium related to transgressive phase |
| af4 | Fan alluvium 4 |
| af5 | Fan alluvium 5 |
| afo | Older fan alluvium, undivided |

### EOLIAN DEPOSITS

| | |
|---|---|
| es | Eolian sand and silt |

### COLLUVIAL DEPOSITS

| | |
|---|---|
| clsy | Younger landslide deposits |
| clso | Older landslide deposits |

### FILL DEPOSITS

| | |
|---|---|
| f | Manmade fill |

### BEDROCK

| | |
|---|---|
| Tn | Neogene sedimentary rocks |
| Pzl | Paleozoic sedimentary rocks, lower part |
| p€ | Proterozoic and Archean rocks |

# DATA COLLECTION AND INTERPRETATION

The hazard from indoor radon is difficult to assess due to the influence of building construction quality and techniques and occupant lifestyle; effective indoor monitoring requires testing every home. However, airborne-radiometric data exist over most of the U.S. and are useful for identifying areas with the potential for an indoor-radon hazard. Muessig (1988) compared airborne radiometrics collected for the National Uranium Resource Evaluation (NURE) with indoor radon in New Jersey, and found that areas with mean equivalent uranium (eU) concentrations greater than 2.4 ppm are associated with radon levels in homes greater than 4 pCi/L (148 Bq/m$^3$). Identification of uranium anomalies using airborne-radiometric data allows follow-up ground surveys in relatively small areas. The surveys include assessment of pertinent geologic factors and measurement of radon in homes. Acquisition of more detailed information may result in building code requirements to reduce the susceptibility of homes to radon.

## Airborne-Radiometric Measurements

### Sampling and Analytical Techniques

The airborne-radiometric survey completed under the NURE program permits delineation of areas of high surface-uranium concentrations that indicate potential for an indoor-radon hazard (Duval and Otton, 1990). Geologic units responsible for the hazard typically are widespread and may affect homes in a large area. NURE data were collected on a coarse scale, generally with 5-kilometer (3-mi) line spacings and 10-kilometer (6-mi) spacings on tie lines. The data, therefore, serve as a reconnaissance tool for regional studies, but more detailed follow-up surveys such as ground-based gamma-ray spectrometry, soil-radon emanometry, and indoor-radon measurements are required to accurately characterize the hazard. Radon hazards resulting from small point sources, such as uranium-mill tailings used for foundation soils, cannot be detected using NURE data.

NURE data (EG&G Geometrics, 1979) were compiled for the eastern Salt Lake Valley and adjacent parts of the Wasatch Range (figure 1). The airborne survey was performed using a helicopter-mounted GeoMetrics GR-800 gamma-ray spectrometer. The GR-800 system contained 37,760 cubic centimeters (2,304 in$^3$) of NaI crystals. Navigation of the helicopter was with visual techniques and 1:24,000 topographic maps, but the flight paths were also documented using a 35-mm tracking camera. The survey was flown at a terrain clearance of between 60 and 210 meters (200 and 700 ft), with an average clearance of 120 meters (400 ft). Data were collected at 1-second intervals along the flight lines. Data-reduction techniques are described in the NURE report (EG&G Geometrics, 1979).

### Data and Discussion

Corrected NURE values for eU, equivalent thorium-232 (eTh), and potassium-40 (K) were used to plot eU, eTh, and K concentration, total gamma, and eU/eTh, eU/K, and eTh/K contour maps (figures 4 through 10). The contour maps were generated by computer and have no geologic bias. The eU and total-gamma contour maps are useful for delineating areas that require ground survey follow-up. The eTh contour map is useful because $^{232}$Th decays to $^{220}$Rn and, although the half-life of this isotope is much shorter than that of $^{222}$Rn, $^{220}$Rn may be a significant contributor to the indoor-radon hazard in buildings built on Th-rich ground (Stranden, 1984). The ratio maps, commonly used in uranium exploration to define areas having the potential for ore deposits, are used here with the eU, eTh, and K contour maps to determine the nature of the source rock from which Rn-generating sediments were derived.

The average apparent uranium concentration for the Salt Lake City 1:250,000-scale quadrangle is 1.65 ppm (EG&G Geometrics, 1979). The area of interest for this study is uranium anomaly A in Sandy (figure 4). Uranium concentrations are greater than 3.2 ppm in the area where high levels of indoor radon were detected in the 1988 UDRC survey (Sprinkel and Solomon, 1990). The anomaly corresponds to locally derived Quaternary unconsolidated deposits along the front of the Wasatch Range. The high uranium values in the Wasatch Range east of anomaly A (figure 4) are located over the Little Cotton-

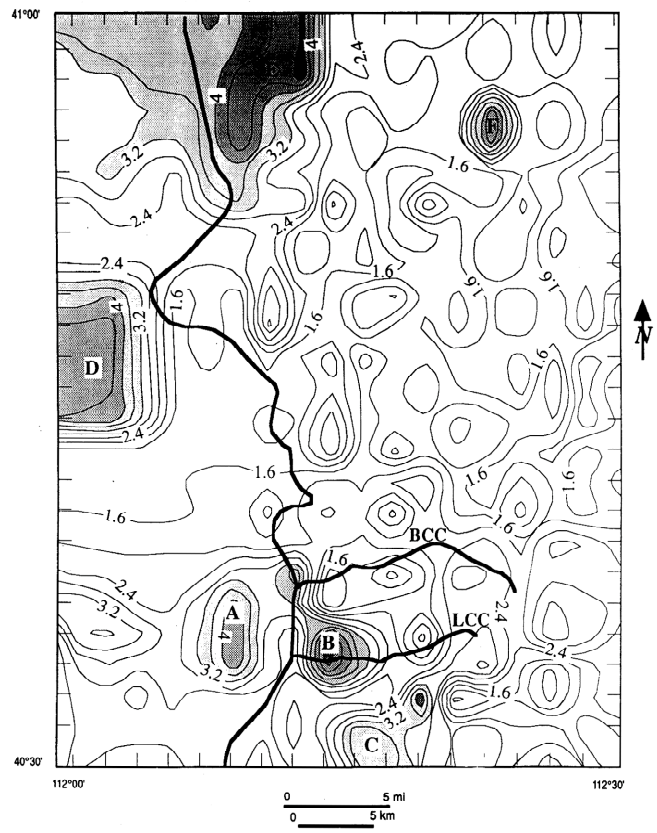


*Figure 4. Equivalent uranium concentrations from the airborne-radiometric survey. The heavy line is the range front. BCC is Big Cottonwood Canyon; LCC is Little Cottonwood Canyon. Anomalies A through F are discussed in the text. Contour interval 0.4 ppm. Anomalies with concentrations greater than 4.0 ppm have light shading between 3.2 and 4.0 ppm, moderate shading between 4.0 and 4.8 ppm, and dark shading greater than 4.8 ppm.*

wood, Alta, and Clayton Peak stocks (anomaly B). This suggests that a significant portion of anomaly A results from granitic material eroded from the stocks.

Uranium anomaly A is coincident with a broader thorium anomaly that reaches values greater than 13 ppm (figure 5), and uranium anomaly B is coincident with even higher values of thorium over the granitic stocks. Diffuse patterns of elevated potassium concentrations (figure 6) are also associated with the uranium and thorium anomalies. The data are compatible with the process of concentration of U, Th, and K in more siliceous igneous rocks during the later stages of igneous-melt differentiation (Nielson and others, 1991).

The total-gamma count represents gamma radiation in the entire 0.4 to 3.0 million electron volts (MeV) range (figure 7). The total-gamma anomalies are much broader than the eU anomalies and thus less useful than the eU data for delineating areas requiring ground surveys.

There are no eU/eTh (figure 8), eU/K (figure 9), or eTh/K anomalies (figure 10) coincident with uranium anomaly A. This is expected given the high concentrations of uranium, thorium, and potassium in the area. If the uranium resulted from non-igneous processes, it would be concentrated relative to both Th and K and the ratio maps would be more useful.

Because high indoor-radon values are associated with uranium anomaly A, other areas with similarly high eU concentrations should be field checked. Anomaly C (figure 4) has such concentrations and is also coincident with an eTh anomaly (figure 5). Anomaly C is in an uninhabited area over different parts of the granitic stocks that produced anomaly B; however, drainage is to the south toward the town of Alpine in northern Utah Valley. Thus, a potential for high eU and related indoor-radon concentrations exists in the Alpine area.

Anomaly D (figure 4), elongated to the west due to a boundary effect of the contouring program, is over Lake Bonneville clays in northern Salt Lake Valley. The eU anomaly is not coincident with an eTh anomaly as in the Sandy area. No additional verification work has been done on this anomaly.

Anomaly E is over exposures of the Precambrian Farmington Canyon Complex, a unit with an average airborne eU concentration of 3.27 ppm (EG&G Geometrics, 1979), and extends westward over gravel derived from the unit (figure 4). An eTh anomaly is coincident with uranium anomaly E but, whereas the greatest uranium concentrations are in the Farmington Canyon Complex, the greatest eTh concentrations are in the gravel (figure 5). Thorium concentrations up to 22 ppm in anomaly E are the highest seen in this study. Although the Farmington Canyon Complex principally underlies uninhabited areas in the Wasatch Range, the gravel was deposited at the base of the range and could serve as a radon source in Wasatch Front communities from Farmington to Bountiful.

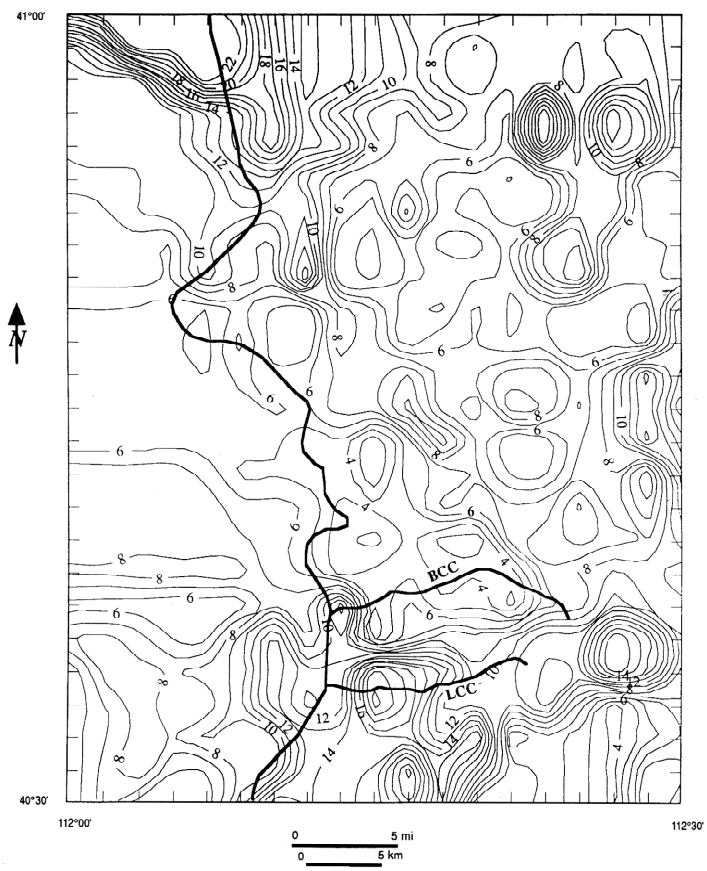


***Figure 5.*** *Equivalent thorium concentrations from the airborne-radiometric survey. See figure 4 for explanation of symbols. Contour interval 1.0 ppm.*

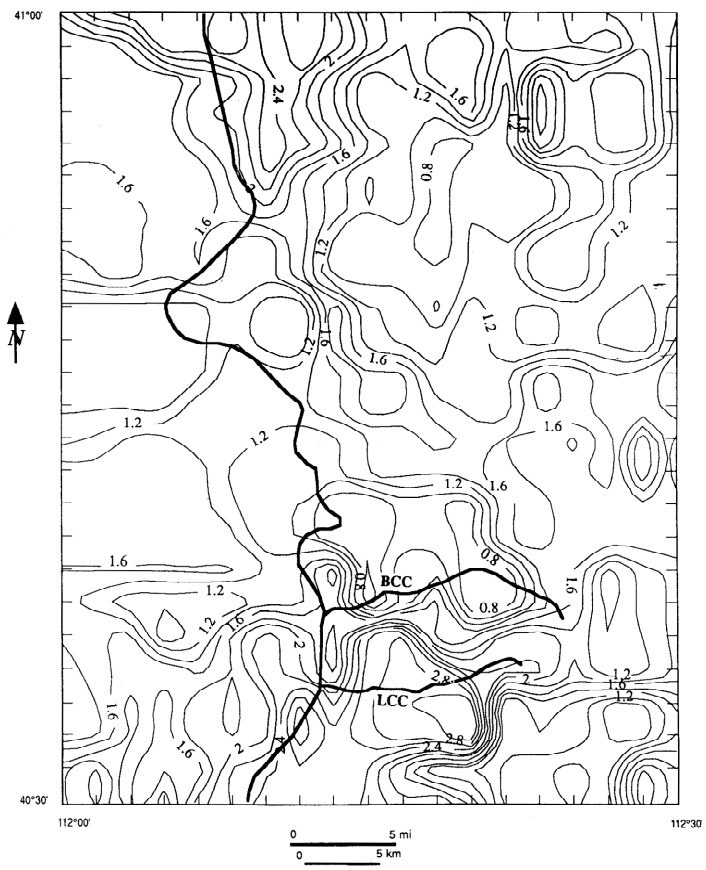


***Figure 6.*** *Potassium concentrations from the airborne-radiometric survey. See figure 4 for explanation of symbols. Contour interval 0.2 percent.*

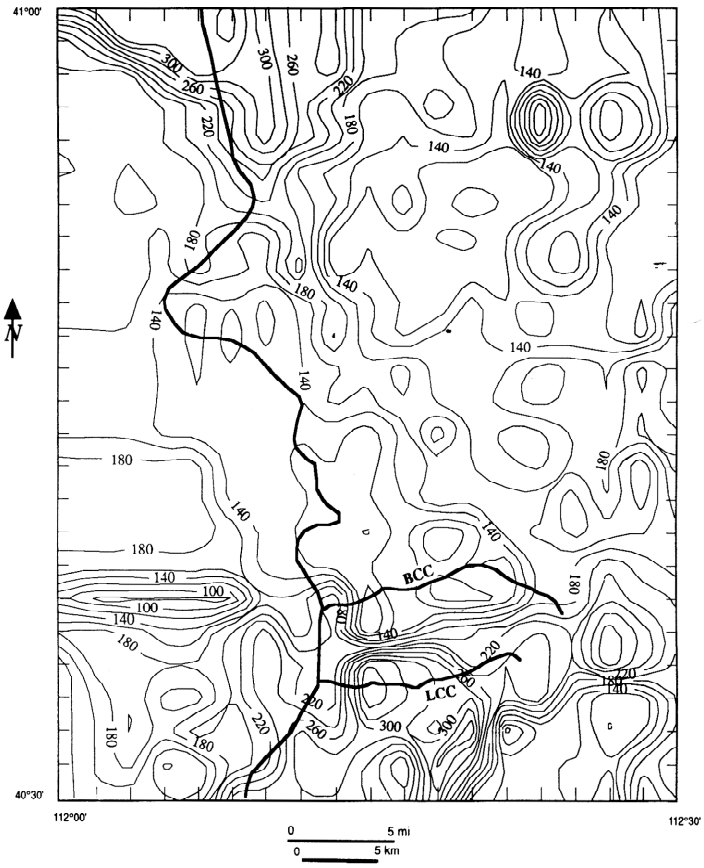


*Figure 7. Total gamma count from the airborne-radiometric survey. See figure 4 for explanation of symbols. Contour interval 20 counts per second.*

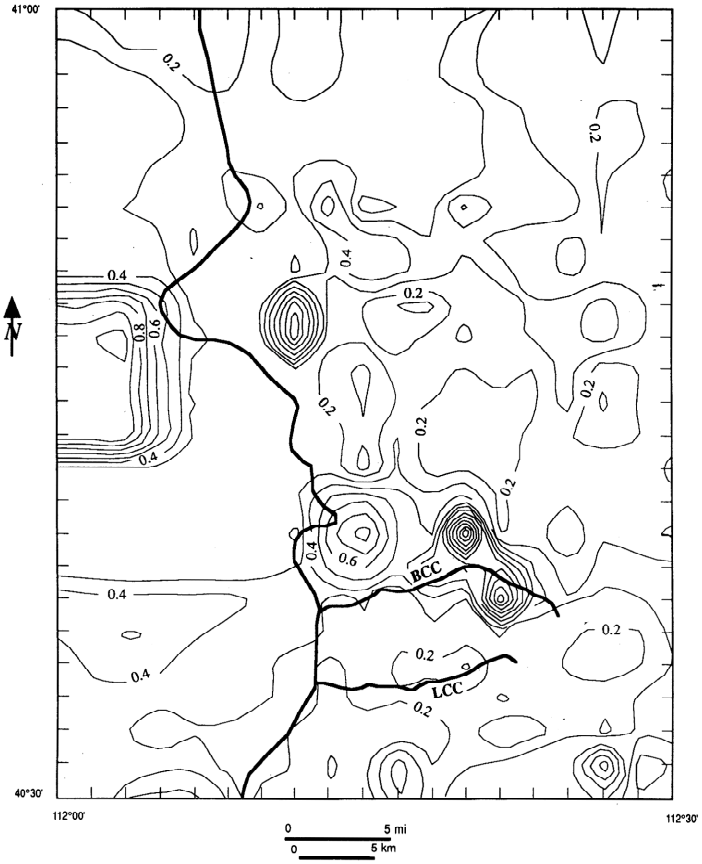


*Figure 8. eU/eTh ratios from the airborne-radiometric survey. See figure 4 for explanation of symbols. Contour interval 0.1.*

Anomaly F is over exposures of the Eocene Wasatch Formation (figure 4) and is also coincident with an eTh anomaly (figure 5). However, anomaly F is in an uninhabited area of southwestern Morgan County and poses little risk of a radon hazard.

## Ground Measurements

### Sampling and Analytical Techniques

Five types of ground data were collected during this study: (1) gamma-ray spectrometry, (2) soil-gas radon emanometry, (3) soil moisture and density, (4) soil texture, and (5) indoor-radon measurements in homes and schools. Gamma-ray spectrometry measures the amount of radioactive parent material in the soil available to decay to radon. Radon emanometry measures the level of radon in soil gas available for migration into buildings. Soil moisture, density, and texture affect the ability of radon to migrate through the soil to building foundations. Soil data were collected at 131 sites in the east Sandy area and 99 sites in the east Provo area. Indoor-radon measurements were made at 153 homes and 12 schools in the east Sandy area, and 66 homes and 4 schools in the east Provo area. These indoor measurements are from targeted surveys, and are in addition to those collected during the 1988 statewide survey (Sprinkel and Solomon, 1990). The results of 53 indoor measurements in the east Sandy area and 86 in the east Provo area from the statewide survey are included in statistical analyses in this report, and are summarized in Solomon and others (1991).

Concentrations of gamma-emitting elements in soil were measured using an Exploranium GR-256 portable, gamma-ray spectrometer with a GPS-21 detector. The detector contained a 3 x 3 inch (7.5 x 7.5 cm) NaI crystal. Values for total gamma, K, eU, and eTh were measured. Peak energy levels used for measurement were 1.46 MeV for K (K has only one emission line), 1.76 MeV for eU (corresponding to $^{214}$Bi), and 2.62 MeV for eTh (corresponding to $^{208}$Tl).

Two techniques were used to measure radon concentrations in soil gas. The first used an RDA-200 portable, alpha-sensitive scintillometer manufactured by EDA Instruments. Scintillator cells are coated with a phosphor sensitive to alpha particles (resulting from the decay of $^{222}$Rn) in the 5.5 MeV range. Individual scintillator cells were calibrated using the UNC Geotech Alpha-track Chamber in Grand Junction, Colorado. The soil-gas sampling system consisted of a 0.4-inch (1-cm) diameter, hollow steel probe that was placed in a hole made by pounding into the soil a rod of slightly smaller diameter than the probe. The probe was inserted to a depth of 26 inches (65

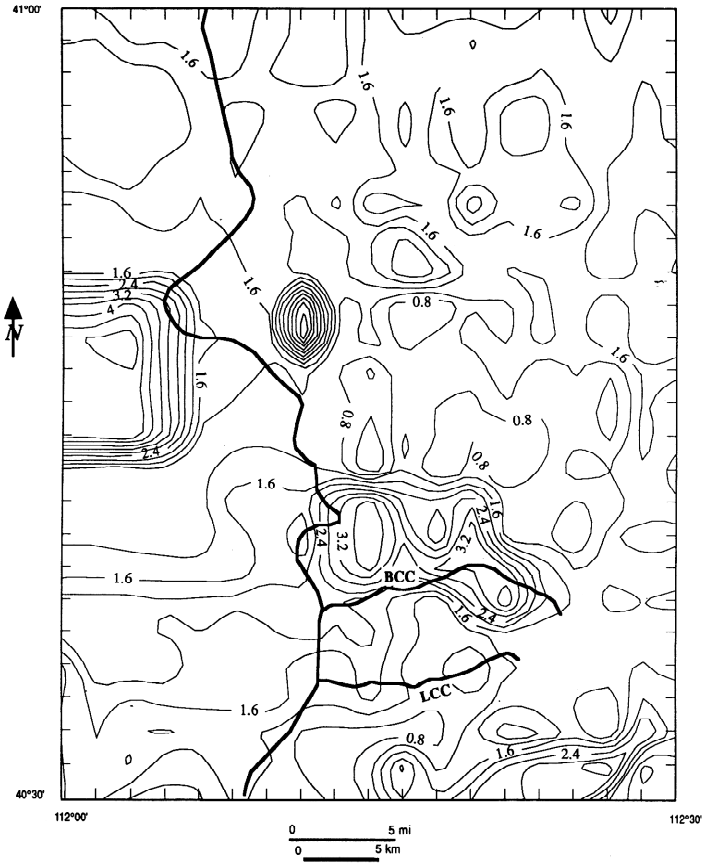


***Figure 9.*** *eU/K ratios from the airborne-radiometric survey. See figure 4 for explanation of symbols. Contour interval 0.4.*

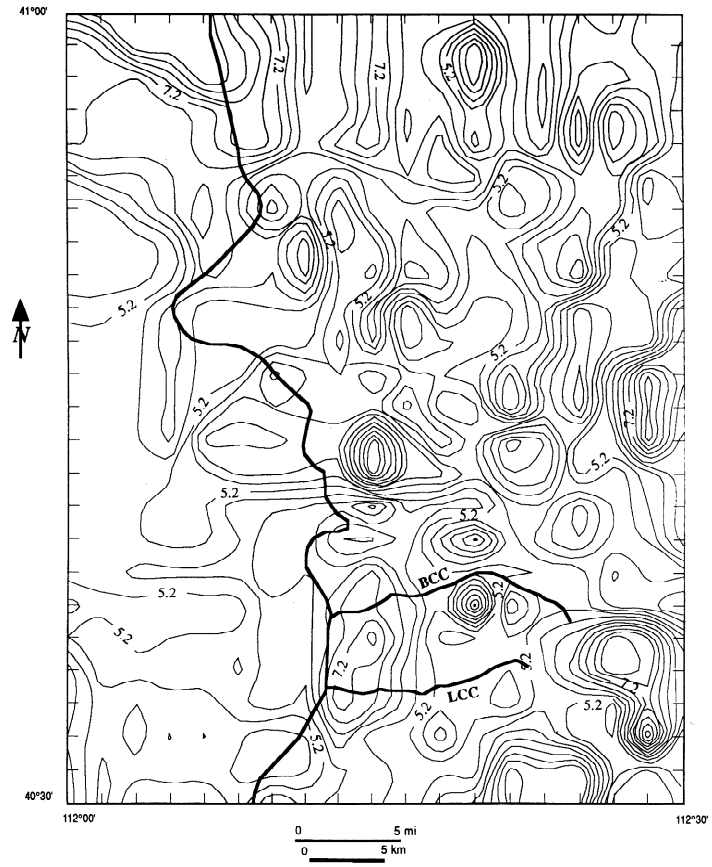


***Figure 10.*** *eTh/K ratios from the airborne-radiometric survey. See figure 4 for explanation of symbols. Contour interval 0.4.*

cm), and samples were collected from perforations in the lower 6 inches (15 cm) of the probe. This depth allowed sample collection below the root zone for grasses, is within the lower B or upper C horizons of most soils, and is about the same as sampling depths which provided consistent and reproducible data to other researchers (Hesselbom, 1985; Reimer and Gundersen, 1989).

Initial scintillometer soil-gas measurements in the east Sandy area identified a pattern of high concentrations up to 2,398 pCi/L (8.87 x $10^4$ Bq/$m^3$). This pattern was confirmed with a second technique using alpha-track detectors (ATDs) manufactured by Alpha Spectra, Inc. ATDs integrate the flux of radon gas over time, and thus average out short-term fluctuations produced by atmospheric variables. The Alpha Spectra units are designed for indoor use and quickly become saturated at higher exposure levels typically found in soil gas. They were therefore left in the ground for only 2 to 3 days. Several ATD surveys were made to evaluate the reproducibility of results, which were standardized for variations in atmospheric conditions during repetitive measurements at several sites.

The flux of radon from soil to the atmosphere can be defined by a diffusion model that depends on depth of source material (Tanner, 1964; Schery and others, 1984). Therefore, the depth at which the measurement is taken is important and, under ideal conditions, all soil-gas samples would be collected at the same depth. However, in the Sandy area, extremely variable soil conditions prohibited maintaining a constant sampling depth and measured values of soil-gas radon must be corrected for depth below the surface. Witcher and Schoenmackers (1990) have derived a relationship for correcting the measured radon concentration to the concentration at an infinite depth. This relationship is given by:

$$C_D = C_Z/(1-\exp[-(Øy_m/D)^{1/2}Z])$$

where:

$C_D$ is the depth-corrected value

$C_Z$ is the concentration at depth Z

$y_m$ is the radon-decay constant (2.1 x $10^{-6}$)

Ø is porosity (0.35)

D is the bulk diffusion coefficient (0.01 $cm^2$/s [1.6 x $10^{-3}$ $in^2$/s]).

ATD data for the Sandy area were corrected using the above equation and constants.

Laboratory measurement of radon from soil samples was also made to determine radon provenance. About 100 grams (3.5 oz) of soil were collected from some sites tested in the field with ATDs. The samples were placed in jars, with an ATD taped to the inside of the lid when the jars were sealed. The ATDs were exposed for a little more than a month.

Wet density, dry density, and moisture content of soils were determined *in situ* using a Campbell Pacific Nuclear 501DR portable probe. The probe contains a gamma source and a gamma-measuring detector for density measurements, and a

fast neutron source and thermal neutron detector for moisture measurements.

Soil texture was estimated for sites where soil-gas samples were collected. Where possible, estimates were based on soil from the depth of gas-sample collection. The soil texture was classified into one of twelve categories used by the U.S. Soil Conservation Service (1975). Classification is based on the less than 2-millimeter (0.08-in) fraction, and is modified by estimates of the volume percent of gravel.

Indoor-radon levels for both the statewide and targeted surveys were measured with ATDs placed in the lowest occupied living space of single-family, owner-occupied homes, as well as in basement rooms of selected schools, or ground-floor rooms of schools without basements. Nineteen detectors were allotted for each school, however some detectors were lost or damaged during the monitoring period. School testing was conducted during the 1990/91 school year in accordance with EPA guidance, which suggests normal school-room occupancy and normal operating procedures for central heating, ventilation, and air conditioning systems during the measurement period (U.S. Environmental Protection Agency, 1989). Duplicate detectors were used to analyze the precision of school measurements, and field blanks (control detectors) were used to determine the extent of exposure to extraneous radiation sources.

## Data and Discussion

Uranium levels from the ground-spectrometer survey are significantly higher in the east Sandy area (5.6 ppm) (table 1) than in the east Provo area (2.6 ppm) (table 2). The distribution of uranium in the two areas, however, is not uniform. In east Sandy, the highest average uranium levels are in upper Pleistocene deltaic deposits of the Provo (regressive) shoreline of the Bonneville lake cycle (7.1 ppm). Uranium levels in upper Pleistocene gravelly alluvium of terraces graded to the Provo shoreline are bimodally distributed; lower levels (4.1 ppm) occur west of the mouth of Big Cottonwood Canyon, whereas higher levels (6.9 ppm) are present elsewhere. In east Provo, the highest average uranium levels are in upper Pleistocene lacustrine gravel of the Bonneville (transgressive) shoreline (3.1 ppm). The distribution of total gamma, eTh, and K parallels that of eU in east Sandy and is consistent with a siliceous igneous rock source (Nielson and others, 1991) (tables 3 and A-3). In east Provo, eU is more concentrated relative to both eTh and K in areas of high eU anomalies, indicating a significant contribution from non-igneous sources (tables 4 and A-4).

Average levels of radon in soil gas from the scintillometer survey are also higher in east Sandy (528 pCi/L [1.95 x $10^4$ Bq/m$^3$]) (table 1) than in east Provo (449 pCi/L [1.66 x $10^4$ Bq/m$^3$]) (table 2). In east Sandy, the highest average levels of radon in soil gas are in the upper Pleistocene terrace deposits noted above (641 pCi/L [2.37 x $10^4$ Bq/m$^3$]). Average levels are lower in the Bonneville shoreline lacustrine gravel (565 pCi/L [2.09 x $10^4$ Bq/m$^3$]), but levels are lowest where the gravel occurs west of the mouth of Big Cottonwood Canyon (296 pCi/L [1.10 x $10^4$ Bq/m$^3$]) compared to similar deposits elsewhere in east Sandy (654 pCi/L [2.42 x $10^4$ Bq/m$^3$]). In east Provo, the highest levels of radon in soil gas are in middle Holocene to upper Pleistocene alluvial fans (679 pCi/L [2.51 x $10^4$ Bq/m$^3$]).

Soil-gas radon measurements from both the east Sandy and east Provo areas are lognormally distributed with many samples of a relatively low concentration, but a few samples with high concentrations (figure 11). This is expected when trace elements, such as radon, are randomly distributed in a homogenous material (Rogers, 1964). Therefore, unconsolidated material in the study areas can be considered homogenous, although inhomogeneities are evident when the material is subdivided into geologic units. However, the correlation between soil-gas radon and surface-uranium concentrations measured at the same sites, although statistically significant, shows considerable scatter (figure 12). The regression line shown in figure 12 was forced to zero and was determined for a sample size of 113. At the 99 percent confidence level, the correlation coefficient of 0.574 exceeds the threshold value of 0.241. The correlation is improved by not forcing the regression to zero, but this is not realistic because there should be essentially no decay product (Rn) if uranium is absent. Additional soil-gas radon concentrations were measured with ATDs to validate the scintillometer readings. The area selected for validation included both the highest soil-gas (figure 13) and indoor-radon concentrations

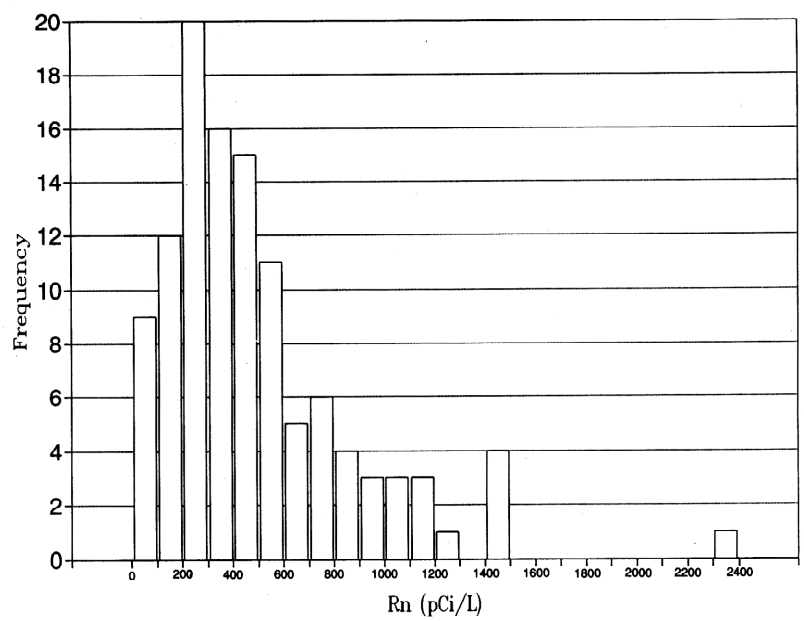


*Figure 11. Histogram of soil-gas radon concentrations from the ground-scintillometer surveys in both the east Sandy and east Provo areas. The distribution of concentrations is log-normal, as expected.*

***Table 3.***

***Statistical summary of additional ground-radiometric data in the east Sandy area. Geologic units were mapped by Personius and Scott (1990, 1992) (figure 2), but units ca, alp, and lbg have been subdivided where they occur on the Big Cottonwood and Little Cottonwood deltas. N is the number of sample sites.***

| Geologic Unit | N | Total Counts | | K | | eTh | | eU/eTh | |
|---|---|---|---|---|---|---|---|---|---|
| | | Avg. ppm | Max. ppm | Avg. % | Max. % | Avg. ppm | Max. ppm | Avg. | Max. |
| Lacustrine Deposits | | | | | | | | | |
| Deposits postdating the Bonneville lake cycle | | | | | | | | | |
| Lacustrine, marsh, and alluvial deposits (laly) | 2 | 12.6 | 13.3 | 1.6 | 1.8 | 9.9 | 10.5 | 0.32 | 0.36 |
| Regressive-phase deposits of Bonneville lake cycle | | | | | | | | | |
| Deltaic deposits (lpd) | 7 | 22.9 | 28.3 | 2.4 | 3.2 | 12.5 | 15.0 | 0.57 | 0.76 |
| Lacustrine gravel (lpg) | 33 | 19.5 | 27.4 | 2.4 | 3.8 | 12.2 | 17.5 | 0.40 | 0.79 |
| Transgressive-phase deposits of Bonneville lake cycle | | | | | | | | | |
| Lacustrine gravel (lbg) | 17 | 18.8 | 24.2 | 2.3 | 2.9 | 12.9 | 16.9 | 0.39 | 0.73 |
| Big Cottonwood | 2 | 20.9 | 24.2 | 2.1 | 2.5 | 11.4 | 12.0 | 0.62 | 0.72 |
| Little Cottonwood | 15 | 18.5 | 23.4 | 2.3 | 2.9 | 13.1 | 16.9 | 0.36 | 0.73 |
| Undivided deposits of Bonneville lake cycle | | | | | | | | | |
| Lacustrine clay and silt (lbpm) | 2 | 17.2 | 19.3 | 2.1 | 2.1 | 12.6 | 14.0 | 0.31 | 0.46 |
| Alluvial Deposits | | | | | | | | | |
| Stream alluvium | | | | | | | | | |
| Unit 1 (al1) | 6 | 23.1 | 25.5 | 2.6 | 3.1 | 15.0 | 19.0 | 0.49 | 0.75 |
| Unit 2 (al2) | 1 | 15.4 | 15.4 | 1.7 | 1.7 | 11.6 | 11.6 | 0.32 | 0.32 |
| Regressive-phase alluvium (alp) | 34 | 22.6 | 28.0 | 2.5 | 3.2 | 13.9 | 18.8 | 0.49 | 0.90 |
| Big Cottonwood | 2 | 14.5 | 16.7 | 1.6 | 1.6 | 10.6 | 11.2 | 0.38 | 0.49 |
| Little Cottonwood | 32 | 23.1 | 28.0 | 2.6 | 3.2 | 14.1 | 18.8 | 0.50 | 0.90 |
| Fan alluvium | | | | | | | | | |
| Unit 1 (af1) | 1 | 19.0 | 19.0 | 2.6 | 2.6 | 14.3 | 14.3 | 0.29 | 0.29 |
| Unit 2 (af2) | 6 | 18.9 | 27.3 | 2.4 | 3.4 | 15.6 | 20.6 | 0.27 | 0.42 |
| Glacial Deposits | | | | | | | | | |
| Outwash of Bells Canyon age (gbco) | 2 | 24.9 | 25.6 | 2.7 | 2.9 | 15.3 | 16.8 | 0.47 | 0.54 |
| Till of Bells Canyon age (gbct) | 2 | 23.1 | 25.5 | 2.9 | 3.3 | 15.9 | 17.0 | 0.36 | 0.37 |
| Eolian Deposits | | | | | | | | | |
| Sand (es) | 8 | 20.5 | 26.2 | 2.5 | 2.9 | 12.2 | 16.2 | 0.43 | 0.64 |
| Colluvial Deposits | | | | | | | | | |
| Debris-flow deposits 1 (cd1) | 0 | – | – | – | – | – | – | – | – |
| Hillslope colluvium (chs) | 2 | 21.5 | 23.7 | 2.9 | 3.4 | 14.9 | 17.5 | 0.39 | 0.46 |
| Colluvium and alluvium (ca) | 8 | 19.6 | 26.1 | 2.2 | 2.6 | 13.5 | 17.2 | 0.43 | 0.53 |
| Big Cottonwood | 4 | 18.3 | 26.1 | 2.0 | 2.6 | 13.4 | 17.2 | 0.40 | 0.49 |
| Little Cottonwood | 4 | 20.9 | 24.3 | 2.4 | 2.5 | 13.6 | 14.8 | 0.46 | 0.53 |
| Fill Deposits | | | | | | | | | |
| Man-made fill (f) | 0 | – | – | – | – | – | – | – | – |
| EAST SANDY TOTAL | 131 | 20.6 | 28.3 | 2.4 | 3.8 | 13.2 | 20.6 | 0.43 | 0.90 |

***Table 4.***
***Statistical summary of additional ground-radiometric data in the east Provo area. Geologic units were mapped by Machette (1989) (figure 3). N is the number of sample sites.***

| Geologic Unit | N | Total Counts | | K | | eTh | | eU/eTh | |
|---|---|---|---|---|---|---|---|---|---|
| | | Avg. ppm | Max. ppm | Avg. % | Max. % | Avg. ppm | Max. ppm | Avg. | Max. |
| Lacustrine Deposits | | | | | | | | | |
| Regressive-phase deposits of Bonneville lake cycle | | | | | | | | | |
| Deltaic deposits (lpd) | 2 | 8.3 | 9.1 | 1.1 | 1.2 | 6.5 | 6.6 | 0.32 | 0.33 |
| Lacustrine gravel (lpg) | 3 | 7.7 | 8.4 | 1.1 | 1.1 | 5.6 | 6.3 | 0.33 | 0.38 |
| Lacustrine sand (lps) | 4 | 9.2 | 10.3 | 1.1 | 1.2 | 6.5 | 7.0 | 0.36 | 0.42 |
| Lacustrine silt and clay (lpm) | 0 | – | – | – | – | – | – | – | – |
| Transgressive-phase deposits of Bonneville lake cycle | | | | | | | | | |
| Lacustrine gravel (lbg) | 2 | 10.4 | 11.0 | 1.3 | 1.3 | 8.1 | 8.4 | 0.39 | 0.49 |
| Lacustrine sand (lbs) | 9 | 10.5 | 13.9 | 1.3 | 1.6 | 8.6 | 12.2 | 0.33 | 0.52 |
| Lacustrine silt and clay (lbm) | 10 | 9.5 | 12.4 | 1.1 | 1.7 | 7.2 | 10.2 | 0.41 | 0.52 |
| Alluvial Deposits | | | | | | | | | |
| Stream alluvium | | | | | | | | | |
| Unit 1 (al1) | 2 | 9.7 | 12.7 | 1.1 | 1.4 | 6.7 | 8.1 | 0.43 | 0.49 |
| Unit 2 (al2) | 8 | 8.5 | 11.0 | 1.1 | 1.3 | 6.3 | 8.9 | 0.40 | 0.55 |
| Regressive-phase alluvium (alp) | 24 | 8.9 | 11.2 | 1.2 | 1.7 | 6.8 | 9.2 | 0.37 | 0.90 |
| Fan alluvium | | | | | | | | | |
| Unit 2 (af2) | 8 | 9.2 | 11.8 | 1.2 | 1.3 | 6.7 | 9.7 | 0.40 | 0.64 |
| Younger fan alluvium (afy) | 19 | 9.3 | 14.1 | 1.1 | 1.8 | 6.4 | 9.4 | 0.46 | 0.68 |
| Regressive-phase fan alluvium (afp) | 6 | 9.6 | 10.5 | 1.2 | 1.3 | 6.3 | 7.5 | 0.44 | 0.55 |
| Transgressive-phase fan alluvium (afb) | 0 | – | – | – | – | – | – | – | – |
| Unit 4 (af4) | 0 | – | – | – | – | – | – | – | – |
| Eolian Deposits | | | | | | | | | |
| Sand and silt (es) | 2 | 8.4 | 9.4 | 1.2 | 1.4 | 6.2 | 6.4 | 0.28 | 0.29 |
| Colluvial Deposits | | | | | | | | | |
| Older landslide deposits (clso) | 0 | – | – | – | – | – | – | – | – |
| EAST PROVO TOTAL | 99 | 9.2 | 14.1 | 1.2 | 1.8 | 6.8 | 12.2 | 0.39 | 0.90 |

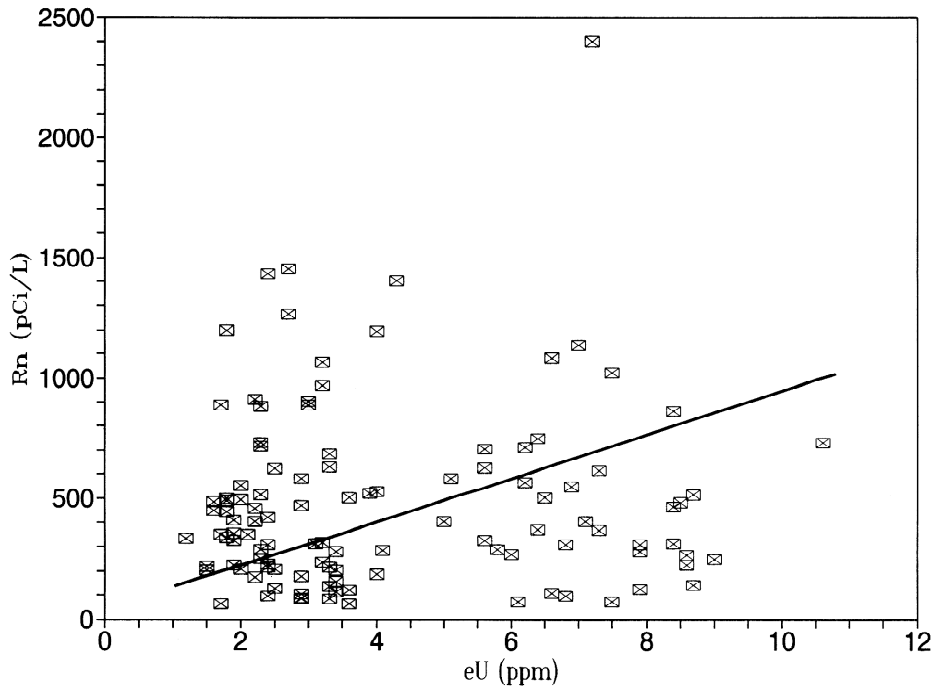


***Figure 12.*** *Scatter plot and linear regression, with regression line forced to zero, of uranium from the ground-spectrometer survey and soil-gas radon from the ground-scintillometer survey. The regression line was determined for a sample size of 113. At the 99 percent confidence level, the correlation coefficient of 0.574 exceeds the threshold value of 0.241.*

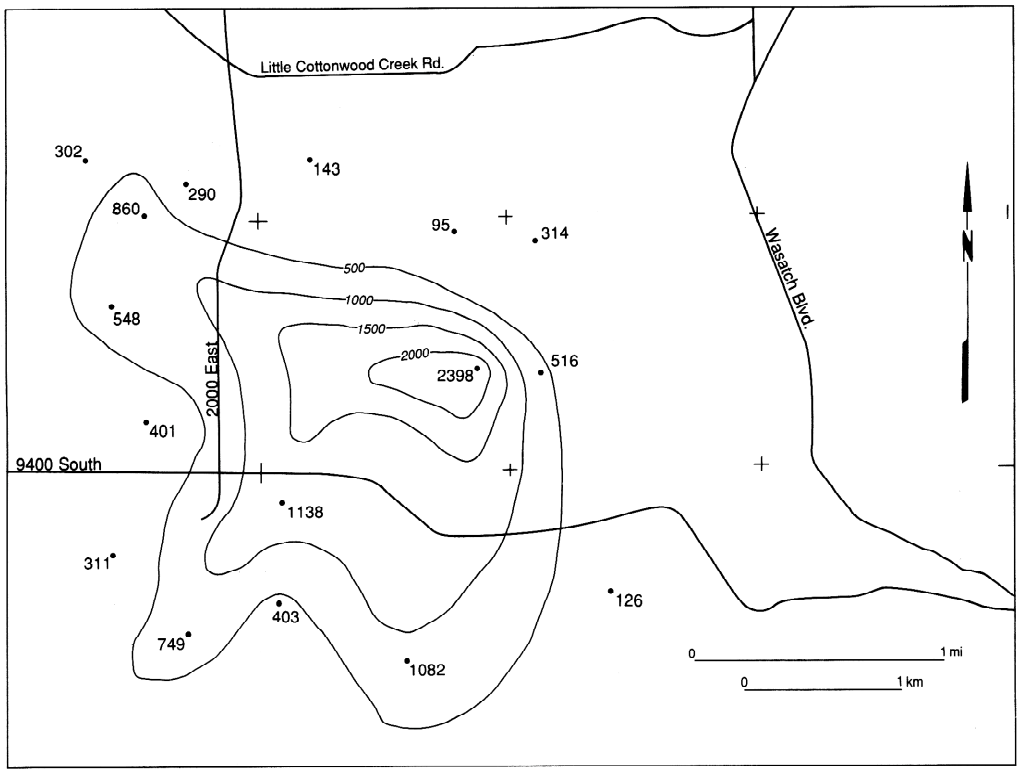


***Figure 13.*** *Contour map of anomalous concentrations of radon in soil gas, east Sandy "hot spot," from the ground-scintillometer survey. Contour interval 500 pCi/L (1.85 x $10^4$ Bq/$m^3$).*

(figure 14) in the east Sandy area. This east Sandy "hot spot," an area of over 4 square miles (10 $km^2$), has an average indoor-radon level of 9.1 pCi/l (337 $Bq/m^3$). Of 28 indoor measurements in the "hot spot," all were greater than 4 pCi/L (148 $Bq/m^3$), with a maximum measurement of 26.2 pCi/L (969 $Bq/m^3$).

ATD field measurements (table 5) were made at three different times in the Sandy area: December, 1990; late March and early April, 1991; and May, 1991. The December and March-April measurements sampled gas concentrations at the same general sites, although different holes and depths were used, to evaluate the reproducibility of results and to standardize for variations in atmospheric conditions. Atmospheric conditions, particularly precipitation and temperature, profoundly affect soil-gas radon levels. Much radon variability occurs in annual cycles because soil-moisture content, and radon partitioning between gas and water, are temperature sensitive. In central Pennsylvania, soil-gas radon concentrations to a depth of 2 meters (7 ft) varied in an annual cycle by a magnitude of ten (Washington and Rose, 1992). The results of the December and March-April surveys, depth corrected, are evaluated graphically on figure 15 using least-squares regression. The calculated correlation coefficient indicates a good linear relationship between the two data sets, although soil-gas radon concentrations are almost uniformly higher in late fall measurements than in those made in the early spring. The sample size is 9. At the 99 percent confidence level, the correlation coefficient of 0.849 exceeds the threshold value of 0.798.

Field and laboratory ATD measurements are directly related (figure 16), showing that field ATDs measure locally derived radon rather than gas that has migrated some distance from another source. The relationship is non-linear because of insufficient laboratory measurement time for the samples to reach equilibrium. However, field measurements can be used to characterize the radon-hazard potential of Quaternary geologic units.

Anomalously high values of soil-gas radon were measured in the same area during both the scintillometer (figure 13) and ATD surveys (figures 17 through 20). The details of the distribution and magnitude are different due to variations in sampling locations and atmospheric conditions during the sampling intervals. A high value of 2,398 pCi/L ($8.87 \times 10^4$ $Bq/m^3$) detected by the scintillometer survey was not confirmed by the ATD surveys, although the scintillometer sample site was not reoccupied for ATD testing because of difficulty in excavating a suitable hole in gravel for proper ATD placement. A localized concentration of radon-generating material cannot be ruled out. However, elevated soil-gas radon levels at the scintillometer site are apparently real because this sample was collected on the grounds of Quail Hollow Elementary School which, with adjacent Albion Middle School, have elevated levels of indoor radon as well (table 6 and figure 14). The anomaly is restricted to upper Pleistocene gravelly alluvium in terraces graded to the Provo (regressive) shoreline, and gravel of the Bonneville (transgressive) shoreline. The radon anomaly corresponds to material near the mouth of Little Cottonwood Canyon derived from uranium-enriched granitic rocks. Radon levels are lower in material near the mouth of Big Cottonwood Canyon derived from uranium-deficient metasedimentary rocks.

Soil permeability affects the rate of soil-gas migration and can be estimated from measurements of moisture, porosity, and particle diameter (Rogers and Nielson, 1990). An attempt was made to measure moisture and density, from which porosity may be calculated, with a moisture-density gauge. However, gravelly soil commonly prevented the necessary access holes from being augered. The few moisture and density measurements made are biased toward sample sites with finer-grained soils. Soil permeability may also be estimated from the textural classification of the soil. Because soil texture did not significantly change between geologic units, permeability estimates of the various units within each area were not attempted. However, soils from east Sandy are generally gravelly sands and are more permeable than the abundant gravelly muddy sands of the east Provo area.

Pore water traps radon and inhibits its migration in soil gas. Conversely, unsaturated porosity facilitates diffusion of radon to the atmosphere. This phenomenon is evident in east Sandy. Most Quaternary units near Big Cottonwood Canyon have lower uranium concentrations than similar units near Little Cottonwood Canyon. However, a few poorly drained (wet) Quaternary units near Big Cottonwood Canyon have high uranium concentrations but low levels of radon in soil gas (see units lpd, al1, and ca on figure 21). Well-drained (dry), transgressive-phase lacustrine gravel deposits (unit lbg, figure 21) near Little Cottonwood Canyon have lower uranium concentrations than their poorly drained counterparts near Big Cottonwood Canyon, but have higher soil-gas radon levels. The relationship between ground water and radon is not as clear in east Provo, possibly because uranium levels are lower and there is a smaller contrast between uranium levels of different geologic units (figure 22). The degree of pore saturation in the survey areas is estimated by tabulating the number of sample sites in each geologic unit with ground-water depths greater than 50 feet (15 m) (tables 1 and 2) (Anderson and others, 1986a, 1986b). Poorly drained geologic units have fewer sample sites with deep ground water than do well-drained units. The 50-foot (15-m) depth does not necessarily indicate a threshold that affects radon migration or diffusion.

Levels of indoor radon are affected by the geologic factors, and reflect differences in these factors between the various geologic units in the two study areas (tables 1, 2, and 6). The highest average indoor-radon levels in both areas occur in houses and schools on upper Pleistocene deposits of the Bonneville (transgressive) shoreline, and in overlying units. In east Sandy these deposits are predominantly gravel and have an average indoor-radon level of 3.5 pCi/L (130 $Bq/m^3$); homes and schools west of the mouth of Big Cottonwood Canyon have lower indoor-radon levels than homes and schools near Little Cottonwood Canyon. Deposits with the highest average indoor-radon levels in east Provo are predominantly silt and clay and average 3.7 pCi/L (137 $Bq/m^3$). In both areas, geologic units with high average indoor-radon levels are commonly characterized by relatively high levels of uranium and soil-gas radon, as well as deeper ground-water levels (tables 1 and 2). Geologic units with low average indoor-radon levels are commonly characterized by relatively low levels of uranium and soil-gas radon; however, poorly drained uraniferous units also commonly have low levels of soil-gas and indoor radon.

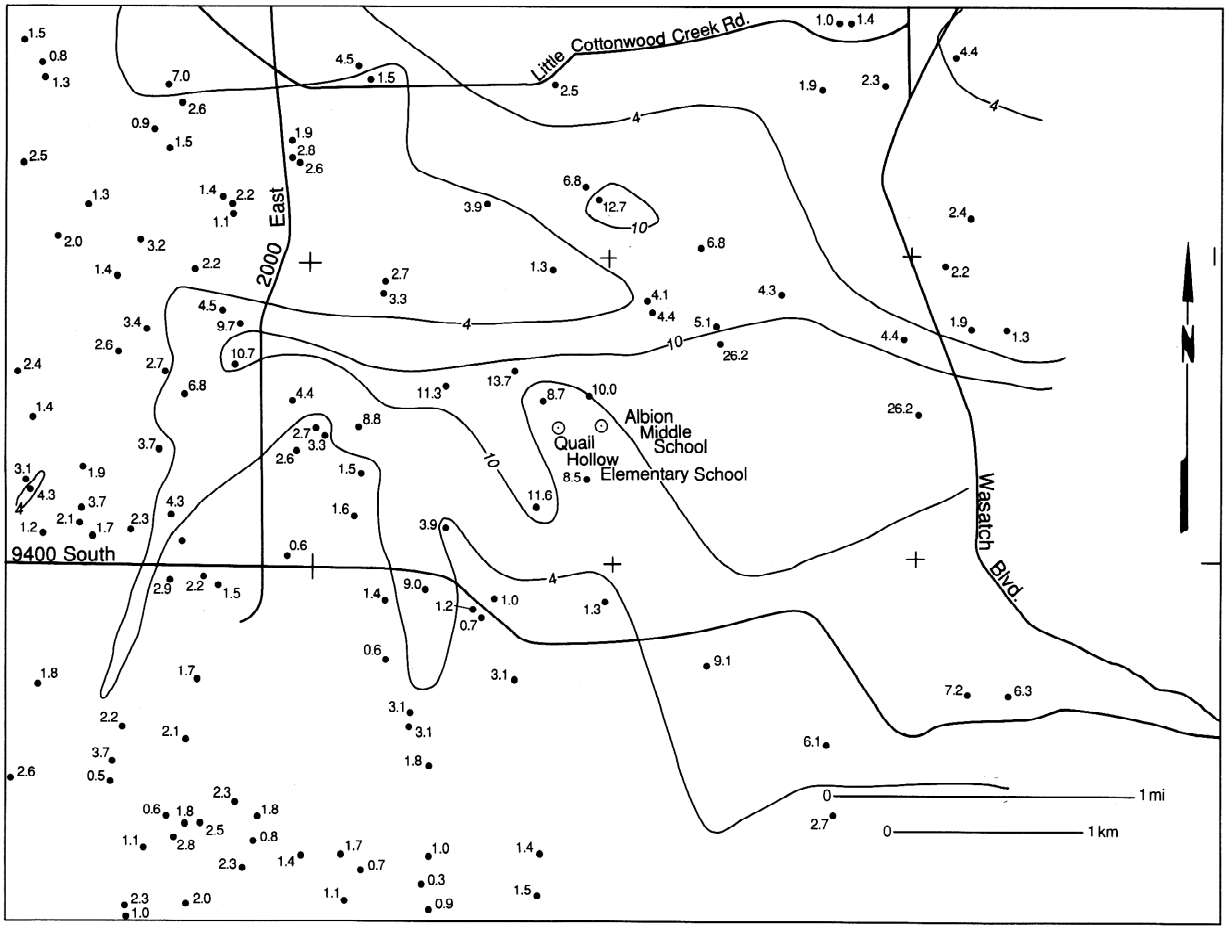


***Figure 14.*** *Contour map of indoor-radon concentrations, east Sandy "hot spot." Contours at 4 and 10 pCi/L (148 and 370 Bq/m$^3$).*

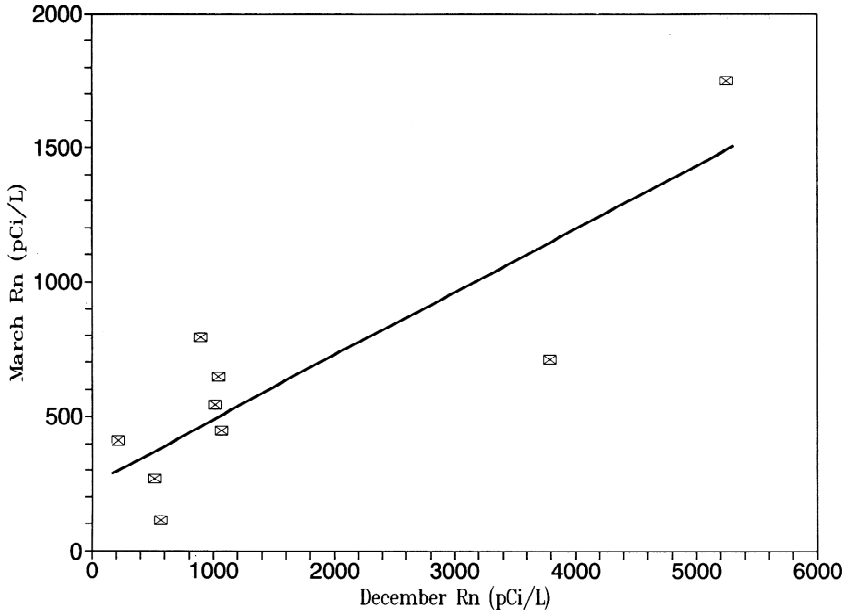


***Figure 15.*** *Linear regression of radon in soil gas, depth-corrected, measured in field with alpha-track detectors. Samples were collected at the same sites during two time intervals, and late fall values are uniformly higher than those measured in early spring. The regression line was determined for a sample size of 9. At the 99 percent confidence level, the correlation coefficient of 0.849 exceeds the threshold value of 0.798.*

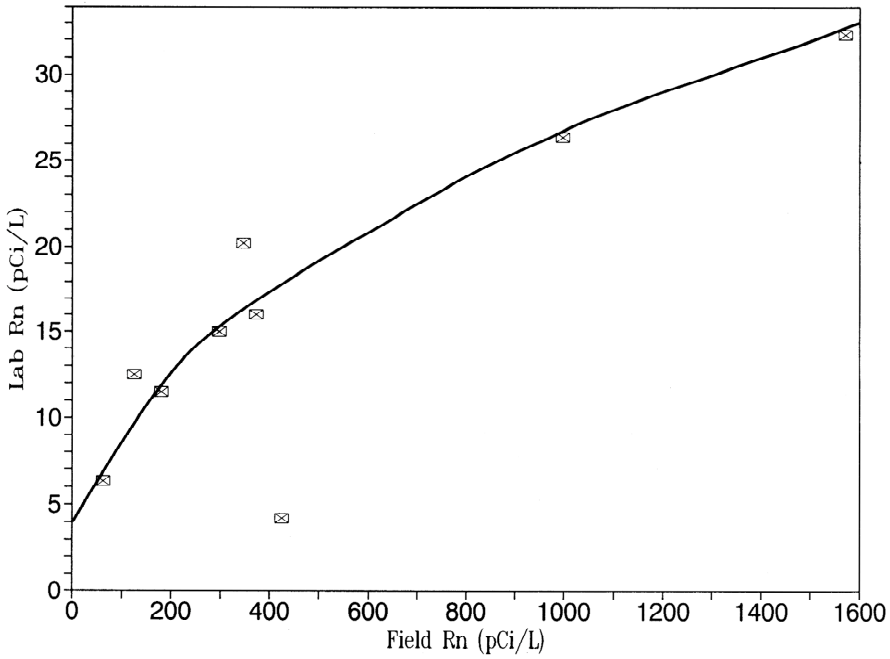


***Figure 16.*** *The relationship between field and laboratory measurements of radon in soil gas. The smooth curve suggests that field measurements of soil-gas radon represent radon that is locally derived, rather than gas that has migrated some distance from other source materials. The non-linearity results from insufficient measurement time for the laboratory samples to reach equilibrium.*

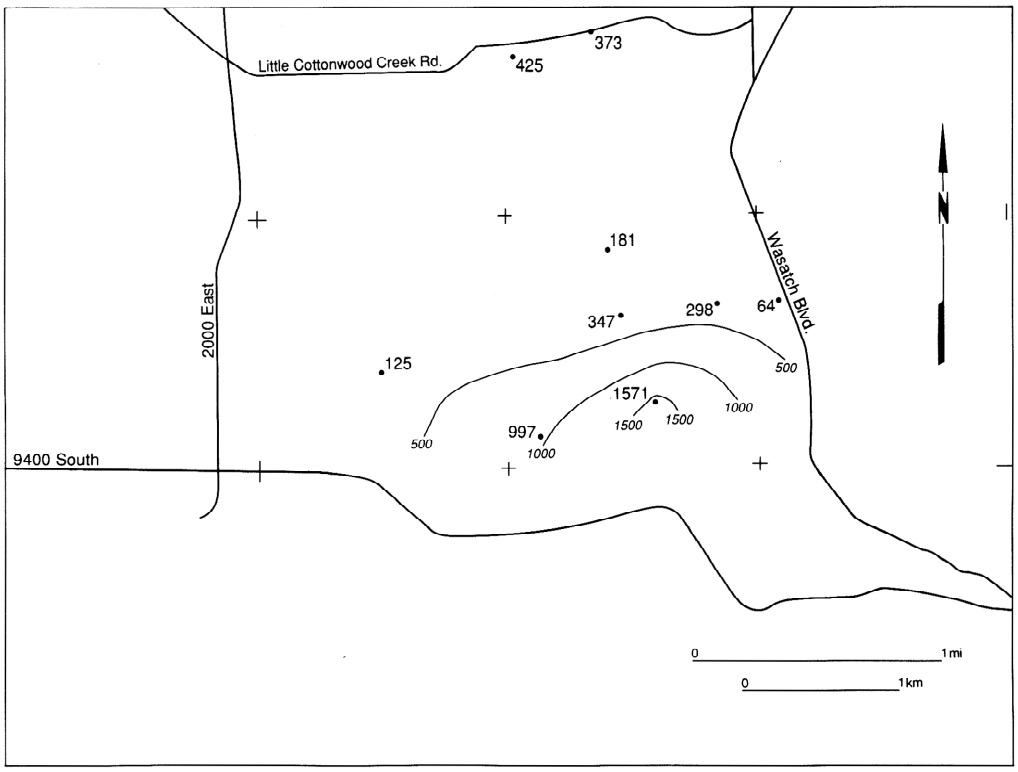


***Figure 17.*** *Contour map of soil-gas radon measured in the field with alpha-track detectors during December, 1990. Contour interval 500 pCi/L ($1.85 \times 10^4$ Bq/m$^3$).*

***Table 5.***

***Soil-gas radon measurements from ATDs, collected in situ (Field Rn) and from laboratory analysis (Lab Rn). Depth-corrected in situ measurements are also listed. In situ measurements, both depth-corrected and uncorrected, are plotted in figures 17 through 20.***

| Station | Date | Field Rn pCi/L | Lab Rn pCi/L | Depth cm | Depth-corrected concentration pCi/L | Moisture % |
|---|---|---|---|---|---|---|
| DLN-1 | 12/11-13/90 | 64.2 | 6.3 | 35.6 | 214.3 | 1 |
| | 03/18-21/91 | 144.3 | – | 43.2 | 411.4 | – |
| DLN-2 | 12/11-13/90 | 298.6 | 15.0 | 40.6 | 894.8 | 9 |
| | 03/18-21/91 | 315.8 | – | 50.8 | 792.9 | – |
| DLN-3 | 12/11-13/90 | 372.8 | 16.0 | 45.7 | 1,016.3 | 8 |
| | 03/18-21/91 | 207.8 | – | 48.3 | 542.5 | – |
| DLN-4 | 03/18-21/91 | 235.7 | – | 43.2 | 671.9 | – |
| DLN-5 | 12/11-13/90 | 424.6 | 4.2 | 50.8 | 1,066.0 | 19 |
| | 03/18-21/91 | 157.0 | – | 43.2 | 447.6 | – |
| DLN-6 | 12/11-13/90 | 347.4 | 20.2 | 40.6 | 1,041.1 | 8 |
| | 03/18-21/91 | 236.2 | – | 45.7 | 643.9 | – |
| DLN-7 | 12/11-13/90 | 180.9 | 11.5 | 38.1 | 571.0 | 3 |
| | 03/18-21/91 | 36.0 | – | 38.1 | 113.6 | – |
| DLN-8 | 12/11-13/90 | 996.8 | 26.4 | 30.5 | 3,791.9 | 3 |
| | 03/19-21/91 | 249.5 | – | 43.2 | 711.3 | – |
| DLN-9 | 12/11-13/90 | 1,571.3 | 32.3 | 35.6 | 5,245.9 | 4 |
| | 03/19-21/91 | 613.9 | – | 43.2 | 1,750.0 | – |
| | 05/05-08/91 | 135.7 | – | 35.6 | 453.0 | – |
| DLN-10 | 12/11-13/90 | 125.3 | 12.5 | 27.9 | 514.7 | 1 |
| | 03/19-21/91 | 93.2 | – | 43.2 | 265.7 | – |
| DLN-11 | 05/05-08/91 | 154.3 | – | 27.9 | 633.8 | – |
| DLN-12 | 05/05-08/91 | 123.0 | – | 27.9 | 505.2 | – |
| DLN-13 | 05/05-08/91 | 321.4 | – | 27.9 | 1,320.1 | – |
| DLN-14 | 05/05-08/91 | 104.2 | – | 27.9 | 428.0 | – |
| DLN-15 | 05/05-08/91 | 103.5 | – | 30.5 | 393.7 | – |
| DLN-16 | 05/05-08/91 | 107.9 | – | 38.1 | 340.6 | – |
| SJL-1 | 03/19-21/91 | 203.1 | – | 43.2 | 579.0 | – |
| | 03/29-04/01/91 | 272.5 | – | 40.6 | 816.6 | – |
| SJL-2 | 03/19-21/91 | 315.8 | – | 38.1 | 996.8 | – |
| SJL-3 | 03/19-21/91 | 912.9 | – | 43.2 | 2,602.4 | – |
| SJL-4 | 03/29-04/01/91 | 540.6 | – | 40.6 | 1,620.1 | – |
| SJL-5 | 03/29-04/01/91 | 402.4 | – | 45.7 | 1,097.0 | – |
| SJL-6 | 03/29-04/01/91 | 432.1 | – | 45.7 | 1,178.0 | – |
| SJL-7 | 03/29-04/01/91 | 734.2 | – | 45.7 | 2,001.5 | – |
| SJL-8 | 03/29-04/01/91 | 426.7 | – | 45.7 | 1,163.2 | – |
| SJL-9 | 03/29-04/01/91 | 418.2 | – | 43.2 | 1,192.2 | – |
| SJL-10 | 03/29-04/01/91 | 703.6 | – | 43.2 | 2,005.8 | – |
| SJL-11 | 03/29-04/01/91 | 331.4 | – | 45.7 | 903.4 | – |
| SJL-12 | 03/29-04/01/91 | 690.4 | – | 45.7 | 1,882.1 | – |
| SJL-13 | 03/29-04/01/91 | 251.1 | – | 38.1 | 792.6 | – |
| SJL-14 | 03/29-04/01/91 | 244.3 | – | 43.2 | 696.4 | – |
| SJL-15 | 03/29-04/01/91 | 452.1 | – | 38.1 | 1,427.0 | – |

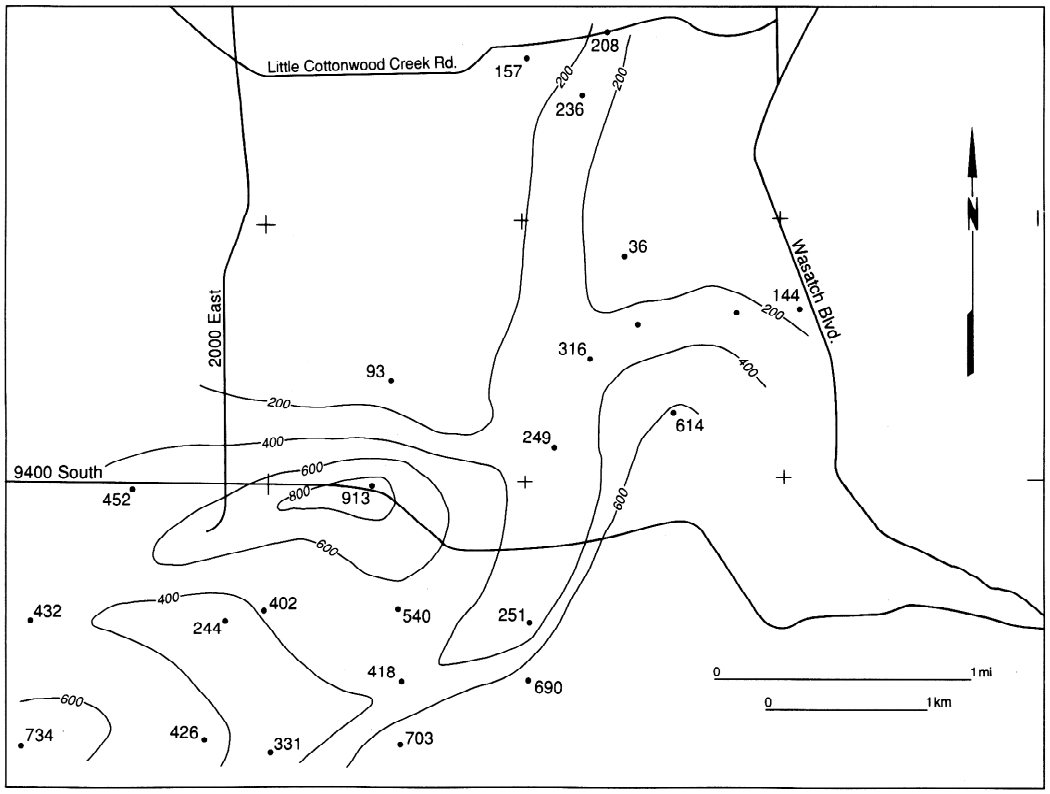


*Figure 18. Contour map of soil-gas radon measured in the field with alpha-track detectors during March and April, 1991. Contour interval 200 pCi/L (7.4 x $10^3$ Bq/$m^3$). Radon levels are generally lower than in December, 1990 (figure 17).*

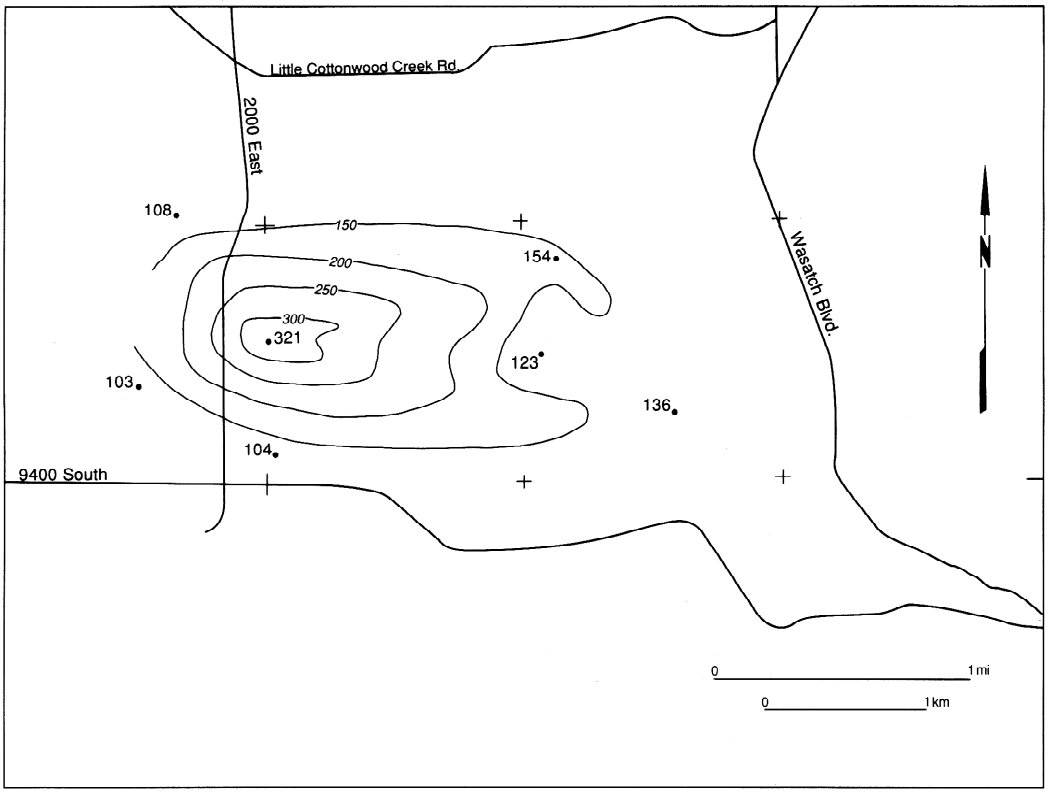


*Figure 19. Contour map of soil-gas radon measured in the field with alpha-track detectors during May, 1991. Contour interval 50 pCi/L (1.85 x $10^3$ Bq/$m^3$). Radon levels have continued their decline beyond March and April measurements (figure 18).*

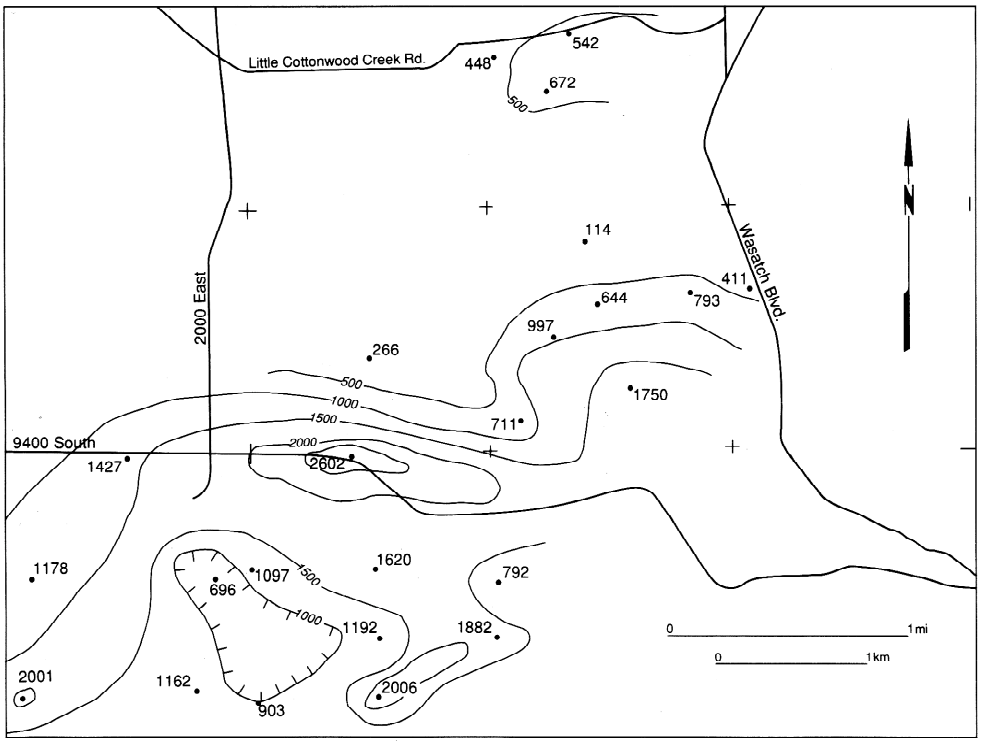


***Figure 20.*** *Contour map of depth-corrected soil-gas radon measured in the field with alpha-track detectors during March and April, 1991. Contour interval 500 pCi/L (1.85 x $10^4$ Bq/$m^3$).*

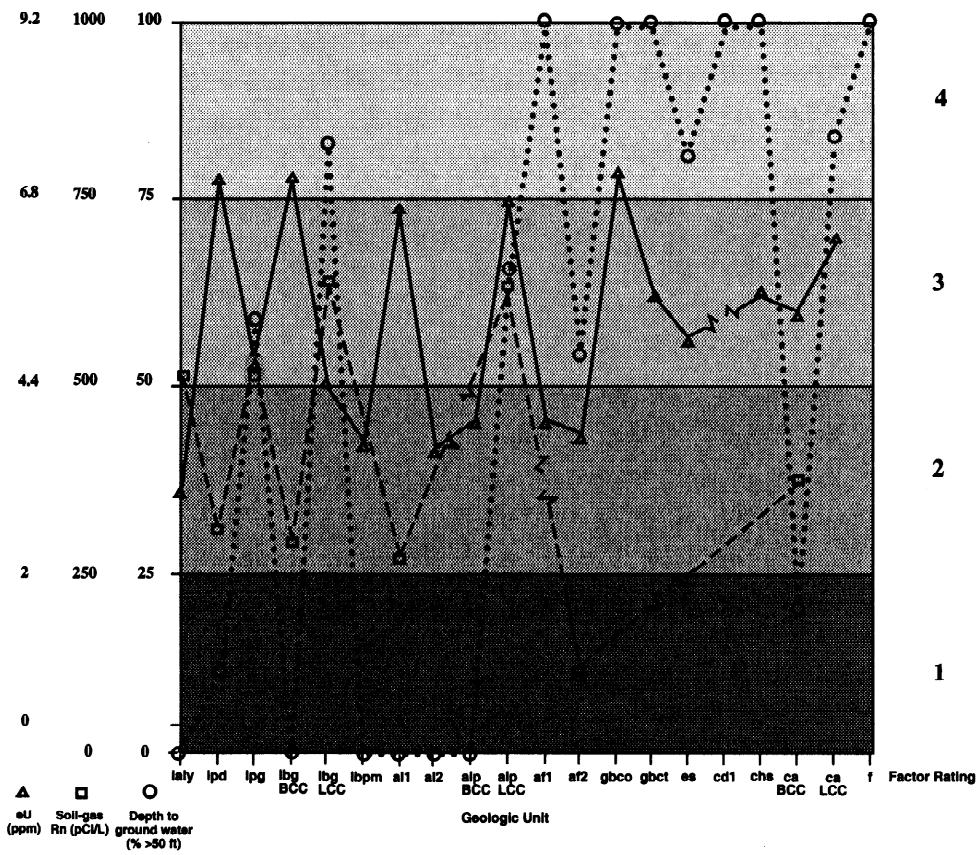


***Figure 21.*** *Average levels of hazard-rating factors in Quaternary geologic units of the east Sandy area. These are the factors used to compile the potential-radon-hazard ratings in table 1; factor ratings are shown at right. The lines which connect the symbols are for clarity and do not imply a spatial relationship between the units. See table 1 for explanation of geologic units.*

***Table 6.***

*Summary of indoor-radon measurements in selected schools, Jordan School District (east Sandy study area) and Provo School District (east Provo study area). Quail Hollow and Albion Schools have rooms with elevated indoor-radon levels, and are located in the east Sandy "hot spot" (figure 14), a high-hazard area (figure 25). Canyon Crest Elementary School also has rooms with elevated indoor-radon levels, and is in a moderate-hazard area of east Provo (figure 26). N is the number of measurements that fall within specified ranges, and does not include the results of duplicate or control detectors.*

| Location | <4 pCi/L | | 4-10 pCi/L | | >10 pCi/L | |
|---|---|---|---|---|---|---|
| | N | % | N | % | N | % |
| Albion Middle School | 5 | 29.4 | 10 | 58.8 | 2 | 11.8 |
| Brighton High School | 18 | 100.0 | 0 | 0.0 | 0 | 0.0 |
| Butler Elementary | 17 | 100.0 | 0 | 0.0 | 0 | 0.0 |
| Canyon View Elementary | 16 | 100.0 | 0 | 0.0 | 0 | 0.0 |
| Cottonwood Heights Elementary | 17 | 100.0 | 0 | 0.0 | 0 | 0.0 |
| Eastmont Middle School | 17 | 100.0 | 0 | 0.0 | 0 | 0.0 |
| Granite Elementary | 16 | 100.0 | 0 | 0.0 | 0 | 0.0 |
| Lone Peak Elementary | 17 | 100.0 | 0 | 0.0 | 0 | 0.0 |
| Mountainview Elementary | 17 | 100.0 | 0 | 0.0 | 0 | 0.0 |
| Quail Hollow Elementary | 11 | 57.9 | 8 | 42.1 | 0 | 0.0 |
| Sunrise Elementary | 17 | 100.0 | 0 | 0.0 | 0 | 0.0 |
| Willow Canyon Elementary | 16 | 100.0 | 0 | 0.0 | 0 | 0.0 |
| Jordan School District Total | 184 | 90.2 | 18 | 8.8 | 2 | 1.0 |
| Canyon Crest Elementary | 1 | 5.6 | 16 | 88.9 | 1 | 5.6 |
| Farrer Middle School | 15 | 100.0 | 0 | 0.0 | 0 | 0.0 |
| Provo High School | 13 | 100.0 | 0 | 0.0 | 0 | 0.0 |
| Sunset View Elementary | 18 | 100.0 | 0 | 0.0 | 0 | 0.0 |
| Provo School District Total | 47 | 73.4 | 16 | 25.0 | 1 | 1.6 |

***Table 7.***

*Radon hazard-potential matrix for the Wasatch Front. Each of three factors are given ratings which range from 1 (lowest potential for contributing to high indoor-radon levels) to 4 (highest potential). Ratings for the three factors are then added, and the composite rating is used to define the three relative hazard-potential categories shown in table 8.*

| Factor Rating | eU ppm | Soil Rn pCi/L | Ground-water Depth % >50 ft |
|---|---|---|---|
| 1 | <2.0 | <250.0 | <25 |
| 2 | 2.0-4.4 | 250.0-500.0 | 25-50 |
| 3 | 4.4-6.8 | 500.1-750.0 | 51-75 |
| 4 | >6.8 | >750.0 | >75 |

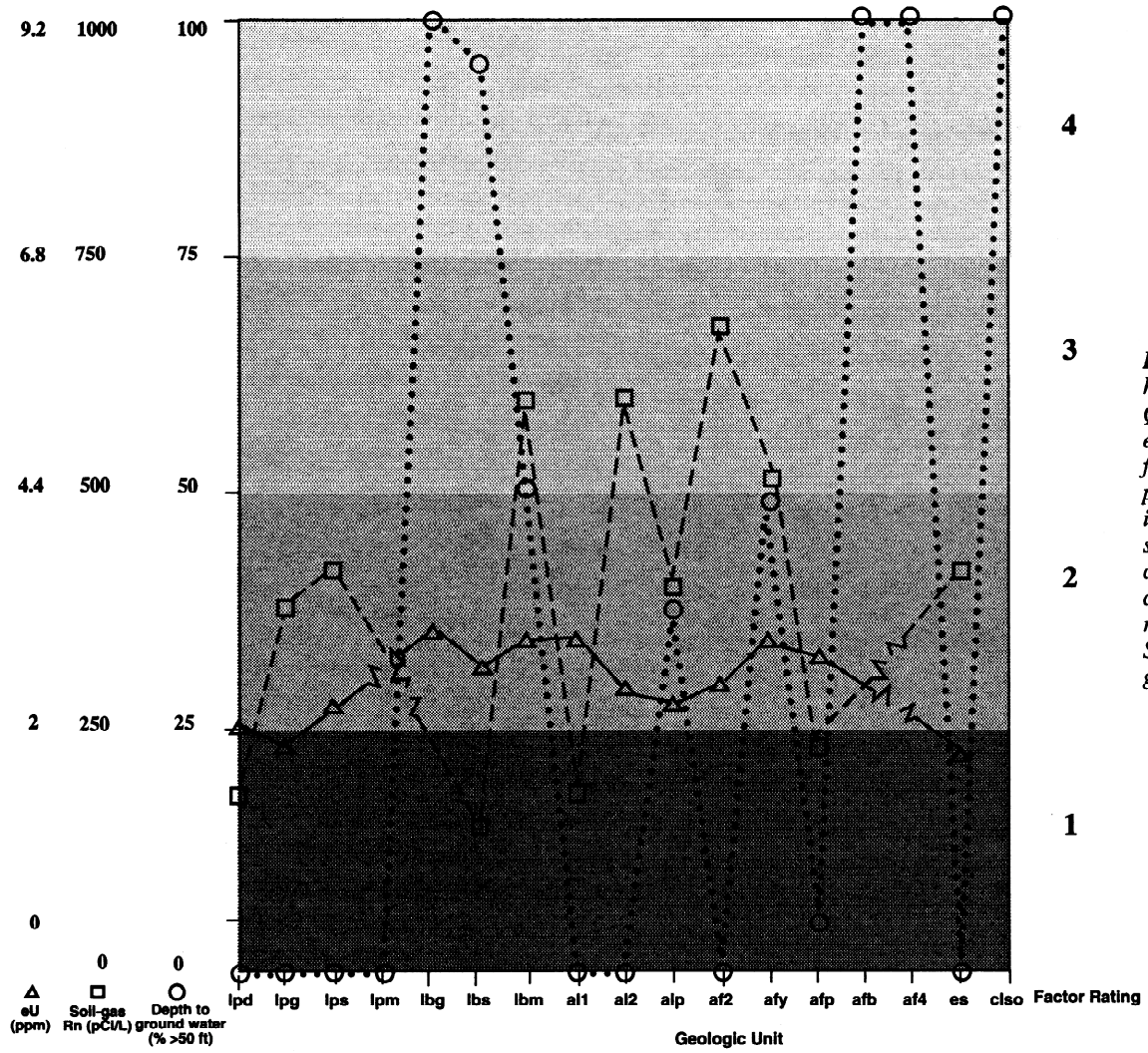


*Figure 22. Average levels of hazard-rating factors in major Quaternary geologic units of the east Provo area. These are the factors used to compile the potential-radon-hazard ratings in table 2; factor ratings are shown at right. The lines which connect the symbols are for clarity and do not imply a spatial relationship between the units. See table 2 for explanation of geologic units.*

## Potential Radon Hazard of Quaternary Geologic Units

Three factors are used in this study to estimate the relative radon-hazard potential of geologic units: (1) uranium concentration, (2) soil-gas radon concentration, and (3) ground-water level. Numerical ratings from 1 to 4 were assigned to each factor, with higher ratings corresponding to conditions favorable for elevated indoor-radon concentrations (table 7). Ratings were assigned to uranium and soil-gas radon by constructing normal probability plots (figures 23 and 24) to identify individual data populations bounded by inflection points in the slope of the data. These populations correspond to groups of related geologic units derived from similar sediment-source areas (McCammon, 1980). Ratings were assigned to ground-water by calculating the percentage of sample sites with a depth to ground water of greater than 50 feet (15 m) to identify the relative degree of saturation within geologic units. Ratings for the three factors were summed for each geologic unit and each unit was placed within one of three radon-hazard-potential categories based on the cumulative totals of the three factors (table 8; figures 21 and 22). The factors are equally weighted because there is insufficient data to independently weight them.

The radon-hazard potential of the study areas (figures 25 and 26) is revised from a preliminary version (Solomon and others, 1991) to incorporate statistical correlations between the three hazard-potential factors and additional indoor-testing results. Boundaries between areas of equal hazard potential are modified from contacts of Quaternary geologic units mapped by Machette (1989) (figure 3) and Personius and Scott (1990, 1992) (figure 2). Each geologic unit listed in tables 1 and 2 has a rating that applies to the unit wherever it occurs in each study area, except for three units which are subdivided between occurrences near Big Cottonwood Canyon and Little Cottonwood Canyon in east Sandy. Upper Pleistocene gravelly alluvium of terraces graded to the Provo (regressive) shoreline, upper Pleistocene lacustrine gravel of the Bonneville (transgressive) shoreline, and Holocene to middle Pleistocene colluvium and alluvium have a moderate hazard potential near Big Cottonwood Canyon, but a high hazard potential elsewhere in

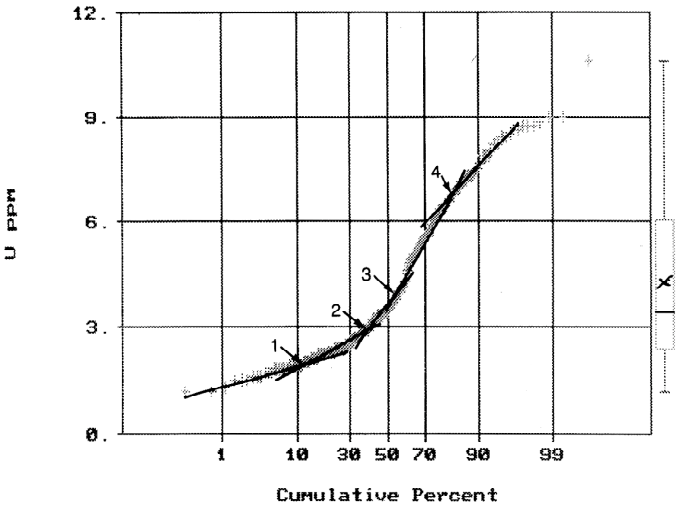


*Figure 23. Normal probability diagram of equivalent uranium concentrations. Factor ratings (table 7) are assigned to values bounded by inflection points "1", "3", and "4". Point "3" separates data sets of equal range. There is also an intermediate inflection point "2". The boxplot to the right of the diagram depicts the limits (the ends of the line which extends outward from the rectangle), quartiles (the ends of the rectangle), median (the solid line within the rectangle), and the arithmetic mean (the "X" within the rectangle) of the data set.*

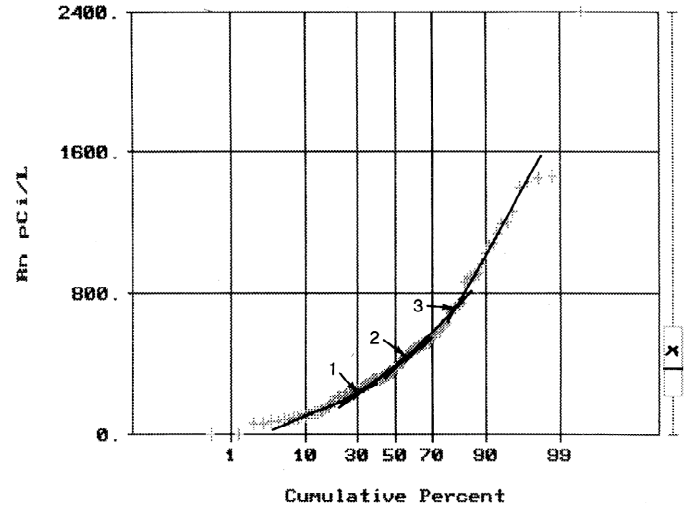


*Figure 24. Normal probability diagram of soil-gas radon concentrations measured with the scintillometer. Factor ratings (table 7) are assigned to values bounded by inflection points "1", "2", and "3", which separate data sets of equal range. The boxplot to the right of the diagram depicts statistical values defined for figure 23.*

east Sandy. Lower ratings for these units near the mouth of Big Cottonwood Canyon reflect shallower ground water, lower levels of soil-gas radon and, for the terrace deposits and colluvium and alluvium, lower levels of eU at that location. The uranium deficiency is a reflection of source rock within the canyon.

Average values of eU, soil-gas Rn, and ground-water depth in both study areas vary directly with hazard category (low, moderate, and high) (table 9) although average values of these factors for individual geologic units (tables 1 and 2) are more diverse. This is expected because hazard categories reflect the interaction of the three hazard-potential factors, and not the influence of any single factor. Average values of total gamma, K, and eTh also vary directly with hazard category (table 10), but this is coincidental and reflects geochemical variations unrelated to the radon-hazard potential. Variations in hazard potential closely parallel average indoor-radon levels for geologic units with sufficiently large indoor-radon sample sizes (see units lbg and alp near Little Cottonwood Canyon, and lpg, figure 27; and units lbs, lbm, alp, afy, and afp, figure 28), and in several units with small sample sizes. The correlation between hazard potential and indoor-radon levels is imperfect in other units because insufficient data are available. For example, most surveyed indoor-radon levels are high in houses underlain by stream alluvium (unit al2) on the northeastern margin of the east Sandy "hot spot" (figure 14), but the hazard potential of this unit is moderate because only one, relatively low measurement of uranium in soil was collected, and ground water is relatively shallow in the area. Lack of access prevented additional sampling of the unit, but further measurements may indicate either that average uranium values are higher, or that average indoor-radon levels are lower.

Although indoor-radon levels are primarily influenced by the three geologic factors considered in this study, other geologic factors not accounted for may locally influence indoor-radon levels. One such factor is permeability. If geologic materials are sufficiently permeable, soil gas can rapidly diffuse into the atmosphere rather than migrate indoors. This effect may be responsible for the discrepancy between hazard potential and average indoor-radon level for eolian sand (unit es) in east Sandy. The hazard potential of this unit is moderate, and is associated with a high level of uranium and deep ground water. However, the average indoor-radon level in 28 houses overlying this unit is only 1.7 pCi/L (62.9 Bq/m$^3$). This is the lowest average indoor-radon level of any unit in east Sandy in which more than two indoor levels were measured. Although high levels of soil-gas radon may have been generated by the eolian sand (soil-gas samples could not be collected from this unit because dry sand in access holes collapsed before the probe could be inserted), the soil-gas migrated through the more permeable sand and into the atmosphere, rather than through less permeable foundation material to the house interior.

The interaction of permeability and grain size complicates regional analysis. East Provo has a lower hazard potential than east Sandy, which is confirmed by lower average indoor-radon levels in east Provo. All three geologic factors considered in this study contribute to this difference, but the factor with the largest contrast between the two areas is the uranium content of

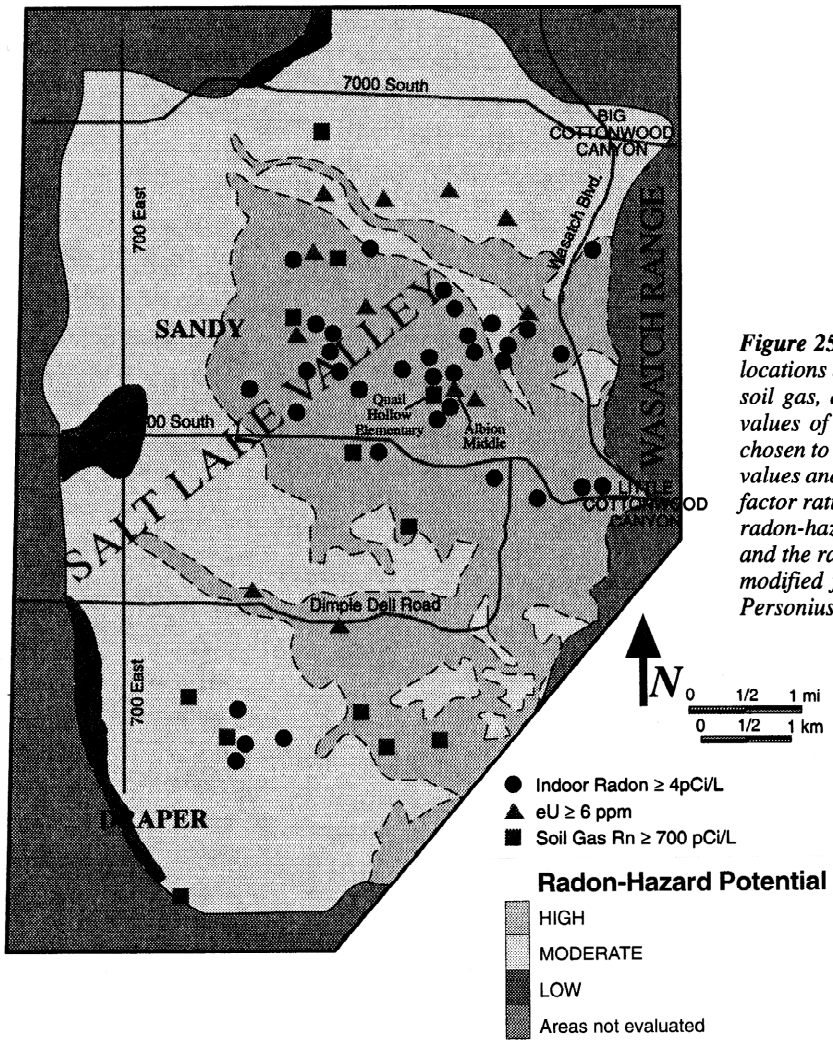


***Figure 25.*** *Map of radon-hazard potential, east Sandy. Approximate locations are shown for measurements of equivalent uranium, radon in soil gas, and indoor radon in excess of threshold values. Threshold values of equivalent uranium and radon in soil gas were arbitrarily chosen to illustrate the geographic relationship between high measured values and hazard ratings, and do not coincide with threshold values of factor ratings in table 7 or with threshold values in figure 21. Areas of radon-hazard potential are based on the data summarized in table 1, and the ratings scheme shown in table 8. Hazard-area boundaries are modified from the contacts of Quaternary geologic units mapped by Personius and Scott (1990, 1992) (figure 2).*

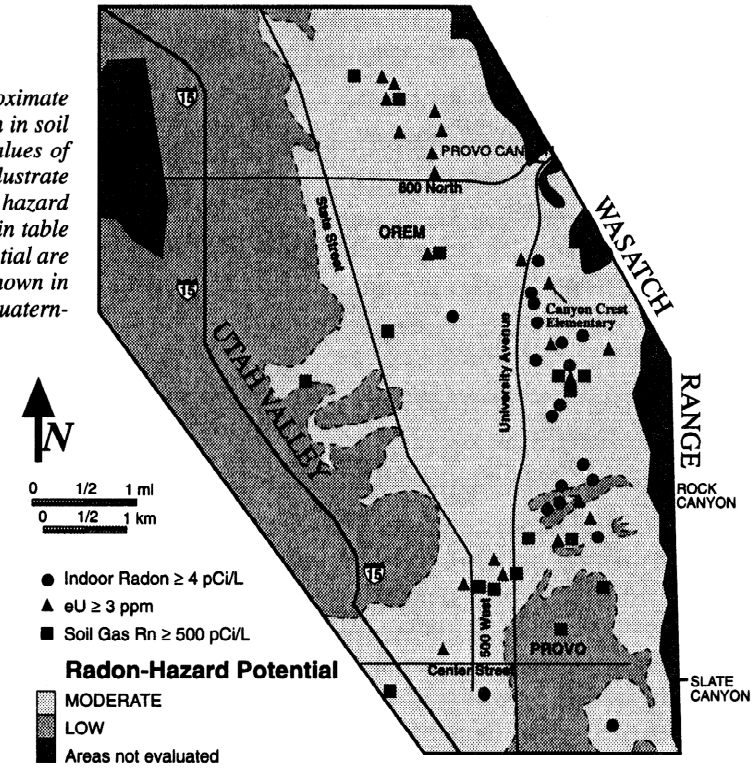


***Figure 26.*** *Map of radon-hazard potential, east Provo. Approximate locations are shown for measurements of equivalent uranium, radon in soil gas, and indoor radon in excess of threshold values. Threshold values of equivalent uranium and radon in soil gas were arbitrarily chosen to illustrate the geographic relationship between high measured values and hazard ratings, and do not coincide with threshold values of factor ratings in table 7 or with threshold values in figure 22. Areas of radon-hazard potential are based on the data summarized in table 2, and the ratings scheme shown in table 8. Hazard-area boundaries are modified from the contacts of Quaternary geologic units mapped by Machette (1989) (figure 3).*

***Table 8.***
*Radon-hazard-potential categories. See table 7 for point value of factors in each category.*

| Hazard Rating | Hazard Potential |
|---|---|
| 3-5 | Low |
| 6-9 | Moderate |
| 10-12 | High |

***Table 9.***
*Statistical summary of field data used as factors to determine radon-hazard-potential categories for Quaternary geologic units. N for eU and soil-gas Rn is the number of sample sites; N for ground-water depth is the number of sites with ground-water depth greater than 50 feet (15 m); N for indoor Rn is the number of sample sites for both this study and the statewide survey (Sprinkel and Solomon, 1990).*

| Hazard Potential | eU | | | | Rn in soil gas | | | | Depth to ground water | | Indoor Rn | | | |
|---|---|---|---|---|---|---|---|---|---|---|---|---|---|---|
| | N | % > 3 ppm | Avg. ppm | Max. ppm | N | % > 500 pCi/L | Avg. pCi/L | Max. pCi/L | N | % > 50 ft | N | % > 4 pCi/L | Avg. pCi/L | Max. pCi/L |
| East Sandy | | | | | | | | | | | | | | |
| Low | 2 | 50 | 3.8 | 5.1 | 2 | 50 | 445 | 580 | 0 | 0 | 1 | 0 | 0.8 | 0.8 |
| Moderate | 72 | 79 | 5.2 | 10.6 | 32 | 34 | 453 | 1,434 | 85 | 52 | 92 | 8 | 2.4 | 26.2 |
| High | 57 | 96 | 6.2 | 8.7 | 22 | 50 | 645 | 2,398 | 125 | 74 | 113 | 27 | 3.5 | 26.2 |
| East Provo | | | | | | | | | | | | | | |
| Low | 17 | 12 | 2.3 | 3.6 | 15 | 13 | 323 | 620 | 1 | 2 | 36 | 3 | 1.7 | 8.1 |
| Moderate | 82 | 29 | 2.6 | 4.6 | 42 | 38 | 490 | 1,463 | 99 | 50 | 116 | 15 | 2.8 | 13.6 |
| High | 0 | – | – | – | 0 | – | – | – | 0 | – | 0 | – | – | – |

***Table 10.***
*Statistical summary of additional ground-radiometric data for radon-hazard-potential categories.*

| Hazard Potential | N | Total Counts | | K | | eTh | | eU/eTh | |
|---|---|---|---|---|---|---|---|---|---|
| | | Avg. ppm | Max. ppm | Avg. % | Max. % | Avg. ppm | Max. ppm | Avg. | Max. |
| East Sandy | | | | | | | | | |
| Low | 2 | 17.2 | 19.3 | 2.1 | 2.1 | 12.6 | 14.0 | 0.31 | 0.46 |
| Moderate | 72 | 19.8 | 28.3 | 2.3 | 3.8 | 12.7 | 20.6 | 0.42 | 0.79 |
| High | 57 | 21.7 | 28.0 | 2.5 | 3.4 | 13.9 | 18.8 | 0.45 | 0.90 |
| East Provo | | | | | | | | | |
| Low | 17 | 8.9 | 10.5 | 1.1 | 1.4 | 6.2 | 7.5 | 0.37 | 0.55 |
| Moderate | 82 | 9.3 | 14.1 | 1.2 | 1.8 | 6.9 | 12.2 | 0.39 | 0.90 |
| High | 0 | – | – | – | – | – | – | – | – |

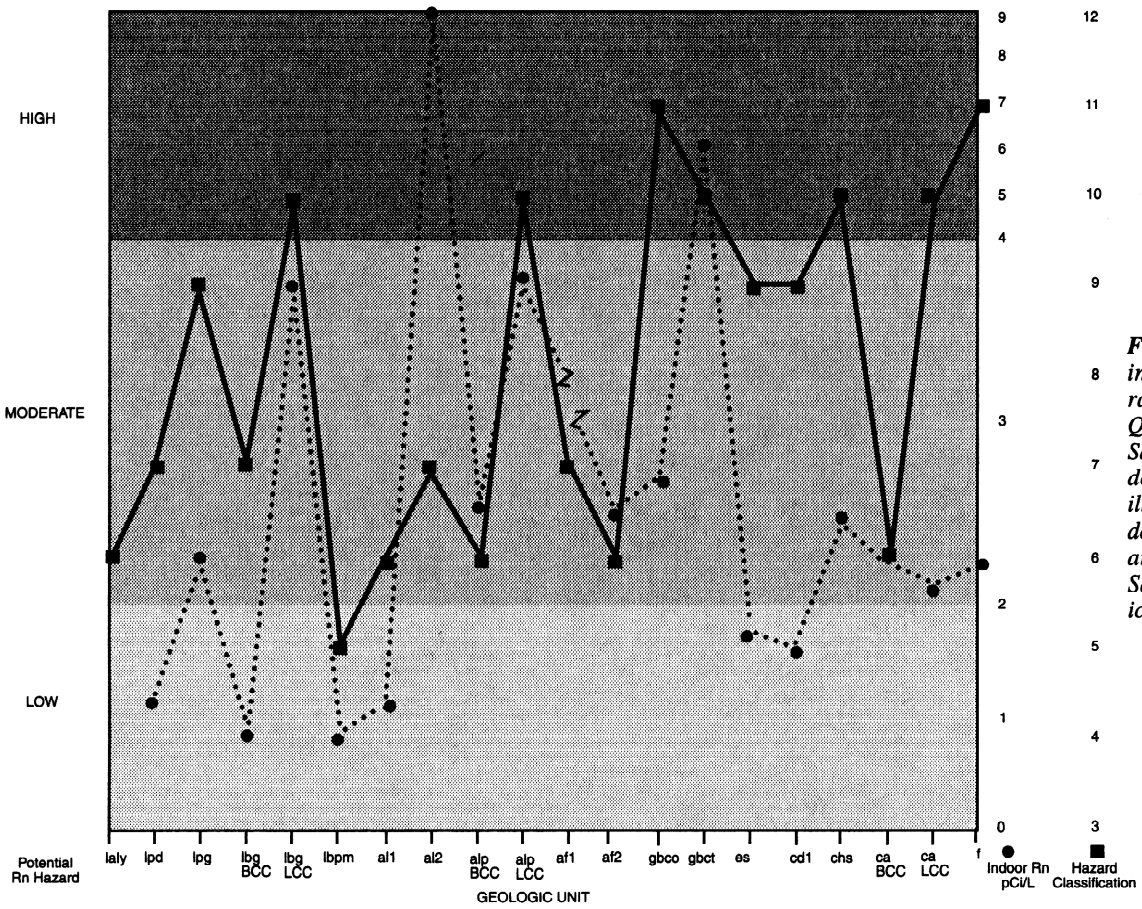


***Figure 27.*** *Comparison of average indoor-radon concentrations and radon-hazard-potential ratings of Quaternary geologic units in the east Sandy area. The vertical scale of indoor radon has been adjusted to illustrate the relationship between indoor-radon concentrations and hazard classification, and is not linear. See table 1 for explanation of geologic units.*

***Figure 28.*** *Comparison of average indoor-radon concentrations and radon-hazard-potential ratings of Quaternary geologic units in the east Provo area. The vertical scale of indoor radon has been adjusted to illustrate the relationship between indoor-radon concentrations and hazard classification, and is not linear. See table 2 for explanation of geologic units.*

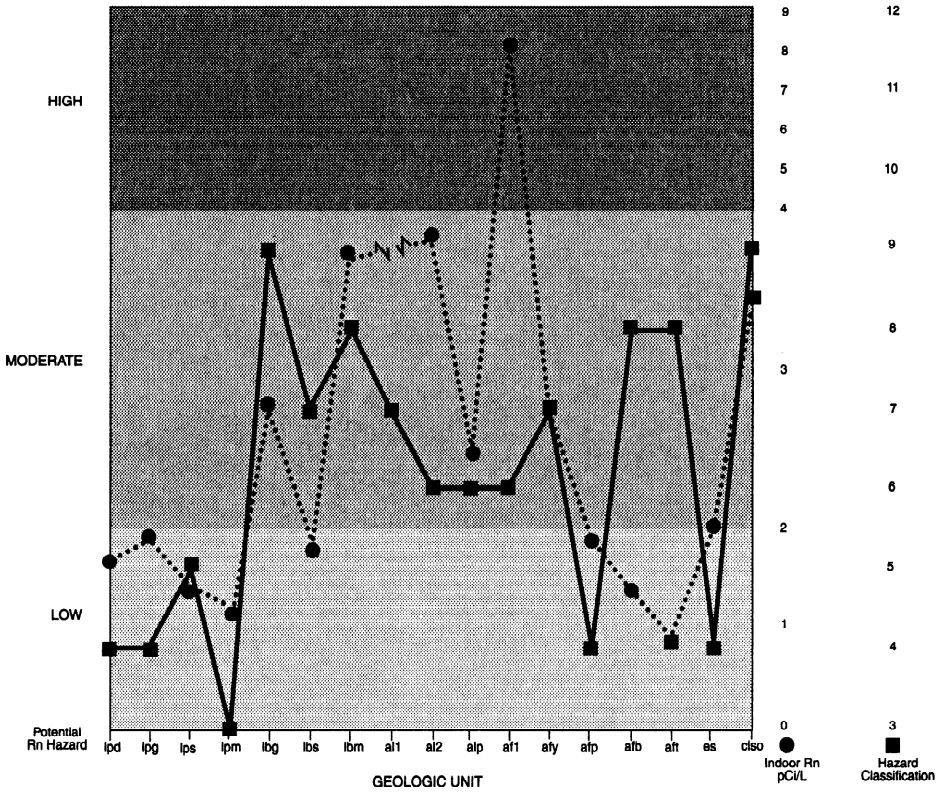

soils. However, the difference between the average indoor-radon level of the two areas is less than expected from the difference in uranium content. The average indoor-radon level in east Provo is only 17 percent less than in east Sandy, but the average uranium content in east Provo is 54 percent less. This inconsistency is explained by the process of radon emanation. Radon atoms escape (emanate) more easily from the solid in which they are produced if that solid has a large ratio of surface area to volume (Tanner, 1980). The ratio of surface area to volume increases in finer grained soil. Soils in both east Sandy and east Provo are gravelly, but the soil matrix in east Provo is finer grained than in east Sandy and the emanation process is thus more effective in east Provo. This effect could be taken into account by assigning numerical scores for a "grain size" factor, with the highest score for the finest grain size. Such a factor, though, would contradict the effect of permeability. Greater permeability facilitates radon migration and, hence, the potential for elevated indoor-radon levels. But permeability generally increases with increasing grain size. Thus, if soil texture alone is used as a surrogate for permeability, a high score for permeability in a coarse-grained soil would ignore the effect of surface area and volume. The solution is to use two factors, both grain size and permeability, but direct measurement of permeability is time consuming. Many investigators use permeabilities estimated from percolation tests conducted for U.S. Soil Conservation Service soil surveys (see, for example, Otton and others, 1988). However, soil-survey permeabilities in the east Sandy and east Provo areas (Swenson and others, 1972; Woodward and others, 1974) do not indicate significant permeability contrasts between Quaternary geologic units. The conflicting effects of both permeability and grain size are considered in this study by the inclusion of soil-gas radon as a hazard factor, because levels of soil-gas radon reflect the influence of both permeability and grain size on radon emanation and migration.

## Cautions When Using This Report

The hazard ratings presented in this report are not an accurate indicator of actual indoor-radon levels because a quantitative relationship between measured geologic factors and indoor-radon levels does not exist. Important non-geologic factors not considered in this report such as building construction and maintenance techniques, lifestyle, and weather can strongly affect indoor-radon levels within areas of similar radon-hazard potential based on geologic data. The scale of the maps precludes identification of small areas of higher and lower radon-hazard potential contained within the hazard-potential areas depicted on the maps. All map boundaries between hazard-potential areas are approximate due to the gradational nature of geologic contacts. Radon-hazard ratings are relative and are specific only to the east Sandy and east Provo study areas. Indoor-radon statistics in this study are based upon volunteer data, and are not based upon a true random sampling. The use of volunteer data may bias indoor-radon statistics toward qualities of volunteers that may not be characteristic of the general population.

# A GEOLOGIC MODEL FOR PREDICTING INDOOR-RADON HAZARD ALONG THE WASATCH FRONT

The rating scheme used to assess the potential indoor-radon hazard in the east Sandy and east Provo areas reflects common depositional patterns and physical conditions of geologic units that influence the hazard in both areas. Such patterns and conditions, as well as the techniques used in this study to identify them, are applicable to the identification of areas susceptible to an indoor-radon hazard elsewhere along the Wasatch Front.

In both study areas, geologic units with the highest hazard potential are upper Pleistocene lacustrine sediments related to the Bonneville (transgressive) phase of the Bonneville lake cycle, as well as younger deposits overlying these transgressive units. These units of highest hazard potential are prevalent in elevated benches, locally refered to as the "east bench," along the range front in the eastern part of both study areas. In east Sandy, drainage from Little Cottonwood Canyon has transported material derived principally from Oligocene granitic rocks with a relatively high uranium content to the Little Cottonwood delta (figure 29). Material transported through Big Cottonwood Canyon to the Big Cottonwood delta is derived from a mixed source whose principal component is the Big Cottonwood Formation, relatively deficient in uranium, but whose secondary components include Oligocene granitic rocks and Precambrian metamorphic and sedimentary rocks with higher uranium contents. Houses on well-drained sediments of the east bench near Little Cottonwood Canyon have the highest indoor-radon levels, with an average of 3.8 pCi/L (141 Bq/m$^3$); 27 percent of these houses have indoor-radon levels above 4 pCi/L (148 Bq/m$^3$). Sediments below the Provo (regressive) level are not well drained. A significant portion of radon derived from the uranium in these deposits migrates with shallow ground water rather than with soil gas and therefore does not enter houses.

Uranium levels in east Sandy, even on the Big Cottonwood delta, are considerably higher than in east Provo due to differences in source material. In east Provo, uranium-enriched sediment derived from the Mineral Fork Formation and Manning Canyon Shale was mixed with uranium-deficient sediment derived from the Oquirrh Formation. This mixed material was transported through canyon mouths and smaller drainages, and deposited as lacustrine sediments at the Bonneville (transgressive) level of the east bench, and in alluvium on the Provo River delta (figure 30). As in east Sandy, Quaternary geologic units with the highest potential for an indoor-radon hazard are well-drained sediments along the range front, whereas poorly drained units toward the valley interior have a lower hazard potential. Indoor-radon levels in east Provo are also highest on the east bench where they average 2.9 pCi/L (107 Bq/m$^3$); 17 percent of homes in this area have indoor-radon levels above 4 pCi/L (148 Bq/m$^3$). In both east Sandy and east Provo uranium content of soils decreases with increasing distance from the range front. This results from increased sediment mixing in valley interiors with material derived from uranium-deficient sources elsewhere in the basin and transported to the study areas

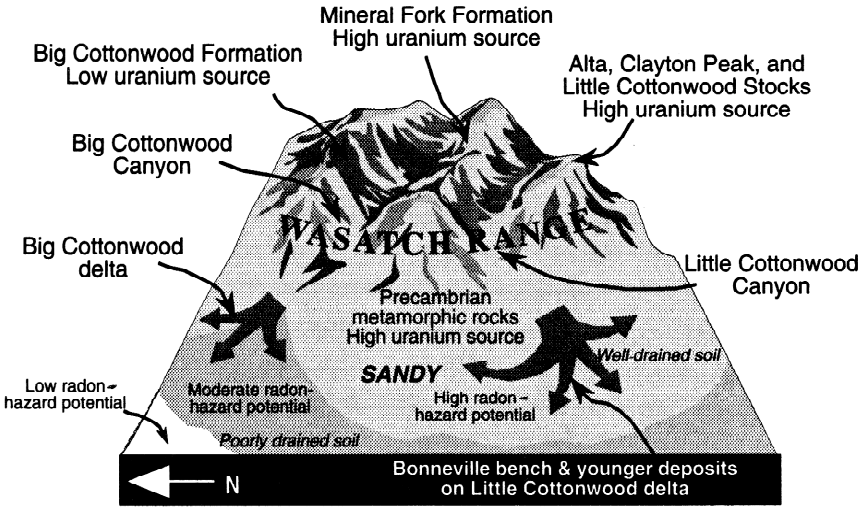


***Figure 29.*** *Sketch of regional geology showing relationship between source and depositional areas, east Sandy. Well-drained, uraniferous deposits with a high radon-hazard potential are derived from rocks in Little Cottonwood Canyon and underlie an elevated bench along the Wasatch Range front. Well-drained but less uraniferous deposits with a moderate radon-hazard potential are derived from rocks in Big Cottonwood Canyon. Poorly drained, uranium-deficient deposits with a low radon-hazard potential are derived from mixed sediment sources and underlie the valley interior.*

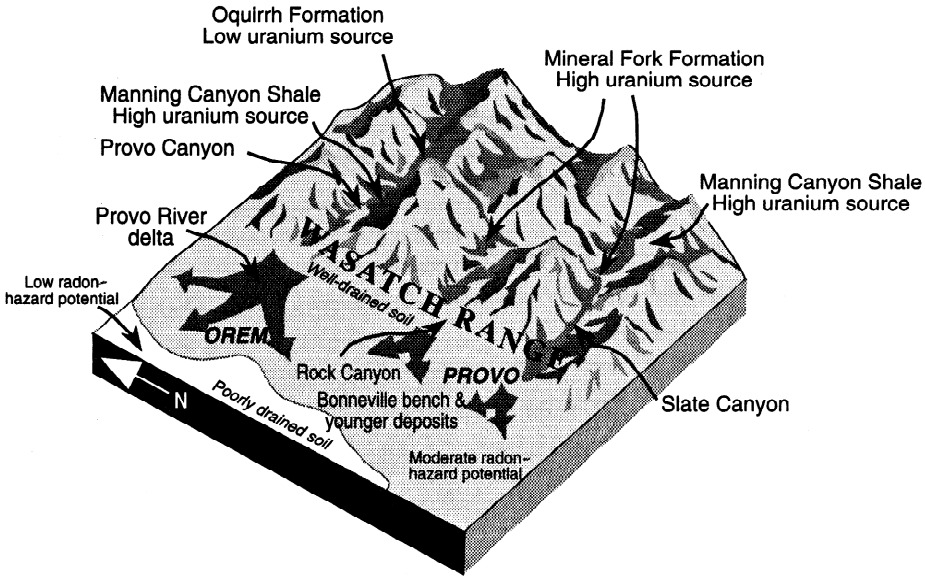


***Figure 30.*** *Sketch of regional geology showing relationship between source and depositional areas, east Provo. Similar depositional patterns in both east Sandy and east Provo resulted in well-drained, uraniferous deposits with the highest radon-hazard potential beneath an elevated bench along the Wasatch Range front. Because uranium levels in east Provo are lower than in east Sandy, bench deposits in east Provo have a moderate radon-hazard potential, rather than high as in east Sandy. As in east Sandy, poorly drained, uranium-deficient deposits in east Provo with a low radon-hazard potential are derived from mixed sediment sources and underlie the valley interior.*

by Lake Bonneville currents.

This combination of distinct source areas with contrasting uranium contents, routes of sediment transport, stratigraphic differentiation in the depositional area, and geomorphic position of well-drained sediments along the range front is a pattern that is likely repeated elsewhere along the Wasatch Front. Techniques used to evaluate potential radon hazard in this study may be applied with equal success in those areas.

## CONCLUSIONS

Airborne-radiometric measurements, particularly NURE data, are an effective means of identifying the regional uranium anomalies that are the source of radon in soil gas along the Wasatch Front. These measurements, in conjunction with regional geologic maps, are used to define areas with the potential for generating high concentrations of indoor radon. This is an efficient method for making rapid, quantitative determinations of potential radon-hazard areas.

Ground surveys using gamma-ray spectrometry and alpha scintillometry can rapidly determine the distribution of uranium and soil-gas radon among various geologic units. However, caution is necessary when interpreting soil-gas radon data. Although soil-gas radon levels measured in both the scintillometer (figure 13) and ATD (figure 20) surveys are of the same order of magnitude, details of survey results differ. Reproducibility of both scintillometer and ATD measurements are affected by atmospheric conditions which preclude extrapolation of soil-gas data to other time periods. Reproducibility of ATD measurements is also affected by the duration of the measurement period. Longer measurements give more accurate results. However, the longer a detector is left in the ground, the more likely it will be damaged or lost. In this study a shorter exposure period was used to ensure a high rate of detector recovery. This may have affected the reproducibility of the ATD survey results, but the extent of this effect is unknown. Soil-gas radon data that are not reproducible are useful for indicating relative differences in the level of radon in soil gas, but are not useful for making quantitative estimates of soil-gas radon levels during any period other than the time of measurement. Soil-gas radon data also cannot be used to make quantitative predictions of indoor-radon levels because of the uncertainty introduced by building construction, building maintenance, and occupant lifestyle.

Although uranium and soil-gas radon concentrations are higher in geologic units with higher hazard potential (table 9), the correlation between uranium concentration at the surface measured during the ground survey and soil-gas radon concentration at shallow depth shows considerable scatter (figure 12). The most likely reason for this discrepancy is that the surface material is different from the material at depth that generates the radon-bearing soil gas. This inhomogeneity may have two causes: development and stratigraphy. Because the study areas are largely developed, much of the surface material consists of either imported or disturbed top soil. When the airborne survey was flown in the late 1970s, there was little development and the surface material probably more closely represented the units that generate the radon in the soil gas. Alternately, if the geologic units are naturally stratified, radon measured from soil gas collected at depth may be generated from beds that are not exposed at the surface. In this case the airborne survey, although flown prior to development, measured uranium in beds different from radon-generating units and this difference persists today.

A combination of airborne and ground surveys was used to identify areas with a higher potential for elevated indoor-radon levels in well-drained sediments along the range front in east Sandy, and a similar radon-hazard area was identified along the range front of east Provo with ground studies only. Field work and interpretation were completed in several weeks. Relevant factors of soil-uranium content, soil-gas radon concentration, and ground-water depth were synthesized into a ratings scheme which identified the relative potential for an indoor-radon hazard in buildings in various geologic units. Several other factors affect the indoor-radon hazard, such as weather, construction type, building maintenance, and lifestyle, but characteristics of these factors vary both spatially and temporally and cannot be accurately or efficiently determined for large geographic areas. The general correlation between the indoor-radon-hazard potential, estimated in this study with only geologic criteria, and measured indoor-radon levels support the utility of this rating scheme for predicting the relative potential for indoor-radon hazard in areas without extensive indoor testing. Determining the relative radon-hazard potential for areas underlain by relatively homogenous geologic units allows priorities to be established for indoor testing and hazard reduction in existing construction and demonstrates the need for radon-resistant new construction.

## ACKNOWLEDGMENTS

This study was supported by a grant from the EPA, administered by the UDRC, under the SIRG Program. Many persons and organizations provided consent for testing on property under their control; this study would not have been possible without them. The preliminary version of this manuscript (Solomon and others, 1991) was reviewed by Douglas A. Sprinkel, UGS, and the final version was reviewed by Gary Christenson, UGS, and Jonathan G. Price, Nevada Bureau of Mines and Geology; we thank them for their critical comments and helpful suggestions.

# REFERENCES CITED


Anderson, L. R., Keaton, J. R., and Bischoff, J. E., 1986a, Liquefaction potential map for Utah County, Utah: Logan, Utah State University, Department of Civil and Environmental Engineering, and Salt Lake City, Dames & Moore Consulting Engineers, 46 p.

Anderson, L. R., Keaton, J. R., Spitzley, J. E., and Allen, A. C., 1986b, Liquefaction potential map for Salt Lake County, Utah: Logan, Utah State University, Department of Civil and Environmental Engineering, and Salt Lake City, Dames & Moore Consulting Engineers, 48 p.

Baker, A. A., 1964, Geology of the Orem quadrangle, Utah: U.S. Geological Survey Map GQ-241, scale 1:24,000.

---1972, Geologic map of the Bridal Veil Falls quadrangle, Utah: U.S. Geological Survey Map GQ-998, scale 1:24,000.

---1973, Geologic map of the Springville quadrangle, Utah: U.S. Geological Survey Map GQ-1103, scale 1:24,000.

Condie, K. C., 1967, Petrology of the late Precambrian tillite(?) association in northern Utah: Geological Society of America Bulletin, v. 78, no. 11, p. 1317-1344.

Crittenden, M. D., Jr., 1976, Stratigraphic and structural setting of the Cottonwood area, Utah, *in* Hill, J. G., editor, Symposium on geology of the Cordilleran hingeline: Denver, Rocky Mountain Association of Geologists, p. 363-379.

Duval, J. S., and Otton, J. K., 1990, Radium distribution and indoor radon in the Pacific Northwest: Geophysical Research Letters, v. 17, no. 6, p. 801-804.

EG&G Geometrics, 1979, Aerial gamma ray and magnetic surveys, Ogden and Salt Lake City quadrangles, Utah: Final Report to the U.S. Department of Energy, v. 1 and 2.

Gundersen, L. C. S., Reimer, G. M., and Agard, S. S., 1988, Correlation between geology, radon in soil gas, and indoor radon in the Reading Prong, *in* Marikos, M. A., and Hansman, R. H., editors, Geologic causes of natural radionuclide anomalies: Missouri Department of Natural Resources, Division of Geology and Land Survey, Special Publication 4, p. 91-102.

Hesselbom, A., 1985, Radon in soil gas - a study of methods and instruments for determining radon concentrations in the ground: Sveriges Geologiska Undersokning (Swedish Geological Survey) Ser. C-803 (in English).

James, L. P., 1979, Geology, ore deposits, and history of the Big Cottonwood mining district, Salt Lake County, Utah: Utah Geological and Mineral Survey Bulletin 114, 98 p.

Machette, M. N., 1989, Preliminary surficial geologic map of the Wasatch fault zone, eastern part of Utah Valley, Utah County and parts of Salt Lake and Juab Counties, Utah: U.S. Geological Survey Miscellaneous Field Studies Map MF-2109, 30 p., scale 1:50,000.

McCammon, R. B., 1980, The statistical treatment of geochemical data, *in* Levinson, A.A., editor, Introduction to exploration geochemistry, 2nd edition: Toronto, Applied Publishing Ltd., p. 835-843.

Muessig, K. W., 1988, Correlation of airborne radiometric data and geologic sources with elevated indoor radon in New Jersey, *in* The 1988 Symposium on Radon and Radon Reduction Technology, preprints: Research Triangle Park, North Carolina, U.S. Environmental Protection Agency, Air and Energy Environmental Research Laboratory, p. V-1.

Nielson, D.L., Linpei, Cui, and Ward, S.H., 1991, Gamma-ray spectrometry and radon emanometry in environmental geophysics, *in* Ward, S.H., editor, Geotechnical and environmental geophysics, v. 1, - review and tutorial: Tulsa, Oklahoma, Society of Exploration Geophysicists, p. 219-250.

Otton, J. K., Schumann, R. R., Owen, D. E., Thurman, Nelson, and Duval, J. S., 1988, Map showing radon potential of rocks and soils in Fairfax County, Virginia: U.S. Geological Survey Miscellaneous Field Studies Map MF-2047, scale 1:48,000.

Oviatt, C.G., Currey, D.R., and Sack, Dorothy, 1992, Radiocarbon chronology of Lake Bonneville, eastern Great Basin, USA: Palaeogeography, Palaeoclimatology, Palaeoecology, v. 99, p. 225-241.

Personius, S. F., and Scott, W. E., 1990, Preliminary surficial geologic map of the Salt Lake City segment and parts of adjacent segments of the Wasatch fault zone, Davis, Salt Lake, and Utah Counties, Utah: U.S. Geological Survey Miscellaneous Field Studies Map MF-2114, scale 1:50,000.

---1992, Surficial geologic map of the Salt Lake City segment and parts of adjacent segments of the Wasatch fault zone, Davis, Salt Lake, and Utah Counties, Utah: U.S. Geological Survey Miscellaneous Investigations Map I-2106, scale 1:50,000.

Reimer, G. M., and Gundersen, L. C. S., 1989, A direct correlation among indoor Rn, soil gas Rn, and geology in the Reading Prong near Boyertown, Pennsylvania: Health Physics, v. 57, no. 1, p. 155-160.

Rogers, J. J. W., 1964, Statistical tests of the homogeneity of the radioactive components of granitic rocks, *in* Makofske, W.J., and Edelstein, M.R., editors, Radon and the environment: Park Ridge, New Jersey, Noyes Publications, p. 51-62.

Rogers, V. C., and Nielson, K. K., 1990, Benchmark and application of the RAETRAD model, *in* The 1990 International Symposium on Radon and Radon Reduction Technology, v. III, preprints: Research Triangle Park, North Carolina, U.S. Environmental Protection Agency, Air and Energy Environmental Research Laboratory, EPA/600/9-90/005c, p. VI-1.

Schery, W. R., Gaeddert, D. H., and Wilkening, M. H., 1984, Factors affecting exhalation of radon from a gravelly sandy loam: Journal of Geophysical Research, v. 89, p. 7299-7309.

Sextro, Richard, 1988, Radon in dwellings, *in* Makofske, W.J., and Edelstein, M.R., editors, Radon and the environment: Park Ridge, New Jersey, Noyes Publications, p. 71-82.

Solomon, B. J., Black, B. D., Nielson, D, L., and Cui, Linpei, 1991, Identification of radon-hazard areas along the Wasatch Front, Utah, using geologic techniques, *in* McCalpin, J. P., editor, Proceedings of the 27th Symposium on Engineering Geology and Geotechnical Engineering: Logan, Utah State University, p. 40-1 - 40-16.

Sprinkel, D. A., 1987 (revised 1988), The potential radon hazard map, Utah: Utah Geological and Mineral Survey Open-File Report 108, 4 p., scale 1:1,000,000.

Sprinkel, D. A., and Solomon, B. J., 1990, Radon hazards in Utah: Utah Geological and Mineral Survey Circular 81, 24 p.

Stranden, Erling, 1984, Thoron ($^{220}$Rn) daughter to radon ($^{222}$Rn) daughter ratios in thorium-rich areas: Health Physics, v. 47, no. 5, p. 784-785.

Swenson, J. L., Jr., Archer, W. M., Donaldson, K. M., Shiozaki, J. J., Broderick, J. H., and Woodward, Lowell, 1972, Soil survey of Utah County, Utah - central part: U.S. Department of Agriculture Soil Conservation Service in cooperation with Utah Agricultural Experiment Station, 161 p.

Tanner, A. B., 1964, Radon migration in the ground, a review, *in* Adams, J. A. S., and Lowder, W. M., editors, The natural radiation environment: University of Chicago Press, p. 161-190.

---1980, Radon migration in the ground - a supplementary review, *in* Gesell, T. F., and Lowder, W. M., editors, Natural Radiation Environment III: Symposium Proceedings, Houston, v. 1, U.S. Department of Energy Report CONF-780422, National Technical Information Service, p. 5-56.

U.S. Environmental Protection Agency, 1989, Radon measurement in schools, an interim report: U.S. Environmental Protection Agency Report EPA-520/1-89-010, 17 p.

U.S. Environmental Protection Agency, U.S. Department of Health and Human Services, and U.S. Public Health Service, 1992, A citizen's guide to radon (second edition): U.S. Environmental Protection Agency, Office of Air and Radiation Report 402-K92-001, 15 p.

U.S. Soil Conservation Service, 1975, Soil taxonomy: Washington, D.C., U.S. Department of Agriculture Handbook No. 436, p. 469-474.

Washington, J. W., and Rose, A. W., 1992, Temporal variability of radon concentration in the interstitial gas of soils in Pennsylvania: Journal of Geophysical Research, v. 97, no. B6, p. 9145-9159.

Witcher, J. C., and Shoenmackers, R., 1990, Time-integrated radon soil-gas surveys in geothermal exploration in the southern Rio Grande rift, New Mexico: New Mexico Research and Development Institute Report, 175 p.

Woodward, Lowell, Harvey, J. L., Donaldson, K. M., Shiozaki, J. J., Leishman, G. W., and Broderick, J. H., 1974, Soil survey of Salt Lake area, Utah: U.S. Department of Agriculture Soil Conservation Service in cooperation with Utah Agricultural Experiment Station, 132 p.

# APPENDIX

*Ground-Survey Data (Except Soil-ATD Measurements)*

***Table A-1***

*Indoor-radon measurements, east Sandy, collected for both this study and the statewide survey (Sprinkel and Solomon, 1990). Measurements are grouped by geologic unit, and are sorted within each unit in descending order by indoor-radon concentration. See table 1 for explanation of geologic units. Specific locations are withheld to protect the confidentiality of survey participants.*

| Sample Number | Geologic Unit | Indoor Radon (pCi/L) | Ground-Water Depth (ft) | Zip Code |
|---|---|---|---|---|
| 483484 | af2 | 3.2 | <10 | 84020 |
| 842197 | af2 | 2.8 | >50 | 84092 |
| 483544 | af2 | 2.7 | <10 | 84020 |
| 839709 | af2 | 2.2 | >50 | 84092 |
| 483524 | af2 | 1.7 | >50 | 84092 |
| 842166 | al1 | 1.1 | <10 | 84093 |
| 842213 | al2 | 26.2 | 10-30 | 84092 |
| 483482 | al2 | 6.8 | 10-30 | 84093 |
| 842193 | al2 | 5.1 | 10-30 | 84093 |
| 839786 | al2 | 4.3 | 10-30 | 84093 |
| 839743 | al2 | 2.5 | <10 | 84093 |
| 483400 | alp bcc | 3.8 | 10-30 | 84121 |
| 483676 | alp bcc | 3.3 | 10-30 | 84121 |
| 483290 | alp bcc | 1.5 | 10-30 | 84121 |
| 839661 | alp bcc | 1.5 | 10-30 | 84121 |
| 1679401 | alp lcc | 13.7 | >50 | 84093 |
| 483231 | alp lcc | 12.7 | 10-30 | 84093 |
| 1679414 | alp lcc | 11.6 | >50 | 84093 |
| 839707 | alp lcc | 11.3 | >50 | 84093 |
| 842241 | alp lcc | 10.7 | >50 | 84093 |
| 483242 | alp lcc | 10.0 | >50 | 84092 |
| 839653 | alp lcc | 9.7 | >50 | 84093 |
| 839752 | alp lcc | 9.0 | >50 | 84092 |
| 839694 | alp lcc | 8.8 | >50 | 84093 |
| 839712 | alp lcc | 8.7 | >50 | 84093 |
| 483176 | alp lcc | 8.5 | >50 | 84093 |
| 842190 | alp lcc | 7.2 | >50 | 84092 |
| 842207 | alp lcc | 7.0 | 10-30 | 84093 |
| 839788 | alp lcc | 6.8 | >50 | 84093 |
| 842230 | alp lcc | 6.8 | 10-30 | 84092 |
| 839681 | alp lcc | 6.3 | >50 | 84092 |
| 839740 | alp lcc | 4.5 | >50 | 84093 |
| 839698 | alp lcc | 4.5 | 10-30 | 84093 |
| 842224 | alp lcc | 4.4 | >50 | 84093 |
| 839732 | alp lcc | 4.4 | 30-50 | 84093 |
| 839679 | alp lcc | 4.3 | >50 | 84093 |
| 842254 | alp lcc | 4.3 | >50 | 84093 |
| 842199 | alp lcc | 4.3 | 10-30 | 84093 |
| 483507 | alp lcc | 4.1 | 30-50 | 84093 |
| 842177 | alp lcc | 3.9 | >50 | 84093 |
| 842163 | alp lcc | 3.9 | 30-50 | 84093 |
| 842211 | alp lcc | 3.7 | >50 | 84093 |
| 483160 | alp lcc | 3.7 | >50 | 84092 |
| 839685 | alp lcc | 3.5 | >50 | 84093 |
| 483167 | alp lcc | 3.4 | >50 | 84093 |
| 839738 | alp lcc | 3.3 | >50 | 84093 |
| 842212 | alp lcc | 3.3 | >50 | 84093 |
| 484575 | alp lcc | 3.2 | >50 | 84092 |
| 839666 | alp lcc | 3.2 | >50 | 84092 |
| 842172 | alp lcc | 3.1 | >50 | 84093 |
| 839777 | alp lcc | 2.9 | >50 | 84092 |
| 842235 | alp lcc | 2.8 | 30-50 | 84093 |
| 839717 | alp lcc | 2.7 | >50 | 84093 |
| 842178 | alp lcc | 2.7 | >50 | 84093 |
| 842192 | alp lcc | 2.7 | >50 | 84093 |
| 839734 | alp lcc | 2.6 | >50 | 84093 |
| 839736 | alp lcc | 2.6 | >50 | 84093 |
| 842240 | alp lcc | 2.6 | 30-50 | 84093 |
| 839733 | alp lcc | 2.6 | 10-30 | 84093 |
| 842176 | alp lcc | 2.5 | 30-50 | 84094 |
| 839702 | alp lcc | 2.5 | 30-50 | 84093 |
| 483515 | alp lcc | 2.4 | >50 | 84093 |
| 839660 | alp lcc | 2.4 | >50 | 84093 |
| 483747 | alp lcc | 2.4 | >50 | 84092 |
| 839719 | alp lcc | 2.3 | >50 | 84093 |
| 839655 | alp lcc | 2.3 | >50 | 84092 |
| 842204 | alp lcc | 2.2 | >50 | 84093 |
| 839701 | alp lcc | 2.2 | >50 | 84092 |
| 839676 | alp lcc | 2.2 | 30-50 | 84093 |
| 839703 | alp lcc | 2.2 | 10-30 | 84093 |
| 1679396 | alp lcc | 2.1 | >50 | 84093 |
| 483766 | alp lcc | 2.1 | 30-50 | 84094 |
| 839735 | alp lcc | 2.0 | >50 | 84093 |
| 839720 | alp lcc | 2.0 | >50 | 84092 |
| 839671 | alp lcc | 1.9 | >50 | 84093 |

***Table A-1** (continued)*

| Sample Number | Geologic Unit | Indoor Radon (pCi/L) | Ground-Water Depth (ft) | Zip Code |
|---|---|---|---|---|
| 839758 | alp lcc | 1.9 | 10-30 | 84093 |
| 842169 | alp lcc | 1.7 | >50 | 84093 |
| 839784 | alp lcc | 1.7 | >50 | 84092 |
| 842206 | alp lcc | 1.6 | >50 | 84093 |
| 842242 | alp lcc | 1.5 | >50 | 84093 |
| 842195 | alp lcc | 1.5 | >50 | 84092 |
| 842167 | alp lcc | 1.5 | 30-50 | 84093 |
| 839687 | alp lcc | 1.5 | 10-30 | 84093 |
| 839691 | alp lcc | 1.5 | 10-30 | 84092 |
| 839787 | alp lcc | 1.4 | >50 | 84093 |
| 842179 | alp lcc | 1.4 | >50 | 84093 |
| 842174 | alp lcc | 1.4 | >50 | 84092 |
| 839663 | alp lcc | 1.4 | 30-50 | 84093 |
| 483252 | alp lcc | 1.3 | 30-50 | 84093 |
| 839699 | alp lcc | 1.3 | 30-50 | 84093 |
| 839706 | alp lcc | 1.3 | 30-50 | 84093 |
| 839730 | alp lcc | 1.2 | 10-30 | 84093 |
| 839690 | alp lcc | 1.1 | >50 | 84093 |
| 839727 | alp lcc | 1.1 | 10-30 | 84121 |
| 839665 | alp lcc | 0.9 | 30-50 | 84093 |
| 842252 | alp lcc | 0.8 | 10-30 | 84093 |
| 839680 | alp lcc | 0.6 | >50 | 84093 |
| 839662 | alp lcc | 0.6 | >50 | 84092 |
| 839723 | alp lcc | 0.5 | >50 | 84092 |
| 483799 | ca bcc | 2.2 | 10-30 | 84121 |
| 839700 | ca lcc | 4.4 | >50 | 84121 |
| 839670 | ca lcc | 3.2 | >50 | 84093 |
| 839757 | ca lcc | 2.7 | >50 | 84092 |
| 839675 | ca lcc | 2.3 | >50 | 84092 |
| 839725 | ca lcc | 1.8 | >50 | 84092 |
| 839678 | ca lcc | 1.2 | >50 | 84092 |
| 839682 | ca lcc | 1.2 | >50 | 84092 |
| 839789 | ca lcc | 1.0 | >50 | 84093 |
| 842248 | ca lcc | 0.7 | >50 | 84092 |
| 839692 | cd1 | 1.9 | >50 | 84121 |
| 842198 | cd1 | 1.3 | >50 | 84121 |
| 483181 | chs | 2.4 | >50 | 84121 |
| 1679391 | es | 3.4 | >50 | 84092 |
| 839741 | es | 3.1 | >50 | 84092 |
| 483760 | es | 3.0 | 30-50 | 84070 |
| 839739 | es | 2.9 | >50 | 84092 |
| 483266 | es | 2.3 | >50 | 84092 |
| 842194 | es | 2.3 | >50 | 84092 |
| 483759 | es | 2.3 | 30-50 | 84121 |
| 483152 | es | 2.0 | >50 | 84092 |
| 842188 | es | 2.0 | >50 | 84092 |
| 483336 | es | 1.8 | >50 | 84092 |
| 839704 | es | 1.8 | >50 | 84092 |
| 839724 | es | 1.7 | >50 | 84092 |
| 842261 | es | 1.7 | >50 | 84092 |
| 1679410 | es | 1.7 | >50 | 84092 |
| 842234 | es | 1.5 | >50 | 84092 |
| 839659 | es | 1.4 | >50 | 84092 |
| 839767 | es | 1.4 | >50 | 84092 |
| 634621 | es | 1.3 | 10-30 | 84121 |
| 483651 | es | 1.2 | 10-30 | 84070 |
| 483549 | es | 1.1 | >50 | 84092 |
| 839656 | es | 1.1 | >50 | 84092 |
| 483518 | es | 1.1 | 30-50 | 84094 |
| 842164 | es | 1.0 | >50 | 84092 |
| 842249 | es | 1.0 | >50 | 84092 |
| 842162 | es | 0.9 | >50 | 84092 |
| 839674 | es | 0.8 | >50 | 84092 |
| 839759 | es | 0.8 | >50 | 84092 |
| 842238 | es | 0.7 | >50 | 84092 |
| 483684 | f | 2.2 | >50 | 84121 |
| 839726 | gbco | 2.7 | >50 | 84092 |
| 842214 | gbct | 6.1 | >50 | 84092 |
| 483580 | lbg bcc | 1.1 | 10-30 | 84121 |
| 1679412 | lbg bcc | 0.5 | 10-30 | 84121 |
| 483803 | lbg lcc | 26.2 | >50 | 84092 |
| 839658 | lbg lcc | 9.1 | >50 | 84092 |
| 839794 | lbg lcc | 4.8 | >50 | 84093 |
| 483547 | lbg lcc | 4.4 | >50 | 84121 |
| 839731 | lbg lcc | 3.1 | >50 | 84092 |
| 842210 | lbg lcc | 2.3 | >50 | 84092 |

***Table A-1** (continued)*

| Sample Number | Geologic Unit | Indoor Radon (pCi/L) | Ground-Water Depth (ft) | Zip Code |
|---|---|---|---|---|
| 842220 | lbg lcc | 1.9 | 10-30 | 84121 |
| 839772 | lbg lcc | 1.8 | >50 | 84092 |
| 842200 | lbg lcc | 1.6 | >50 | 84092 |
| 842170 | lbg lcc | 1.4 | 30-50 | 84121 |
| 839718 | lbg lcc | 1.3 | >50 | 84092 |
| 842202 | lbg lcc | 1.0 | >50 | 84092 |
| 842250 | lbg lcc | 1.0 | >50 | 84092 |
| 839797 | lbg lcc | 1.0 | 30-50 | 84121 |
| 842180 | lbg lcc | 0.9 | >50 | 84092 |
| 839760 | lbg lcc | 0.3 | >50 | 84092 |
| 483608 | lbpm | 0.8 | <10 | 84020 |
| 483640 | lpd | 1.3 | 10-30 | 84094 |
| 483806 | lpd | 0.9 | 10-30 | 84092 |
| 483241 | lpg | 8.8 | >50 | 84092 |
| 483177 | lpg | 6.2 | >50 | 84092 |
| 842236 | lpg | 4.6 | 30-50 | 84092 |
| 1679393 | lpg | 4.0 | >50 | 84092 |
| 483386 | lpg | 3.7 | >50 | 84092 |
| 1679381 | lpg | 3.7 | >50 | 84092 |
| 839705 | lpg | 3.5 | >50 | 84092 |
| 483538 | lpg | 3.0 | >50 | 84070 |
| 839654 | lpg | 2.8 | >50 | 84092 |
| 839721 | lpg | 2.8 | >50 | 84092 |
| 842221 | lpg | 2.7 | >50 | 84092 |
| 839729 | lpg | 2.6 | >50 | 84092 |
| 839696 | lpg | 2.5 | >50 | 84092 |
| 842203 | lpg | 2.5 | >50 | 84092 |
| 842233 | lpg | 2.4 | >50 | 84092 |
| 483480 | lpg | 2.2 | >50 | 84092 |
| 839744 | lpg | 2.2 | >50 | 84092 |
| 842251 | lpg | 2.2 | >50 | 84092 |
| 483247 | lpg | 2.1 | >50 | 84092 |
| 839693 | lpg | 1.8 | >50 | 84092 |
| 842175 | lpg | 1.8 | >50 | 84092 |
| 839668 | lpg | 1.8 | >50 | 84092 |
| 839770 | lpg | 1.7 | >50 | 84092 |
| 483270 | lpg | 1.7 | 10-30 | 84121 |
| 483564 | lpg | 1.6 | 30-50 | 84092 |
| 483485 | lpg | 1.6 | 10-30 | 84070 |
| 842165 | lpg | 1.5 | >50 | 84092 |
| 842227 | lpg | 1.4 | >50 | 84092 |
| 839722 | lpg | 1.3 | >50 | 84092 |
| 839776 | lpg | 1.3 | >50 | 84092 |
| 842253 | lpg | 1.2 | >50 | 84093 |
| 483599 | lpg | 1.2 | 10-30 | 84121 |
| 842255 | lpg | 1.1 | >50 | 84092 |
| 483584 | lpg | 0.9 | 30-50 | 84094 |
| 634596 | lpg | 0.9 | 30-50 | 84070 |
| 483519 | lpg | 0.9 | 10-30 | 84121 |
| 483471 | lpg | 0.8 | 10-30 | 84070 |
| 842181 | lpg | 0.6 | >50 | 84092 |
| 483722 | lpg | 0.6 | >50 | 84070 |
| 484542 | lpg | 0.5 | >50 | 84092 |
| 842182 | lpg | 0.5 | >50 | 84092 |
| 483741 | lpg | 0.5 | 30-50 | 84070 |

***Table A-2***

***Indoor-radon measurements, east Provo, collected for both this study and the statewide survey (Sprinkel and Solomon, 1990). Measurements are grouped by geologic unit, and are sorted within each unit in descending order by indoor-radon concentration. See table 2 for explanation of geologic units. Specific locations are withheld to protect the confidentiality of survey participants.***

| Sample Number | Geologic Unit | Indoor Radon (pCi/L) | Ground-Water Depth (ft) | Zip Code |
|---|---|---|---|---|
| 483390 | af2 | 8.2 | 10-30 | 84604 |
| 483300 | af4 | 0.9 | >50 | 84604 |
| 634598 | afb | 1.4 | >50 | 84604 |
| 842189 | afp | 8.1 | 10-50 | 84604 |
| 842205 | afp | 3.1 | <10 | 84606 |
| 839802 | afp | 1.6 | <10 | 84606 |
| 839768 | afp | 1.5 | <10 | 84606 |
| 842245 | afp | 1.1 | <10 | 84606 |
| 842229 | afp | 1.0 | <10 | 84606 |
| 839710 | afp | 1.0 | <10 | 84601 |
| 842215 | afp | 0.8 | <10 | 84606 |
| 842228 | afp | 0.7 | <10 | 84606 |
| 483743 | afp | 0.5 | >50 | 84604 |
| 483348 | afy | 10.2 | 10-50 | 84604 |
| 839684 | afy | 7.8 | >50 | 84604 |
| 483508 | afy | 7.0 | >50 | 84604 |
| 842185 | afy | 6.5 | >50 | 84604 |
| 483388 | afy | 5.4 | <10 | 84601 |
| 839801 | afy | 4.1 | 10-50 | 84604 |
| 842209 | afy | 3.9 | >50 | 84604 |
| 839711 | afy | 3.2 | 10-50 | 84604 |
| 483829 | afy | 3.1 | >50 | 84604 |
| 839792 | afy | 3.0 | >50 | 84604 |
| 839779 | afy | 2.4 | >50 | 84606 |
| 839754 | afy | 2.4 | >50 | 84604 |
| 842243 | afy | 2.2 | >50 | 84604 |
| 483375 | afy | 2.2 | <10 | 84601 |
| 839715 | afy | 2.1 | >50 | 84604 |
| 839764 | afy | 2.1 | >50 | 84604 |
| 483341 | afy | 2.1 | >50 | 84601 |
| 842244 | afy | 2.0 | >50 | 84604 |
| 839673 | afy | 2.0 | <10 | 84606 |
| 842187 | afy | 1.6 | <10 | 84606 |
| 839756 | afy | 1.6 | 10-50 | 84606 |
| 483800 | afy | 1.5 | >50 | 84601 |
| 842168 | afy | 1.5 | 10-50 | 84604 |
| 839778 | afy | 1.4 | >50 | 84604 |
| 839785 | afy | 1.4 | 10-50 | 84604 |
| 634601 | afy | 1.3 | >50 | 84604 |
| 483268 | afy | 1.3 | <10 | 84601 |
| 839781 | afy | 1.3 | 10-50 | 84604 |
| 483573 | afy | 1.2 | >50 | 84604 |
| 842225 | afy | 1.2 | <10 | 84606 |
| 839753 | afy | 0.8 | >50 | 84604 |
| 483808 | afy | 0.7 | <10 | 84601 |
| 483198 | afy | 0.7 | 10-50 | 84601 |
| 839790 | afy | 0.6 | 10-50 | 84604 |
| 483764 | al2 | 6.5 | <10 | 84604 |
| 483820 | al2 | 1.0 | <10 | 84604 |
| 483826 | alp | 6.3 | 10-50 | 84604 |
| 483744 | alp | 4.6 | 10-50 | 84058 |
| 483314 | alp | 4.0 | >50 | 84057 |
| 483516 | alp | 3.9 | >50 | 84058 |
| 483802 | alp | 3.9 | 10-50 | 84604 |
| 483309 | alp | 3.7 | >50 | 84604 |
| 483394 | alp | 3.7 | >50 | 84057 |
| 634591 | alp | 3.7 | >50 | 84057 |
| 483779 | alp | 3.5 | 10-50 | 84058 |
| 483605 | alp | 3.4 | 10-50 | 84057 |
| 483191 | alp | 3.3 | >50 | 84057 |
| 483828 | alp | 3.3 | 10-50 | 84058 |
| 483603 | alp | 2.9 | >50 | 84057 |
| 483387 | alp | 2.8 | >50 | 84057 |
| 483378 | alp | 2.7 | 10-50 | 84058 |
| 483812 | alp | 2.3 | 10-50 | 84058 |
| 483624 | alp | 2.2 | >50 | 84057 |
| 483173 | alp | 2.0 | <10 | 84058 |
| 634629 | alp | 1.8 | 10-50 | 84057 |
| 483202 | alp | 1.7 | <10 | 84058 |
| 483742 | alp | 1.7 | 10-50 | 84057 |
| 483207 | alp | 1.6 | >50 | 84057 |
| 483491 | alp | 1.4 | 10-50 | 84058 |
| 483269 | alp | 1.3 | 10-50 | 84058 |
| 634595 | alp | 1.3 | 10-50 | 84057 |
| 483279 | alp | 1.1 | 10-50 | 84058 |

***Table A-2** (continued)*

| Sample Number | Geologic Unit | Indoor Radon (pCi/L) | Ground-Water Depth (ft) | Zip Code |
|---|---|---|---|---|
| 483398 | alp | 1.1 | 10-50 | 84057 |
| 483287 | alp | 1.0 | >50 | 84604 |
| 483226 | alp | 1.0 | 10-50 | 84058 |
| 634580 | alp | 0.6 | >50 | 84057 |
| 483791 | alp | 0.2 | 10-50 | 84058 |
| 483733 | clso | 3.4 | >50 | 84604 |
| 483537 | es | 3.8 | 10-50 | 84057 |
| 483704 | es | 2.7 | 10-50 | 84057 |
| 483735 | es | 2.0 | 10-50 | 84057 |
| 483512 | es | 0.9 | 10-50 | 84058 |
| 483715 | es | 0.6 | 10-50 | 84057 |
| 839799 | lbg | 3.7 | >50 | 84604 |
| 483805 | lbg | 2.7 | >50 | 84604 |
| 483711 | lbg | 2.6 | >50 | 84604 |
| 842260 | lbg | 2.1 | >50 | 84604 |
| 483505 | lbm | 13.6 | 10-50 | 84604 |
| 842246 | lbm | 9.1 | >50 | 84604 |
| 483525 | lbm | 8.7 | 10-50 | 84604 |
| 839800 | lbm | 8.4 | 10-50 | 84604 |
| 842237 | lbm | 5.5 | >50 | 84604 |
| 842183 | lbm | 4.1 | >50 | 84604 |
| 839686 | lbm | 4.0 | 10-50 | 84604 |
| 842201 | lbm | 3.9 | >50 | 84604 |
| 483748 | lbm | 3.3 | >50 | 84057 |
| 839771 | lbm | 3.2 | >50 | 84604 |
| 839689 | lbm | 2.9 | >50 | 84601 |
| 839714 | lbm | 2.9 | 10-50 | 84604 |
| 483271 | lbm | 2.9 | 10-50 | 84604 |
| 839762 | lbm | 2.7 | >50 | 84604 |
| 483310 | lbm | 2.6 | 10-50 | 84604 |
| 839765 | lbm | 2.2 | 10-50 | 84604 |
| 634599 | lbm | 2.1 | 10-50 | 84604 |
| 839742 | lbm | 1.8 | 10-50 | 84604 |
| 839755 | lbm | 1.4 | 10-50 | 84604 |
| 839793 | lbm | 1.1 | >50 | 84604 |
| 839796 | lbm | 1.1 | 10-50 | 84604 |
| 483789 | lbm | 0.9 | >50 | 84604 |
| 483331 | lbm | 0.7 | >50 | 84604 |

| Sample Number | Geologic Unit | Indoor Radon (pCi/L) | Ground-Water Depth (ft) | Zip Code |
|---|---|---|---|---|
| 483393 | lbm | 0.7 | >50 | 84604 |
| 483807 | lbs | 9.9 | >50 | 84604 |
| 483723 | lbs | 2.1 | >50 | 84604 |
| 483776 | lbs | 2.0 | >50 | 84604 |
| 839783 | lbs | 2.0 | >50 | 84604 |
| 839782 | lbs | 1.9 | >50 | 84604 |
| 1679375 | lbs | 1.9 | >50 | 84604 |
| 842259 | lbs | 1.7 | >50 | 84604 |
| 842186 | lbs | 1.6 | >50 | 84604 |
| 842196 | lbs | 1.0 | >50 | 84604 |
| 483453 | lbs | 0.9 | >50 | 84604 |
| 842171 | lbs | 0.9 | >50 | 84604 |
| 1679407 | lbs | 0.9 | >50 | 84604 |
| 483289 | lbs | 0.8 | >50 | 84604 |
| 483389 | lbs | 0.8 | >50 | 84604 |
| 483817 | lbs | 0.8 | >50 | 84604 |
| 839795 | lbs | 0.7 | >50 | 84606 |
| 839774 | lbs | 0.7 | >50 | 84604 |
| 839761 | lpd | 2.3 | 10-50 | 84604 |
| 483550 | lpd | 2.2 | 10-50 | 84057 |
| 839697 | lpd | 1.7 | 10-50 | 84604 |
| 483343 | lpd | 1.5 | 10-50 | 84058 |
| 483734 | lpd | 0.6 | 10-50 | 84058 |
| 483452 | lpg | 2.5 | 10-50 | 84604 |
| 483361 | lpg | 2.4 | 10-50 | 84604 |
| 483714 | lpg | 2.2 | 10-50 | 84058 |
| 483781 | lpg | 2.2 | 10-50 | 84058 |
| 483359 | lpg | 1.5 | 10-50 | 84058 |
| 483757 | lpg | 1.5 | 10-50 | 84058 |
| 483513 | lpg | 1.4 | 10-50 | 84057 |
| 483285 | lpg | 1.3 | 10-50 | 84058 |
| 839769 | lpm | 1.9 | <10 | 84606 |
| 842247 | lpm | 1.6 | <10 | 84606 |
| 1679399 | lpm | 1.3 | <10 | 84606 |
| 839798 | lpm | 0.8 | <10 | 84606 |
| 839775 | lpm | 0.5 | <10 | 84606 |
| 483493 | lps | 1.7 | <10 | 84058 |
| 839716 | lps | 1.7 | 10-50 | 84606 |
| 483662 | lps | 0.8 | 10-50 | 84058 |

***Table A-3.***

***Ground-survey data, east Sandy, exclusive of indoor- and soil-ATD measurements. Measurements are grouped by geologic unit, and are sorted within each unit in descending order by eU concentration. See table 1 for explanation of geologic units.***

| Sample Number | Geologic Unit | Total Counts (ppm) | eK (%) | eU (ppm) | eTh (ppm) | eU/eTh | Soil Gas Rn (pCi/L) | Ground-Water Depth (ft) |
|---|---|---|---|---|---|---|---|---|
| S-008 | af1 | 19.0 | 2.6 | 4.2 | 14.3 | 0.29 | – | >50 |
| S-041 | af2 | 27.3 | 3.4 | 6.0 | 19.2 | 0.31 | – | >50 |
| S-116 | af2 | 16.5 | 1.6 | 5.2 | 12.3 | 0.42 | – | 10-30 |
| S-096 | af2 | 16.8 | 1.8 | 4.0 | 14.1 | 0.28 | – | >50 |
| S-005 | af2 | 18.4 | 2.4 | 3.6 | 17.1 | 0.21 | 120 | <10 |
| S-010 | af2 | 15.8 | 2.6 | 2.9 | 10.3 | 0.28 | – | >50 |
| S-007 | af2 | 18.8 | 2.6 | 2.3 | 20.6 | 0.11 | – | 30-50 |
| S-112 | al1 | 25.5 | 2.6 | 9.0 | 14.2 | 0.63 | 246 | <10 |
| S-102 | al1 | 24.6 | 2.7 | 8.5 | 11.4 | 0.75 | 482 | <10 |
| S-083 | al1 | 24.7 | 3.1 | 7.9 | 12.5 | 0.63 | – | <10 |
| S-130 | al1 | 21.9 | 2.1 | 6.4 | 16.2 | 0.40 | – | 10-30 |
| S-104 | al1 | 21.8 | 2.2 | 6.2 | 16.5 | 0.38 | – | <10 |
| S-004 | al1 | 19.9 | 2.8 | 2.9 | 19.0 | 0.15 | 82 | <10 |
| S-118 | al2 | 15.4 | 1.7 | 3.7 | 11.6 | 0.32 | – | 10-30 |
| S-131 | alp bcc | 16.7 | 1.6 | 5.5 | 11.2 | 0.49 | – | 10-30 |
| S-125 | alp bcc | 12.2 | 1.6 | 2.6 | 10.0 | 0.26 | – | 10-30 |
| S-064 | alp lcc | 26.3 | 2.8 | 8.7 | 15.3 | 0.57 | 516 | >50 |
| S-084 | alp lcc | 20.8 | 2.2 | 8.7 | 9.7 | 0.90 | 143 | 30-50 |
| S-037 | alp lcc | 28.0 | 3.0 | 8.7 | 16.6 | 0.52 | – | >50 |
| S-073 | alp lcc | 23.4 | 2.3 | 8.4 | 12.1 | 0.69 | 861 | >50 |
| S-120 | alp lcc | 25.1 | 2.7 | 8.4 | 16.4 | 0.51 | 314 | 30-50 |
| S-127 | alp lcc | 26.5 | 2.9 | 8.2 | 15.6 | 0.53 | – | 10-30 |
| S-122 | alp lcc | 23.5 | 2.2 | 8.2 | 13.9 | 0.59 | – | 10-30 |
| S-045 | alp lcc | 25.4 | 2.5 | 7.9 | 16.1 | 0.49 | 311 | >50 |
| S-038 | alp lcc | 27.8 | 3.2 | 7.9 | 17.8 | 0.44 | 279 | >50 |
| S-075 | alp lcc | 25.3 | 2.8 | 7.5 | 14.3 | 0.52 | 1021 | 10-30 |
| S-105 | alp lcc | 25.0 | 2.8 | 7.5 | 18.8 | 0.40 | – | <10 |
| S-039 | alp lcc | 24.2 | 2.8 | 7.3 | 12.6 | 0.58 | 368 | >50 |
| S-126 | alp lcc | 25.1 | 2.8 | 7.3 | 12.0 | 0.61 | – | 10-30 |
| S-063 | alp lcc | 25.1 | 2.7 | 7.2 | 14.8 | 0.49 | 2398 | >50 |
| S-047 | alp lcc | 24.0 | 2.5 | 7.1 | 14.6 | 0.49 | 402 | >50 |
| S-065 | alp lcc | 24.8 | 2.9 | 7.1 | 16.4 | 0.43 | – | >50 |
| S-046 | alp lcc | 21.0 | 2.2 | 7.0 | 11.6 | 0.60 | 1138 | >50 |
| S-040 | alp lcc | 26.9 | 3.1 | 7.0 | 16.9 | 0.41 | – | >50 |
| S-061 | alp lcc | 22.3 | 2.3 | 6.9 | 12.5 | 0.55 | 548 | >50 |
| S-062 | alp lcc | 21.4 | 2.2 | 6.8 | 9.4 | 0.72 | 95 | 30-50 |
| S-076 | alp lcc | 24.8 | 2.5 | 6.8 | 15.8 | 0.43 | – | >50 |

***Table A-3** (continued)*

| Sample Number | Geologic Unit | Total Counts (ppm) | eK (%) | eU (ppm) | eTh (ppm) | eU/eTh | Soil Gas Rn (pCi/L) | Ground-Water Depth (ft) |
|---|---|---|---|---|---|---|---|---|
| S-072 | alp lcc | 24.1 | 2.7 | 6.5 | 13.7 | 0.47 | 503 | 30-50 |
| S-129 | alp lcc | 23.9 | 2.7 | 6.5 | 15.6 | 0.42 | – | 10-30 |
| S-092 | alp lcc | 19.8 | 2.2 | 6.0 | 12.7 | 0.47 | – | >50 |
| S-074 | alp lcc | 17.5 | 1.8 | 5.8 | 9.0 | 0.64 | 290 | >50 |
| S-081 | alp lcc | 19.3 | 2.3 | 5.4 | 11.4 | 0.47 | – | >50 |
| S-066 | alp lcc | 21.8 | 2.5 | 5.3 | 15.4 | 0.34 | – | >50 |
| S-068 | alp lcc | 16.0 | 1.6 | 5.2 | 10.5 | 0.50 | – | >50 |
| S-067 | alp lcc | 22.3 | 3.1 | 5.0 | 13.2 | 0.38 | – | >50 |
| S-069 | alp lcc | 21.1 | 2.9 | 4.9 | 15.7 | 0.31 | – | >50 |
| S-052 | alp lcc | 22.9 | 2.7 | 4.3 | 17.8 | 0.24 | – | >50 |
| S-014 | alp lcc | 13.5 | 1.6 | 3.2 | 11.5 | 0.28 | 1069 | >50 |
| S-110 | ca bcc | 26.1 | 2.6 | 8.4 | 17.2 | 0.49 | 466 | 10-30 |
| S-117 | ca bcc | 18.9 | 2.0 | 5.9 | 15.2 | 0.39 | – | <10 |
| S-124 | ca bcc | 14.0 | 1.7 | 4.1 | 10.6 | 0.39 | 283 | 10-30 |
| S-119 | ca bcc | 14.1 | 1.8 | 3.6 | 10.4 | 0.35 | – | >50 |
| S-113 | ca lcc | 24.3 | 2.5 | 7.7 | 14.8 | 0.52 | – | 30-50 |
| S-115 | ca lcc | 21.0 | 2.0 | 7.2 | 14.5 | 0.50 | – | >50 |
| S-128 | ca lcc | 21.4 | 2.4 | 6.7 | 12.7 | 0.53 | – | 10-30 |
| S-056 | ca lcc | 16.8 | 2.4 | 3.8 | 12.9 | 0.29 | – | >50 |
| S-095 | chs | 23.7 | 3.4 | 5.7 | 17.5 | 0.33 | – | >50 |
| S-094 | chs | 19.2 | 2.3 | 5.6 | 12.2 | 0.46 | – | >50 |
| S-082 | es | 24.0 | 2.6 | 8.2 | 12.8 | 0.64 | – | <10 |
| S-044 | es | 26.2 | 2.9 | 6.4 | 16.2 | 0.40 | – | >50 |
| S-048 | es | 20.0 | 2.5 | 5.4 | 10.7 | 0.50 | – | >50 |
| S-078 | es | 21.0 | 2.7 | 5.3 | 10.8 | 0.49 | – | >50 |
| S-049 | es | 19.9 | 2.4 | 4.7 | 11.6 | 0.41 | – | >50 |
| S-077 | es | 19.5 | 2.6 | 4.5 | 9.8 | 0.46 | – | >50 |
| S-080 | es | 17.9 | 2.1 | 3.8 | 13.0 | 0.29 | – | >50 |
| S-054 | es | 15.6 | 2.3 | 2.7 | 12.7 | 0.21 | – | >50 |
| S-089 | gbco | 25.6 | 2.9 | 7.4 | 13.7 | 0.54 | – | >50 |
| S-090 | gbco | 24.2 | 2.5 | 6.6 | 16.8 | 0.39 | – | >50 |
| S-091 | gbct | 25.5 | 3.3 | 6.3 | 17.0 | 0.37 | – | >50 |
| S-093 | gbct | 20.6 | 2.4 | 5.1 | 14.8 | 0.34 | – | >50 |
| S-003 | laly | 11.9 | 1.4 | 3.3 | 9.3 | 0.35 | 138 | <10 |
| S-002 | laly | 13.3 | 1.8 | 3.0 | 10.5 | 0.29 | 905 | <10 |
| S-109 | lbg bcc | 24.2 | 2.5 | 8.6 | 12.0 | 0.72 | 265 | 10-30 |
| S-108 | lbg bcc | 17.5 | 1.7 | 5.6 | 10.7 | 0.52 | 327 | 30-50 |

***Table A-3** (continued)*

| Sample Number | Geologic Unit | Total Counts (ppm) | eK (%) | eU (ppm) | eTh (ppm) | eU/eTh | Soil Gas Rn (pCi/L) | Ground-Water Depth (ft) |
|---|---|---|---|---|---|---|---|---|
| S-042 | lbg lcc | 23.2 | 2.5 | 7.9 | 10.9 | 0.72 | 126 | >50 |
| S-114 | lbg lcc | 22.2 | 2.2 | 7.2 | 14.6 | 0.49 | – | 30-50 |
| S-043 | lbg lcc | 19.6 | 2.1 | 6.6 | 9.9 | 0.67 | 1082 | >50 |
| S-050 | lbg lcc | 23.4 | 2.8 | 5.4 | 15.9 | 0.34 | – | >50 |
| S-051 | lbg lcc | 22.6 | 2.6 | 5.3 | 15.8 | 0.34 | – | >50 |
| S-029 | lbg lcc | 21.3 | 2.6 | 5.0 | 12.9 | 0.39 | 404 | >50 |
| S-079 | lbg lcc | 18.6 | 2.3 | 4.9 | 13.8 | 0.36 | – | >50 |
| S-106 | lbg lcc | 16.5 | 1.8 | 4.8 | 11.0 | 0.44 | – | 10-30 |
| S-055 | lbg lcc | 17.0 | 2.3 | 4.3 | 11.9 | 0.36 | – | >50 |
| S-018 | lbg lcc | 17.3 | 2.5 | 3.4 | 13.3 | 0.26 | 203 | >50 |
| S-053 | lbg lcc | 20.2 | 2.6 | 3.4 | 16.9 | 0.20 | – | >50 |
| S-011 | lbg lcc | 15.5 | 2.3 | 3.2 | 13.0 | 0.25 | – | >50 |
| S-009 | lbg lcc | 17.5 | 2.9 | 2.7 | 15.6 | 0.17 | – | >50 |
| S-013 | lbg lcc | 11.3 | 1.6 | 2.2 | 9.8 | 0.22 | 912 | >50 |
| S-012 | lbg lcc | 11.3 | 1.4 | 1.8 | 10.6 | 0.17 | 1198 | >50 |
| S-087 | lbpm | 19.3 | 2.1 | 5.1 | 11.2 | 0.46 | 580 | 10-30 |
| S-001 | lbpm | 15.0 | 2.0 | 2.4 | 14.0 | 0.17 | 309 | <10 |
| S-121 | lpd | 26.1 | 2.4 | 9.0 | 14.1 | 0.64 | – | 10-30 |
| S-103 | lpd | 26.2 | 3.0 | 8.8 | 15.0 | 0.59 | – | 10-30 |
| S-111 | lpd | 23.8 | 2.2 | 8.6 | 13.2 | 0.65 | 223 | 10-30 |
| S-071 | lpd | 21.8 | 2.0 | 7.3 | 11.5 | 0.63 | 613 | 10-30 |
| S-059 | lpd | 28.3 | 3.2 | 7.3 | 14.6 | 0.50 | – | >50 |
| S-100 | lpd | 22.5 | 2.7 | 6.6 | 8.7 | 0.76 | 110 | 10-30 |
| S-123 | lpd | 11.8 | 1.4 | 2.4 | 10.2 | 0.24 | – | 10-30 |
| S-097 | lpg | 25.5 | 2.2 | 10.6 | 13.5 | 0.79 | 730 | 10-30 |
| S-035 | lpg | 27.2 | 3.2 | 8.0 | 13.3 | 0.60 | – | 30-50 |
| S-026 | lpg | 21.8 | 2.1 | 7.5 | 13.7 | 0.55 | 72 | 30-50 |
| S-036 | lpg | 25.5 | 3.1 | 7.0 | 12.6 | 0.56 | – | >50 |
| S-101 | lpg | 24.5 | 2.7 | 6.8 | 16.9 | 0.40 | 309 | 10-30 |
| S-028 | lpg | 27.4 | 3.2 | 6.4 | 17.5 | 0.37 | 749 | >50 |
| S-025 | lpg | 23.8 | 2.6 | 6.4 | 13.7 | 0.47 | 371 | >50 |
| S-030 | lpg | 24.6 | 3.4 | 6.3 | 8.3 | 0.76 | – | 30-50 |
| S-086 | lpg | 22.5 | 2.5 | 6.2 | 12.7 | 0.49 | 711 | <10 |
| S-060 | lpg | 22.5 | 2.4 | 6.2 | 13.7 | 0.45 | 564 | 30-50 |
| S-088 | lpg | 20.6 | 2.0 | 6.1 | 13.4 | 0.46 | 73 | 10-30 |
| S-099 | lpg | 19.7 | 2.4 | 6.0 | 8.6 | 0.70 | 270 | 10-30 |
| S-085 | lpg | 20.4 | 2.6 | 5.6 | 12.0 | 0.47 | 702 | 10-30 |
| S-027 | lpg | 22.4 | 2.7 | 5.6 | 13.1 | 0.43 | 624 | >50 |

***Table A-3** (continued)*

| Sample Number | Geologic Unit | Total Counts (ppm) | eK (%) | eU (ppm) | eTh (ppm) | eU/eTh | Soil Gas Rn (pCi/L) | Ground-Water Depth (ft) |
|---|---|---|---|---|---|---|---|---|
| S-032 | lpg | 21.2 | 2.8 | 5.6 | 9.1 | 0.62 | – | 30-50 |
| S-034 | lpg | 21.0 | 2.6 | 5.5 | 12.3 | 0.45 | – | >50 |
| S-031 | lpg | 25.7 | 3.8 | 5.0 | 11.2 | 0.45 | – | 30-50 |
| S-107 | lpg | 16.0 | 1.8 | 4.9 | 10.8 | 0.45 | – | 10-30 |
| S-070 | lpg | 15.8 | 1.8 | 4.1 | 12.2 | 0.34 | – | >50 |
| S-098 | lpg | 19.2 | 2.2 | 4.0 | 14.4 | 0.28 | 1194 | 10-30 |
| S-033 | lpg | 22.0 | 3.4 | 4.0 | 8.8 | 0.45 | – | 10-30 |
| S-015 | lpg | 17.8 | 2.4 | 3.7 | 14.1 | 0.26 | – | 30-50 |
| S-017 | lpg | 12.9 | 1.7 | 3.4 | 9.6 | 0.35 | 114 | 30-50 |
| S-023 | lpg | 17.5 | 2.2 | 3.3 | 16.5 | 0.20 | – | 30-50 |
| S-022 | lpg | 12.8 | 1.6 | 3.2 | 7.9 | 0.41 | 968 | >50 |
| S-021 | lpg | 13.5 | 1.9 | 2.4 | 9.8 | 0.24 | 1434 | 30-50 |
| S-057 | lpg | 15.1 | 2.0 | 2.3 | 13.3 | 0.17 | – | >50 |
| S-006 | lpg | 11.8 | 1.7 | 2.2 | 8.5 | 0.26 | 456 | >50 |
| S-024 | lpg | 17.8 | 2.7 | 2.2 | 16.8 | 0.13 | – | 30-50 |
| S-016 | lpg | 13.1 | 1.9 | 1.9 | 8.6 | 0.22 | 354 | 30-50 |
| S-058 | lpg | 16.2 | 2.5 | 1.9 | 13.1 | 0.15 | – | >50 |
| S-019 | lpg | 11.0 | 1.8 | 1.5 | 8.0 | 0.19 | 220 | >50 |
| S-020 | lpg | 13.8 | 1.9 | 1.2 | 12.8 | 0.09 | 332 | >50 |

***Table A-4***

***Ground-survey data, east Provo, exclusive of indoor- and soil-ATD measurements. Measurements are grouped by geologic unit, and are sorted within each unit in descending order by eU concentration. See table 2 for explanation of geologic units.***

| Sample Number | Geologic Unit | Total Counts (ppm) | eK (%) | eU (ppm) | eTh (ppm) | eU/eTh | Soil Gas Rn (pCi/L) | Ground-Water Depth (ft) |
|---|---|---|---|---|---|---|---|---|
| P-037 | af2 | 8.8 | 1.1 | 3.4 | 5.3 | 0.64 | 281 | 10-30 |
| P-046 | af2 | 11.8 | 1.3 | 3.3 | 6.7 | 0.49 | – | 10-50 |
| P-011 | af2 | 8.8 | 1.1 | 2.7 | 5.9 | 0.46 | 1454 | <10 |
| P-091 | af2 | 7.8 | 0.9 | 2.7 | 6.9 | 0.39 | 1264 | <10 |
| P-047 | af2 | 9.1 | 1.2 | 2.5 | 5.4 | 0.46 | – | 10-50 |
| P-061 | af2 | 9.9 | 1.3 | 1.9 | 8.6 | 0.22 | 354 | 10-30 |
| P-062 | af2 | 10.5 | 1.3 | 1.9 | 9.7 | 0.20 | 224 | 10-30 |
| P-010 | af2 | 7.1 | 1.0 | 1.8 | 4.8 | 0.38 | 497 | <10 |
| P-044 | afp | 10.5 | 1.2 | 3.6 | 6.5 | 0.55 | 65 | <10 |
| P-016 | afp | 9.8 | 1.1 | 3.3 | 6.1 | 0.54 | – | 10-50 |
| P-033 | afp | 10.2 | 1.2 | 2.9 | 6.3 | 0.46 | 468 | <10 |
| P-041 | afp | 9.2 | 1.0 | 2.9 | 7.5 | 0.39 | 180 | <10 |
| P-038 | afp | 9.5 | 1.3 | 2.3 | 5.2 | 0.44 | 253 | <10 |
| P-036 | afp | 8.2 | 1.2 | 1.5 | 6.0 | 0.25 | 202 | <10 |
| P-056 | afy | 14.1 | 1.7 | 4.6 | 9.4 | 0.49 | – | >50 |
| P-034 | afy | 11.2 | 1.3 | 4.3 | 7.0 | 0.61 | 1405 | <10 |
| P-067 | afy | 11.2 | 1.4 | 4.0 | 7.3 | 0.55 | 527 | >50 |
| P-021 | afy | 9.6 | 1.1 | 3.3 | 5.7 | 0.58 | 683 | 10-50 |
| P-068 | afy | 12.2 | 1.6 | 3.3 | 8.9 | 0.37 | 215 | >50 |
| P-012 | afy | 7.8 | 0.7 | 3.0 | 6.4 | 0.47 | 889 | >50 |
| P-019 | afy | 9.3 | 0.8 | 2.9 | 7.6 | 0.38 | 87 | 10-50 |
| P-039 | afy | 10.9 | 1.3 | 2.9 | 6.5 | 0.45 | – | <10 |
| P-054 | afy | 8.8 | 1.1 | 2.8 | 4.1 | 0.68 | – | 10-50 |
| P-089 | afy | 10.8 | 1.8 | 2.7 | 6.5 | 0.42 | – | >50 |
| P-030 | afy | 7.1 | 1.0 | 2.6 | 3.8 | 0.68 | – | >50 |
| P-051 | afy | 8.8 | 1.1 | 2.6 | 6.4 | 0.41 | – | <10 |
| P-035 | afy | 7.9 | 0.9 | 2.4 | 5.9 | 0.41 | 214 | 10-50 |
| P-084 | afy | 6.3 | 0.6 | 2.4 | 3.9 | 0.62 | – | >50 |
| P-020 | afy | 7.5 | 0.8 | 2.3 | 7.0 | 0.33 | 716 | 10-50 |
| P-023 | afy | 8.8 | 1.2 | 2.3 | 5.2 | 0.44 | 290 | <10 |
| P-083 | afy | 6.9 | 0.9 | 2.0 | 7.0 | 0.29 | – | >50 |
| P-007 | afy | 8.8 | 1.4 | 1.9 | 6.6 | 0.29 | 325 | 10-50 |
| P-005 | afy | 8.1 | 0.9 | 1.8 | 5.9 | 0.31 | 336 | 10-50 |
| P-001 | al1 | 12.7 | 1.4 | 4.0 | 8.1 | 0.49 | 187 | <10 |
| P-092 | al1 | 6.7 | 0.7 | 1.9 | 5.2 | 0.37 | – | <10 |
| P-052 | al2 | 10.1 | 1.2 | 3.9 | 7.1 | 0.55 | 519 | <10 |
| P-002 | al2 | 11.0 | 1.3 | 2.8 | 7.5 | 0.37 | – | <10 |

*Table A-4 (continued)*

| Sample Number | Geologic Unit | Total Counts (ppm) | eK (%) | eU (ppm) | eTh (ppm) | eU/eTh | Soil Gas Rn (pCi/L) | Ground-Water Depth (ft) |
|---|---|---|---|---|---|---|---|---|
| P-048 | al2 | 9.5 | 1.2 | 2.6 | 7.5 | 0.35 | – | <10 |
| P-065 | al2 | 8.0 | 1.1 | 2.4 | 5.5 | 0.44 | – | <10 |
| P-050 | al2 | 8.4 | 1.0 | 2.0 | 8.9 | 0.22 | – | <10 |
| P-099 | al2 | 6.6 | 1.0 | 1.9 | 3.5 | 0.54 | 407 | <10 |
| P-013 | al2 | 6.8 | 1.0 | 1.9 | 4.1 | 0.46 | – | <10 |
| P-093 | al2 | 7.6 | 0.9 | 1.7 | 5.9 | 0.29 | 887 | <10 |
| P-079 | alp | 9.1 | 1.0 | 3.3 | 7.5 | 0.44 | 630 | >50 |
| P-058 | alp | 10.6 | 1.2 | 3.3 | 8.2 | 0.40 | 86 | >50 |
| P-070 | alp | 11.2 | 1.6 | 3.2 | 7.5 | 0.43 | 318 | >50 |
| P-026 | alp | 10.0 | 1.2 | 3.2 | 6.5 | 0.49 | – | >50 |
| P-073 | alp | 6.7 | 0.8 | 2.8 | 4.2 | 0.67 | – | <10 |
| P-059 | alp | 5.7 | 0.3 | 2.8 | 3.1 | 0.90 | – | >50 |
| P-066 | alp | 9.9 | 1.3 | 2.7 | 7.2 | 0.38 | – | >50 |
| P-086 | alp | 10.6 | 1.5 | 2.5 | 7.9 | 0.32 | 129 | 10-50 |
| P-076 | alp | 8.6 | 1.1 | 2.5 | 5.7 | 0.44 | – | 10-50 |
| P-080 | alp | 9.5 | 1.2 | 2.3 | 7.9 | 0.29 | 734 | 10-50 |
| P-078 | alp | 8.9 | 1.2 | 2.2 | 6.6 | 0.33 | 403 | >50 |
| P-055 | alp | 10.6 | 1.4 | 2.2 | 7.8 | 0.28 | – | 10-50 |
| P-072 | alp | 11.1 | 1.7 | 2.2 | 9.2 | 0.24 | – | 10-50 |
| P-074 | alp | 6.9 | 1.0 | 2.1 | 3.9 | 0.54 | – | 10-50 |
| P-075 | alp | 9.0 | 1.3 | 2.1 | 7.0 | 0.30 | – | 10-50 |
| P-071 | alp | 8.4 | 1.1 | 2.1 | 6.3 | 0.33 | – | >50 |
| P-097 | alp | 9.2 | 1.3 | 2.0 | 6.7 | 0.30 | 551 | 10-50 |
| P-085 | alp | 8.3 | 1.1 | 2.0 | 7.2 | 0.28 | 492 | 10-50 |
| P-022 | alp | 7.9 | 1.0 | 1.8 | 6.7 | 0.27 | 445 | 10-50 |
| P-060 | alp | 8.8 | 1.3 | 1.8 | 6.5 | 0.28 | – | >50 |
| P-082 | alp | 8.4 | 1.2 | 1.8 | 8.3 | 0.22 | – | 10-50 |
| P-024 | alp | 9.9 | 1.4 | 1.7 | 8.3 | 0.20 | 62 | 10-50 |
| P-096 | alp | 6.8 | 0.9 | 1.6 | 5.8 | 0.28 | 486 | 10-50 |
| P-049 | alp | 8.1 | 1.1 | 1.3 | 6.6 | 0.20 | – | 10-50 |
| P-098 | es | 9.4 | 1.4 | 1.8 | 6.4 | 0.28 | 490 | 10-50 |
| P-095 | es | 7.3 | 0.9 | 1.7 | 5.9 | 0.29 | 349 | 10-50 |
| P-031 | lbg | 11.0 | 1.3 | 3.8 | 7.8 | 0.49 | – | >50 |
| P-032 | lbg | 9.7 | 1.3 | 2.4 | 8.4 | 0.29 | – | >50 |
| P-003 | lbm | 9.2 | 1.0 | 3.6 | 6.9 | 0.52 | 503 | >50 |
| P-027 | lbm | 12.4 | 1.7 | 3.6 | 7.7 | 0.47 | – | >50 |
| P-029 | lbm | 10.0 | 1.0 | 3.5 | 7.5 | 0.47 | – | >50 |
| P-015 | lbm | 9.9 | 1.3 | 3.2 | 7.7 | 0.42 | 237 | >50 |

***Table A-4** (continued)*

| Sample Number | Geologic Unit | Total Counts (ppm) | eK (%) | eU (ppm) | eTh (ppm) | eU/eTh | Soil Gas Rn (pCi/L) | Ground-Water Depth (ft) |
|---|---|---|---|---|---|---|---|---|
| P-017 | lbm | 9.4 | 0.9 | 3.1 | 6.4 | 0.48 | 314 | 10-50 |
| P-057 | lbm | 10.1 | 1.0 | 2.9 | 10.2 | 0.28 | 580 | >50 |
| P-025 | lbm | 8.2 | 1.0 | 2.4 | 6.2 | 0.39 | 229 | 10-50 |
| P-064 | lbm | 7.7 | 1.0 | 2.4 | 5.9 | 0.41 | – | >50 |
| P-004 | lbm | 10.2 | 1.3 | 2.3 | 8.0 | 0.29 | 884 | 10-50 |
| P-090 | lbm | 8.1 | 1.2 | 2.1 | 5.4 | 0.39 | – | 10-50 |
| P-069 | lbm | – | – | – | – | – | 1463 | 10-50 |
| P-063 | lbs | 12.3 | 1.5 | 3.4 | 10.7 | 0.32 | 158 | >50 |
| P-042 | lbs | 11.3 | 1.5 | 3.4 | 7.6 | 0.45 | – | >50 |
| P-040 | lbs | 13.9 | 1.6 | 3.4 | 12.2 | 0.28 | – | <10 |
| P-043 | lbs | 9.5 | 1.2 | 3.0 | 5.8 | 0.52 | – | >50 |
| P-028 | lbs | 8.6 | 1.0 | 2.9 | 5.7 | 0.51 | – | >50 |
| P-045 | lbs | 10.0 | 1.1 | 2.5 | 8.1 | 0.31 | 207 | >50 |
| P-014 | lbs | 11.3 | 1.6 | 2.4 | 10.0 | 0.24 | 97 | >50 |
| P-081 | lbs | 10.8 | 1.6 | 1.6 | 10.2 | 0.16 | – | >50 |
| P-088 | lbs | 6.9 | 0.8 | 1.5 | 6.9 | 0.22 | – | >50 |
| P-018 | lpd | 7.5 | 0.9 | 2.2 | 6.6 | 0.33 | 175 | 10-50 |
| P-008 | lpd | 9.1 | 1.2 | 2.0 | 6.4 | 0.31 | 205 | 10-50 |
| P-094 | lpg | 8.4 | 1.1 | 2.4 | 6.3 | 0.38 | 420 | 10-50 |
| P-087 | lpg | 8.0 | 1.1 | 2.1 | 6.1 | 0.34 | 349 | 10-50 |
| P-100 | lpg | 6.7 | 1.0 | 1.2 | 4.4 | 0.27 | – | 10-50 |
| P-053 | lps | 10.3 | 1.1 | 2.9 | 6.9 | 0.42 | 106 | 10-50 |
| P-006 | lps | 9.7 | 1.2 | 2.5 | 7.0 | 0.36 | 619 | 10-50 |
| P-009 | lps | 9.2 | 1.2 | 2.3 | 5.6 | 0.41 | 513 | <10 |
| P-077 | lps | 7.6 | 0.9 | 1.6 | 6.4 | 0.25 | 447 | 10-50 |